The Experimental Task in the 10 keV … 10 GeV Energy Range

- **Sources, Cosmic Gamma Radiation:**
  - ☆ Typical Intensities ~10^{-3}… 10^{-6} ph cm^{-2} s^{-1}
  - ☆ Continuum Radiation, Lines of Largely-Different Widths
  - ☆ Embedded / Occulted Sources
  - ☆ Examples:
    - ☞ Active Galaxies and Black-Hole Radiation Phenomena
    - ☞ Hot PlasmaSupernova Remnants
    - ☞ Interstellar-Medium Interactions
    - ☞ Cosmic Background Radiation Spectrum

- **Instrumental Constraints:**
  - ☆ Low Interaction Cross Sections
  - ☆ No/Problematic Reflecting Surfaces
  - ☆ Instrumental Background

Roland Diehl

X-Ray Telescopes: Concentrating Radiation

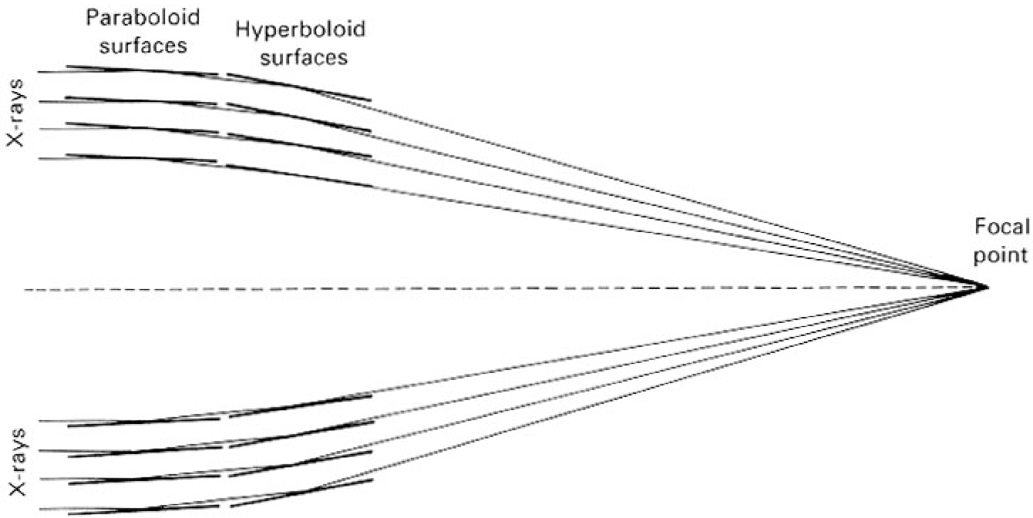

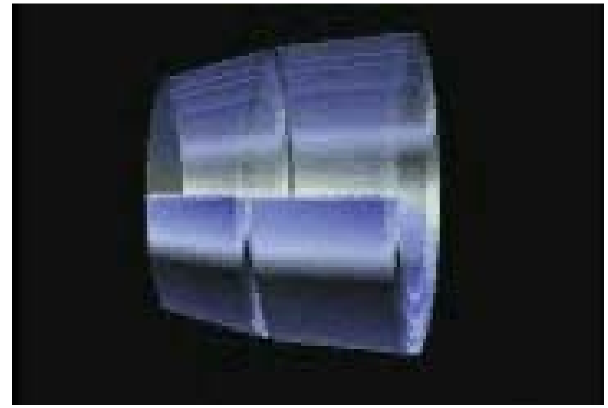

☆ Concentration of Cosmic Radiation

- Signal ~ Telescope Area
- Background ~ Detector Volume

☞ Signal/Background Ratio Improves with Radiation Concentration

Metal Surface Reflectivity

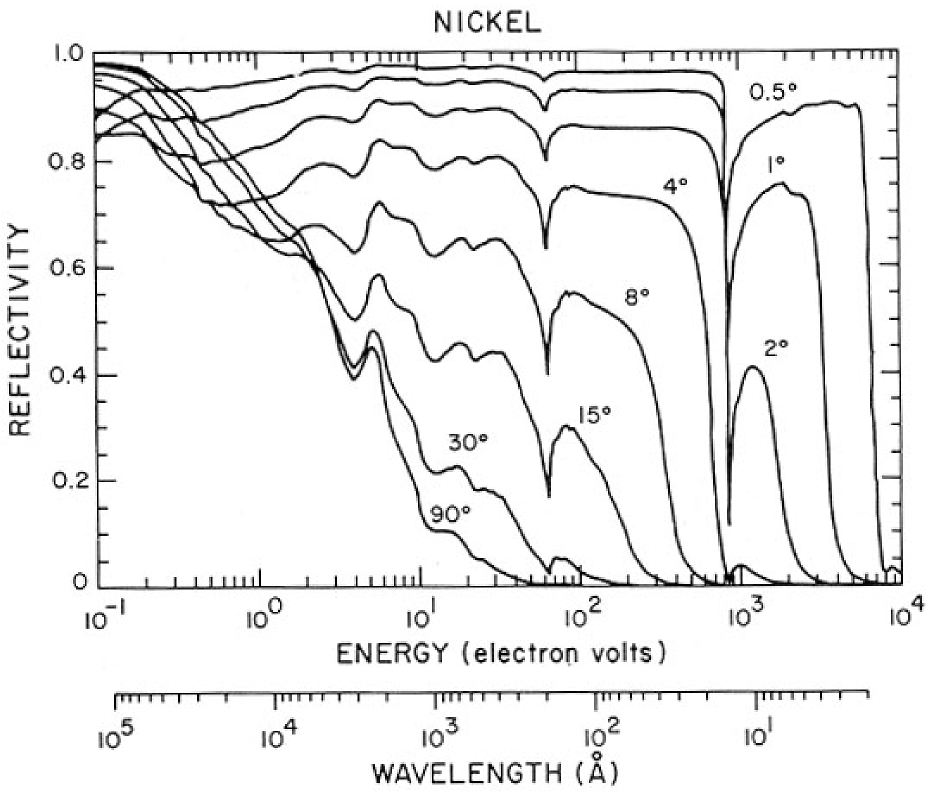

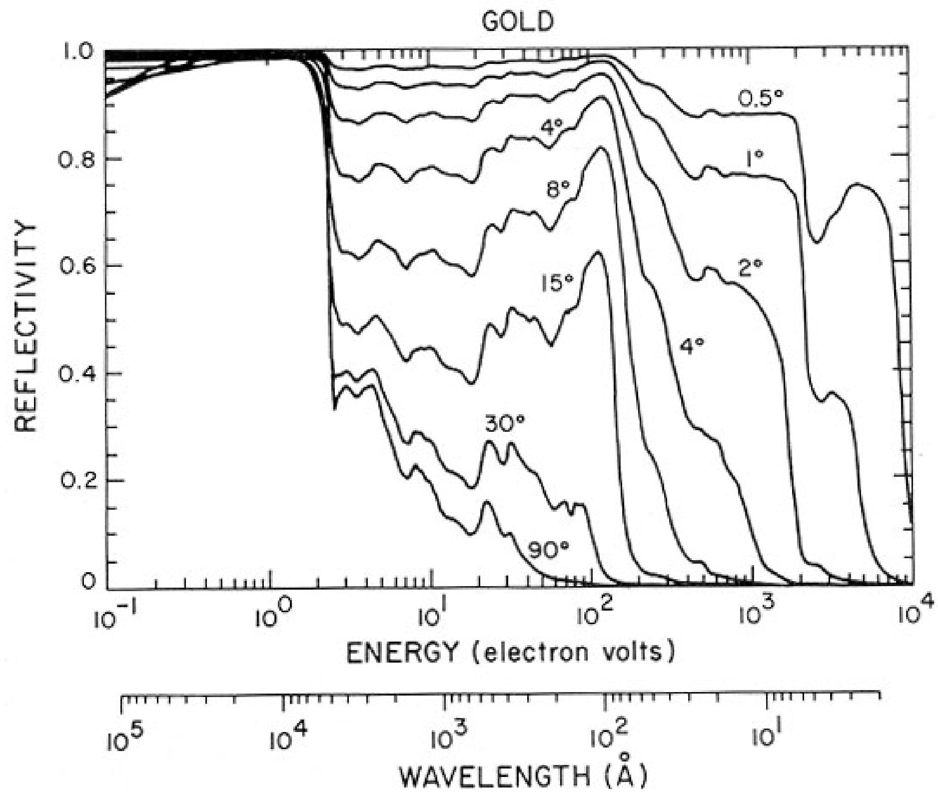

Roland Diehl

Focusing Gamma-Rays through Crystal Diffraction

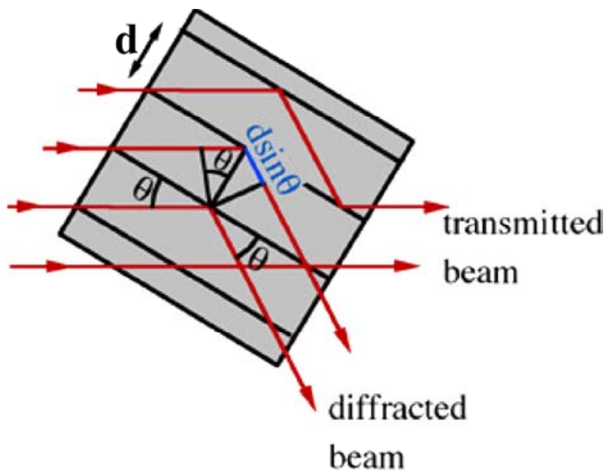

λ(511 keV) = $2.42632 \cdot 10^{-2}$ Å

Bragg condition

$2d\sin\theta = n\lambda$

d[220] = 2.0004Å
arcsin(λ/2d) = 0.347°

courtesy P.von Ballmoos

Focusing Gamma-Rays: e.g. 511 keV Photons

λ(511 keV) = $2.42632 \cdot 10^{-2}$ Å

Bragg condition

$2d\sin\theta = n\lambda$

d[220] = 2.0004Å

arcsin(λ/2d) = 0.347°

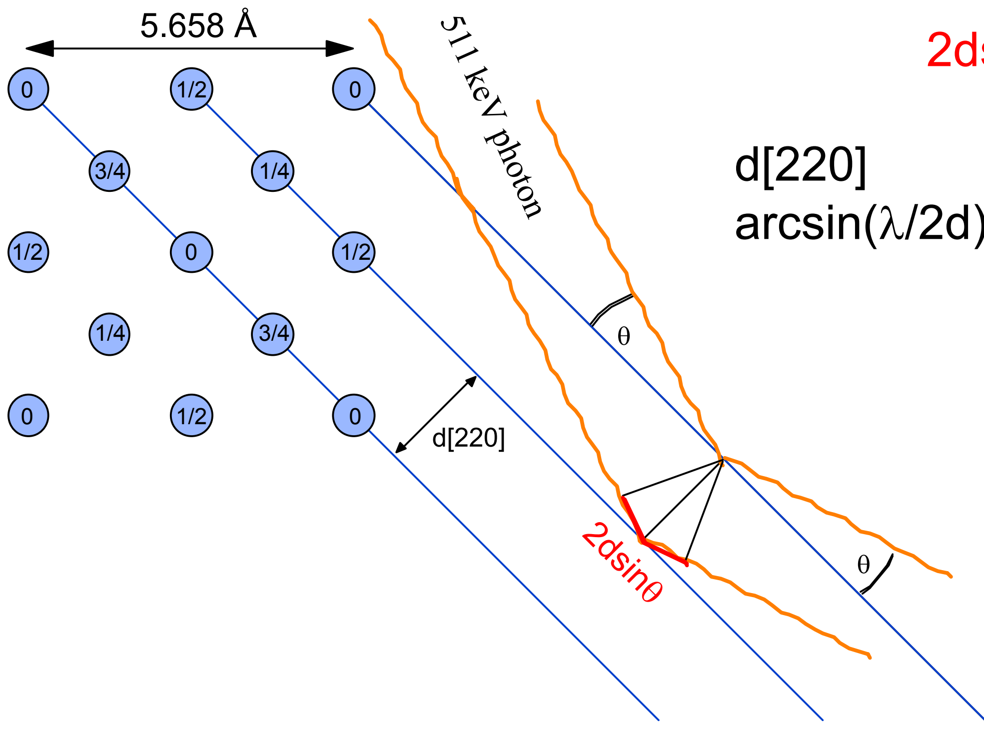

courtesy P.von Ballmoos

Roland Diehl

Crystal Diffraction Lenses: Bragg vs Laue Geometry

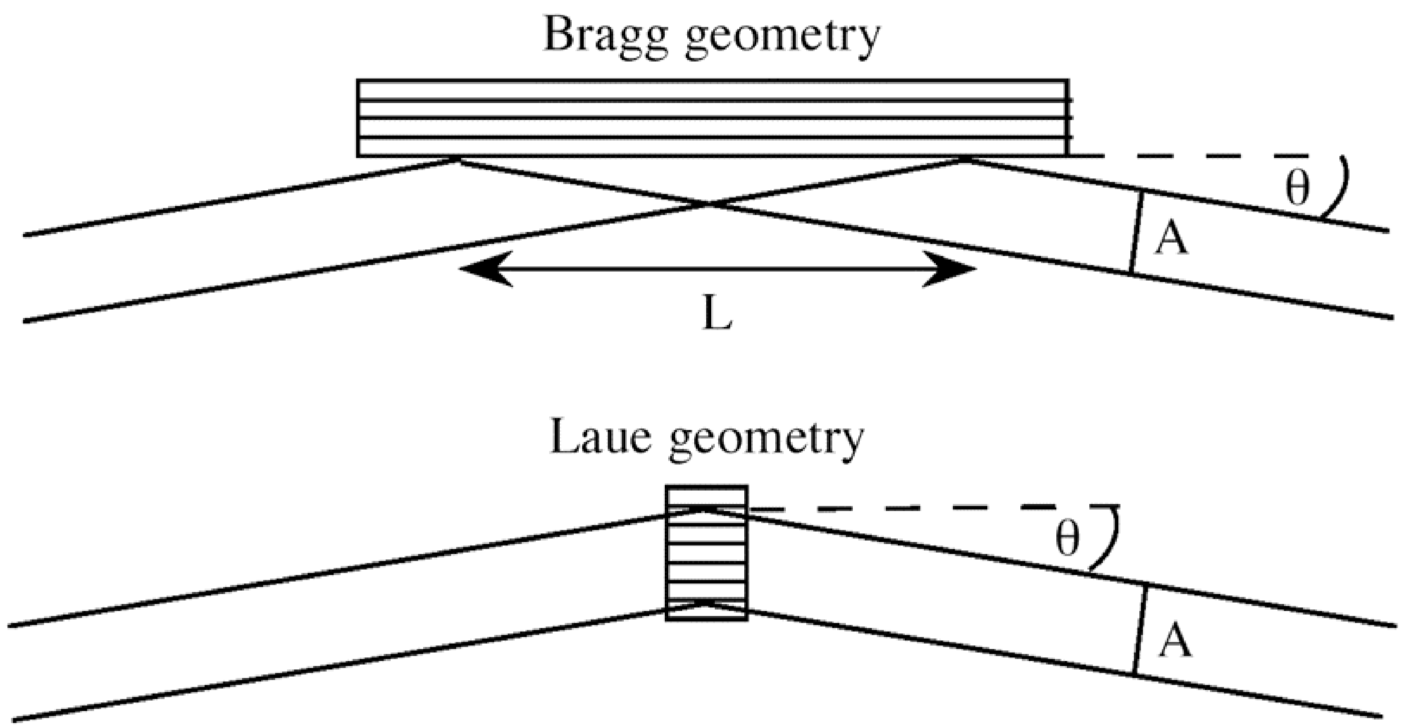

courtesy P.von Ballmoos

Focusing Gamma-Rays: Laue Lens Telescope

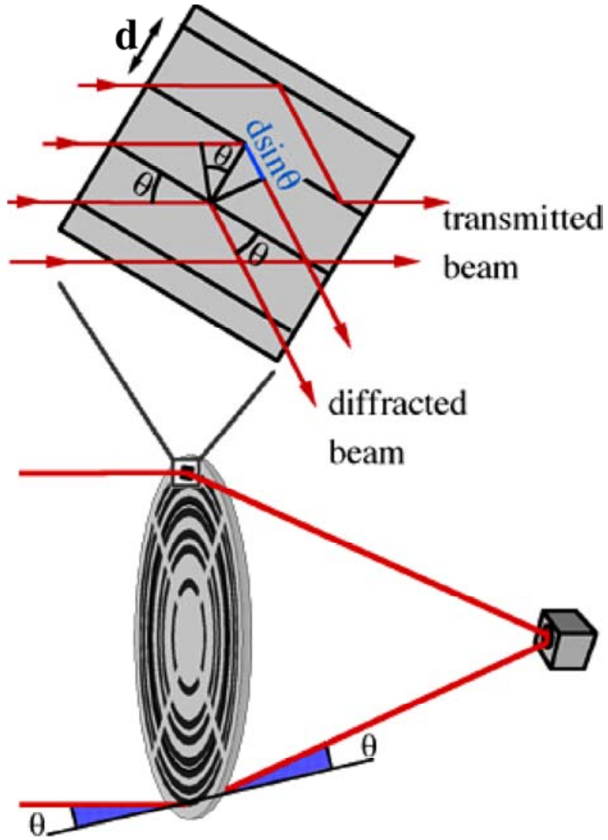

λ(511 keV)	=	$2.42632 \cdot 10^{-2}$ Å
Bragg condition		
$2d\sin\theta$	=	$n\lambda$
d[220]	=	2.0004Å
arcsin(λ/2d)	=	0.347°

Laue-type Gamma-ray lens

2θ	=	0.695°
ex. radius [220]	=	10.1 cm
=> focal lenght	=	8.2 m

narrow band Laue lens : higher orders at larger radia (CLAIRE)
broad band Laue lens : most efficient order at all radia (MAX)

courtesy P.von Ballmoos

Energy Bandpass ΔE and Field of View Δθ

- perfect monocrystal

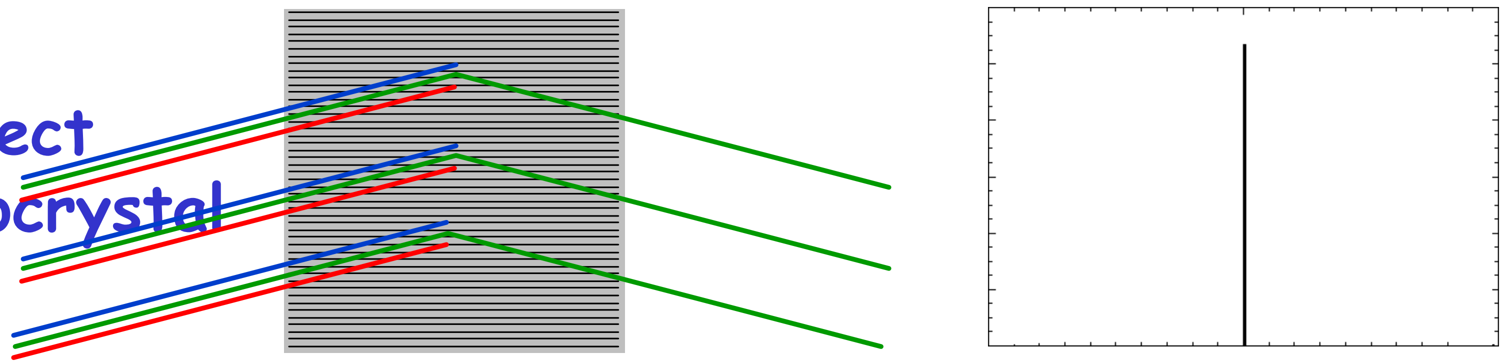

ΔE / $\Delta\theta$

- mosaic crystal

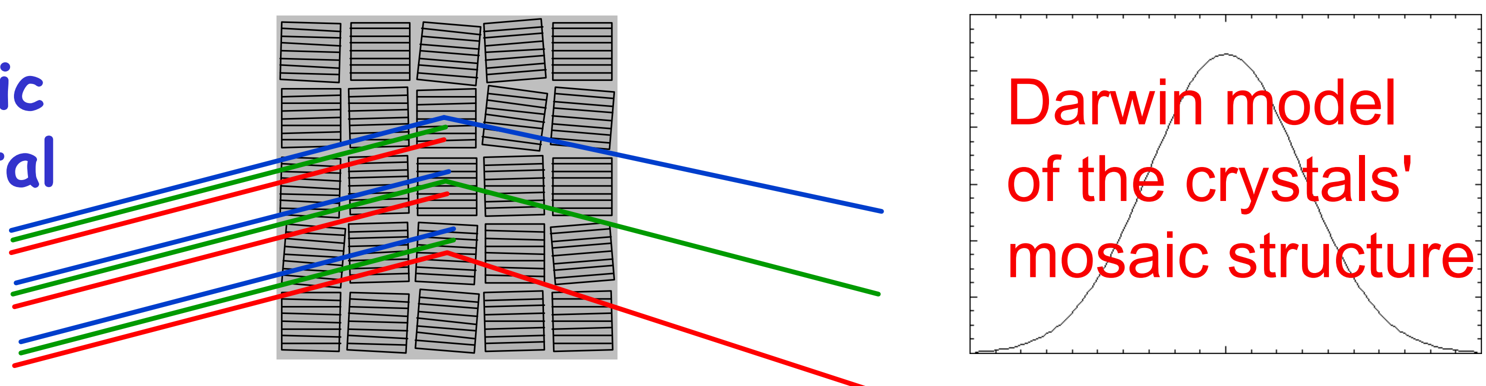

ΔE / $\Delta\theta$

courtesy P.von Ballmoos

Thickness of Diffraction Crystal

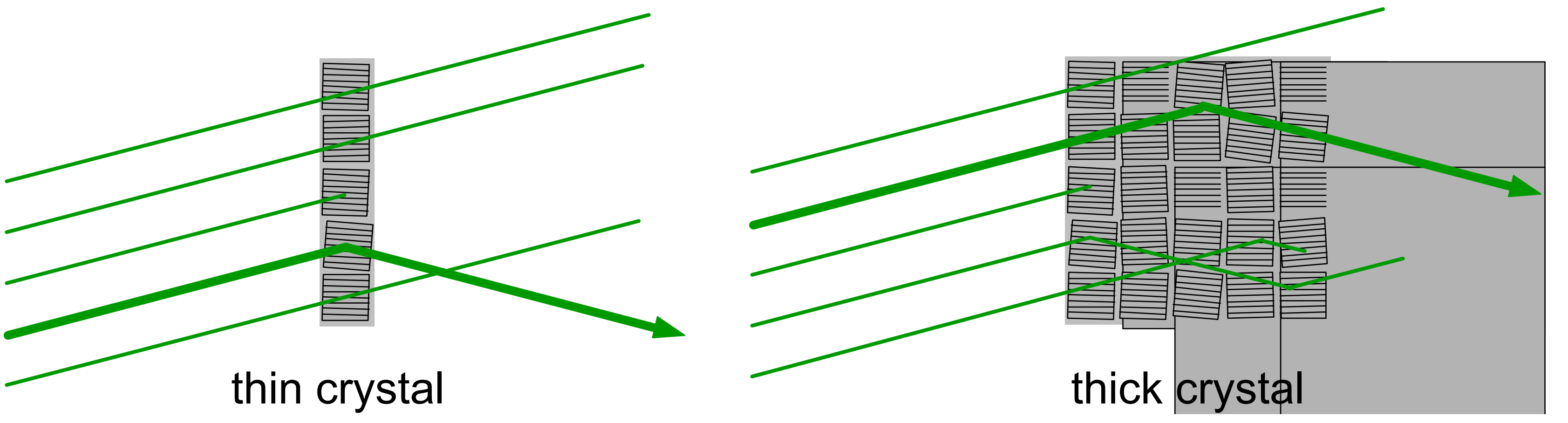

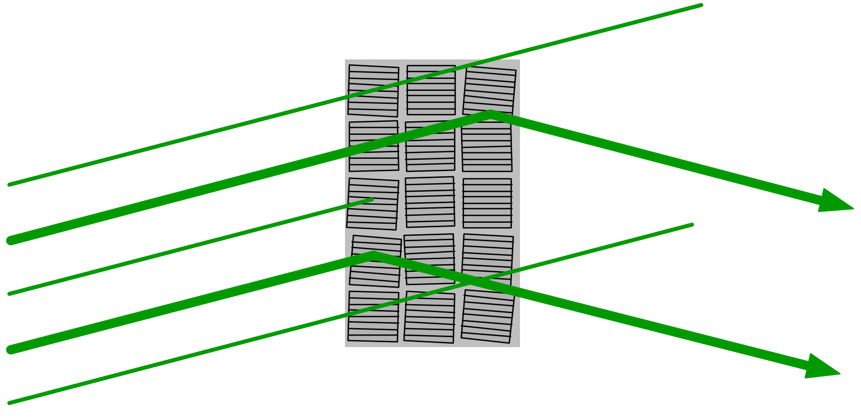

optimal thickness - energy dependent !

courtesy P.von Ballmoos

Performance Parameters of a Ge Lens:

Focussing Gamma-Rays of Specific Energy Onto a Detector

Diffraction Efficiency for Ge [440] Planes

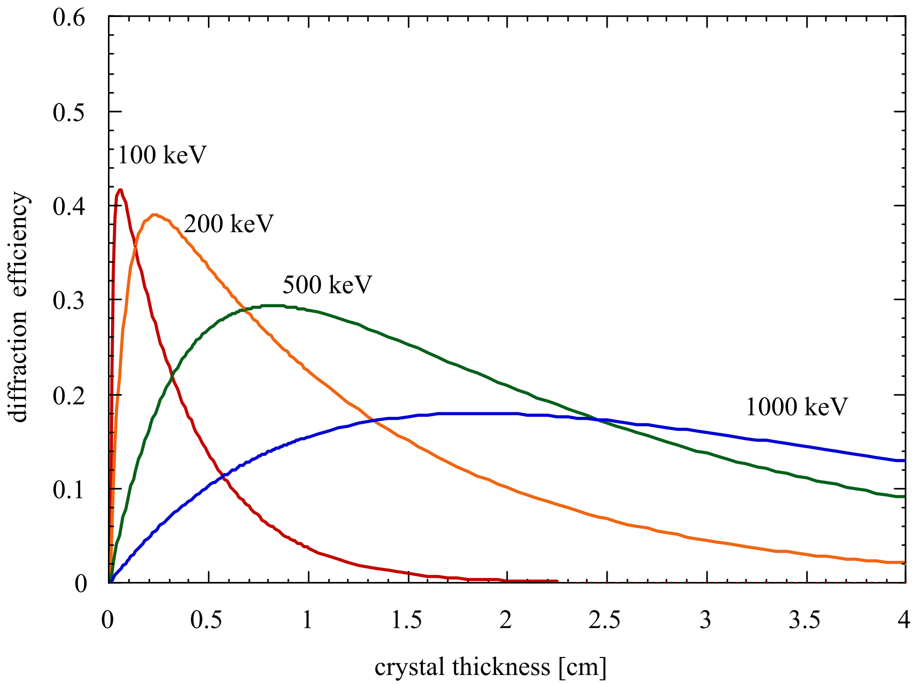

Ge [111] lens ring - diffracting area

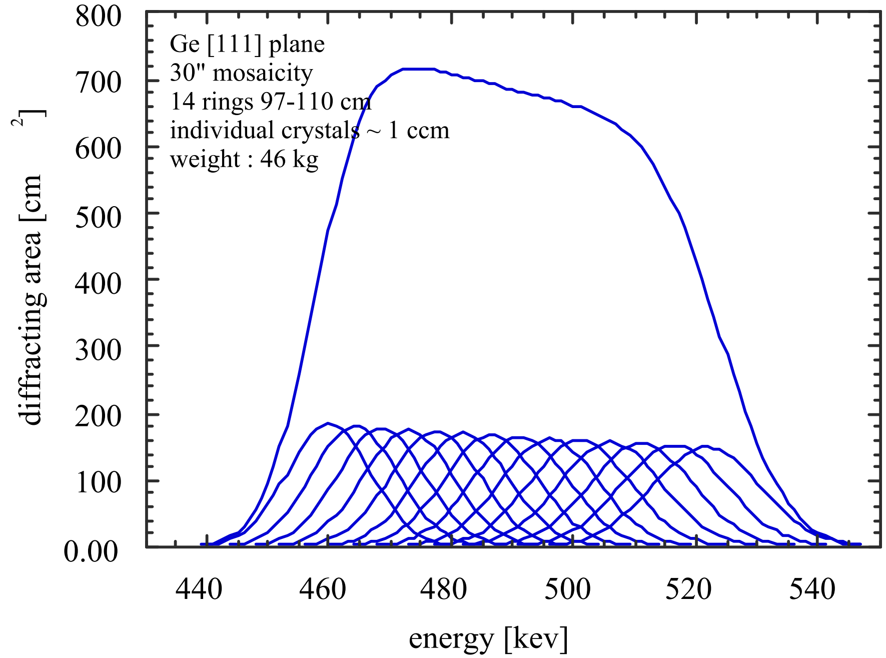

$$r_{th}(\theta)=0.5(1-e^{-2\alpha T})(e^{-\mu T}) \text{ at } E_{Bragg}$$

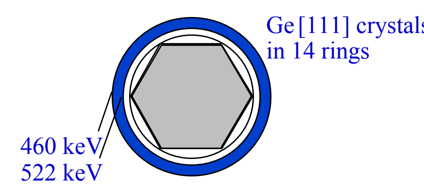

μ: Absorption coefficient

T: crystal thickness

$\alpha(\theta)$: diffraction coefficient

$\alpha(\theta) \sim F^2\lambda^3/V^2\sin(\theta) \sim \theta^{5/3}/E^2$

Efficiency Decreases with Increasing Energy and Order

courtesy P.von Ballmoos

Roland Diehl

the principle of a tunable Laue Lens

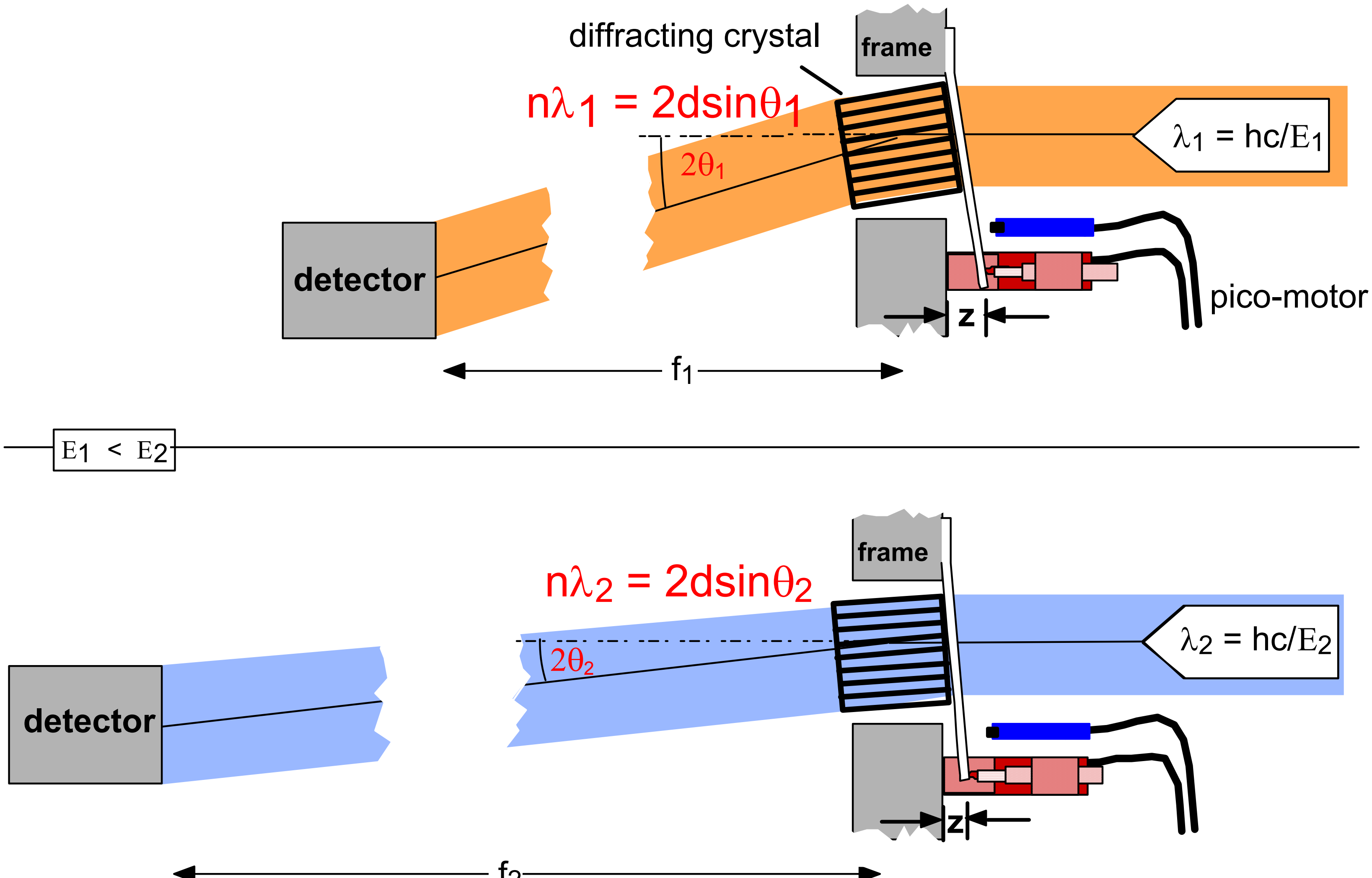

courtesy P.von Ballmoos

Balloon Experiment with Laue Lens: "Claire" (Gap->Bordeaux, June 2001)

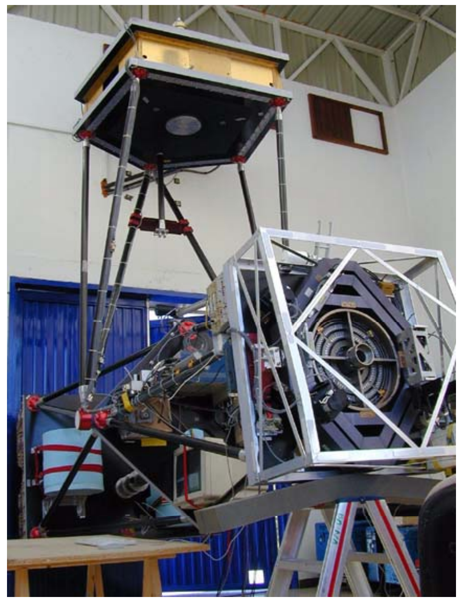

courtesy P.von Ballmoos

CLAIRE 2001 : Laue lens and fine pointing system

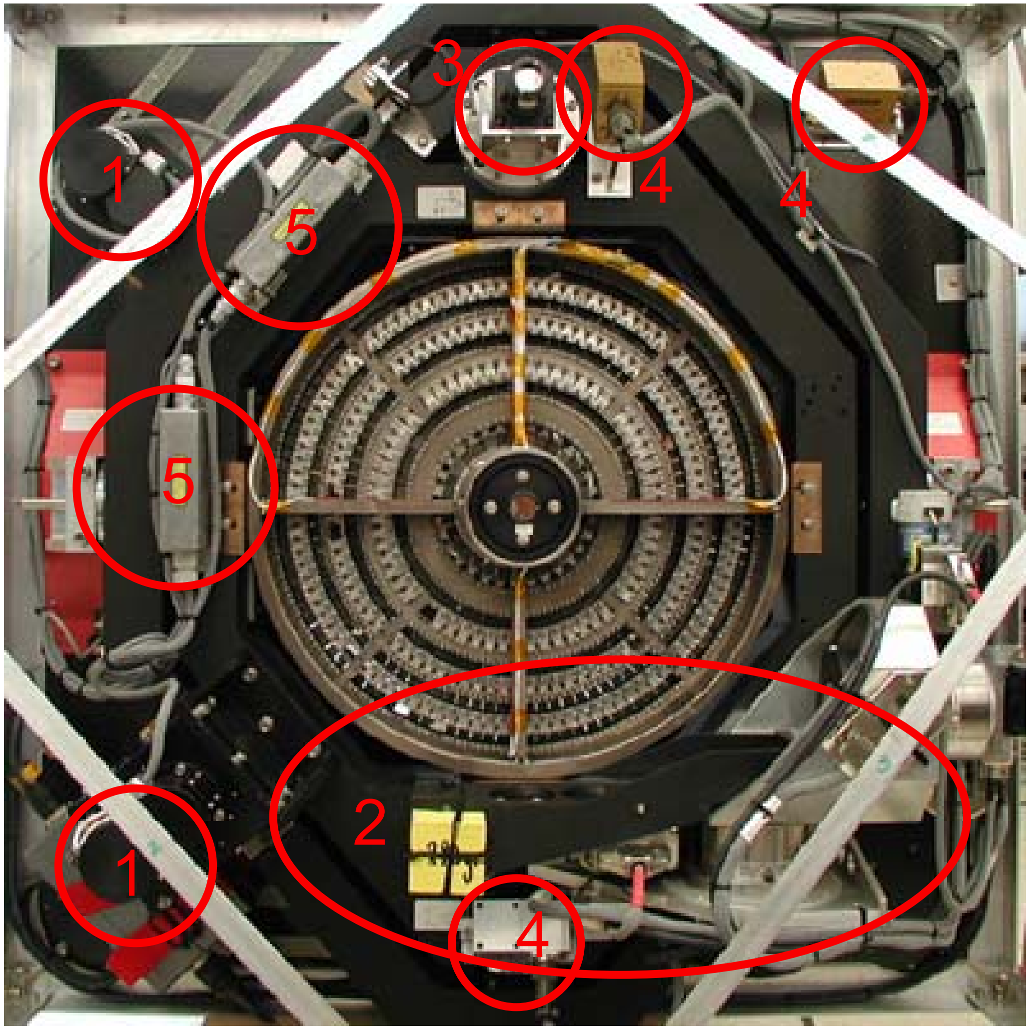

lens

- 576 Ge crystals
- A_{geo} = 511 cm^2
- E_{diff} = 170 keV, $\Delta E \approx 1.5$ keV
- FOV ≈ 45 arcsec

optical axis

- invar. pixel of rotating CCD

fine pointing

- Geneva actuators 1
- precision sun sensor 2
- wide field CCD camera 3
- inclinometers 4
- mechanical & laser gyros 5

=> stability ≈ 3 arcsec

courtesy P.von Ballmoos

CLAIRE 2001 : Ge detector matrix and ACS

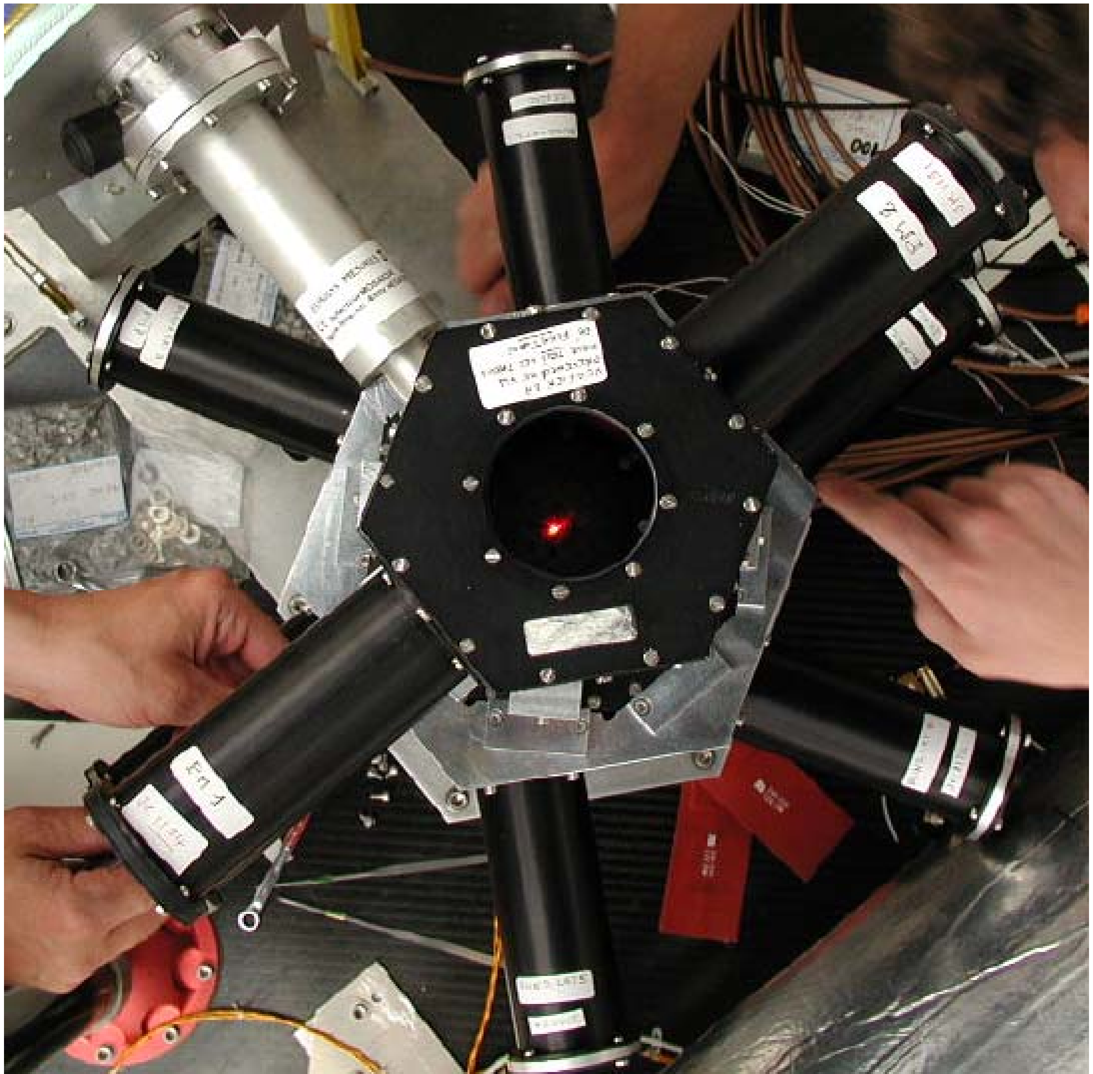

detector
- 3x3 matrix
- high purity Ge
- 1.5*1.5*4cm

cooling
- pressurized N dewar

ACS system
- CsI shield
- BGO collimator

courtesy P.von Ballmoos

Proposed Laue Lens Space Mission

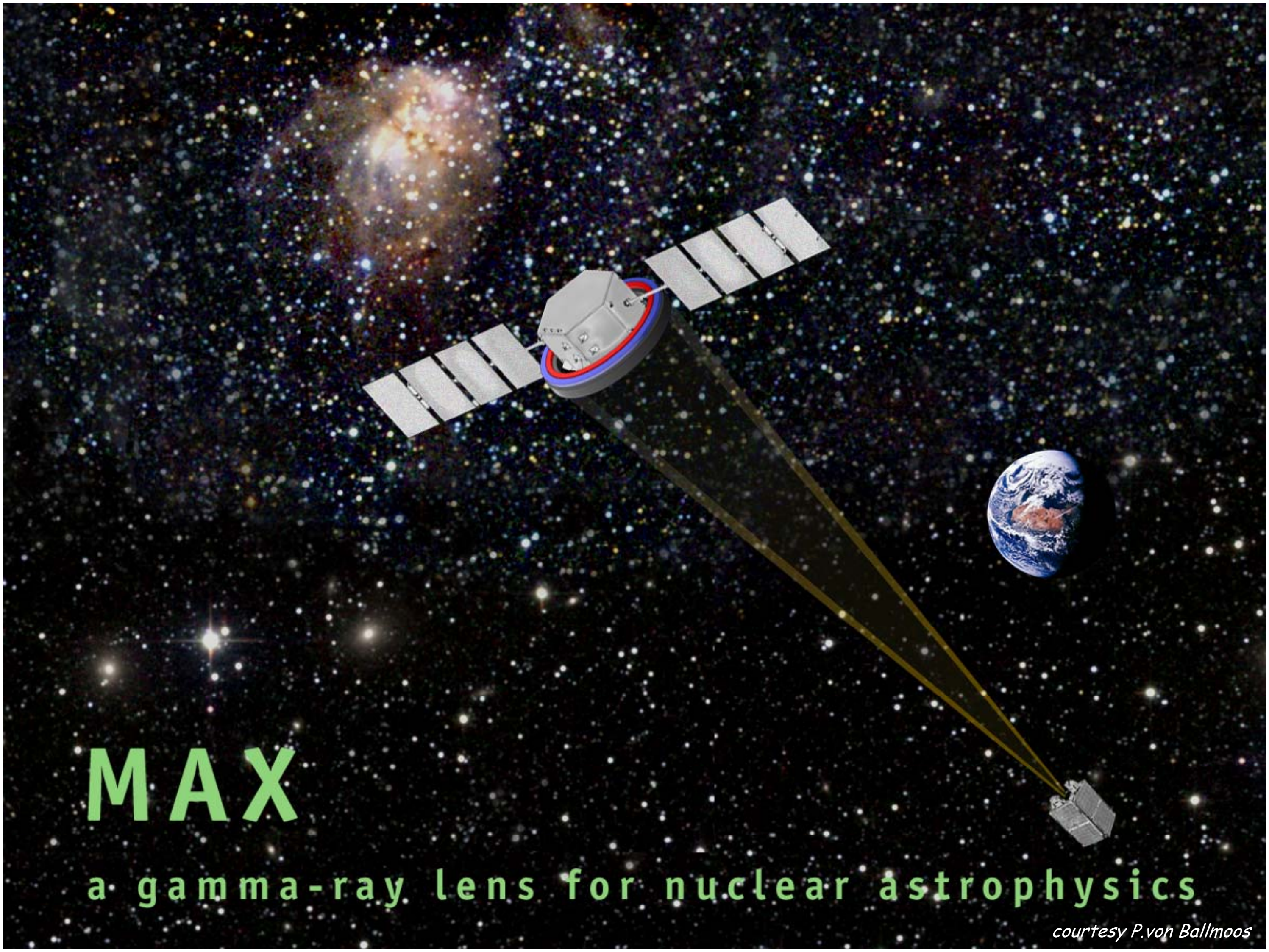

Interaction of HE photons with matter

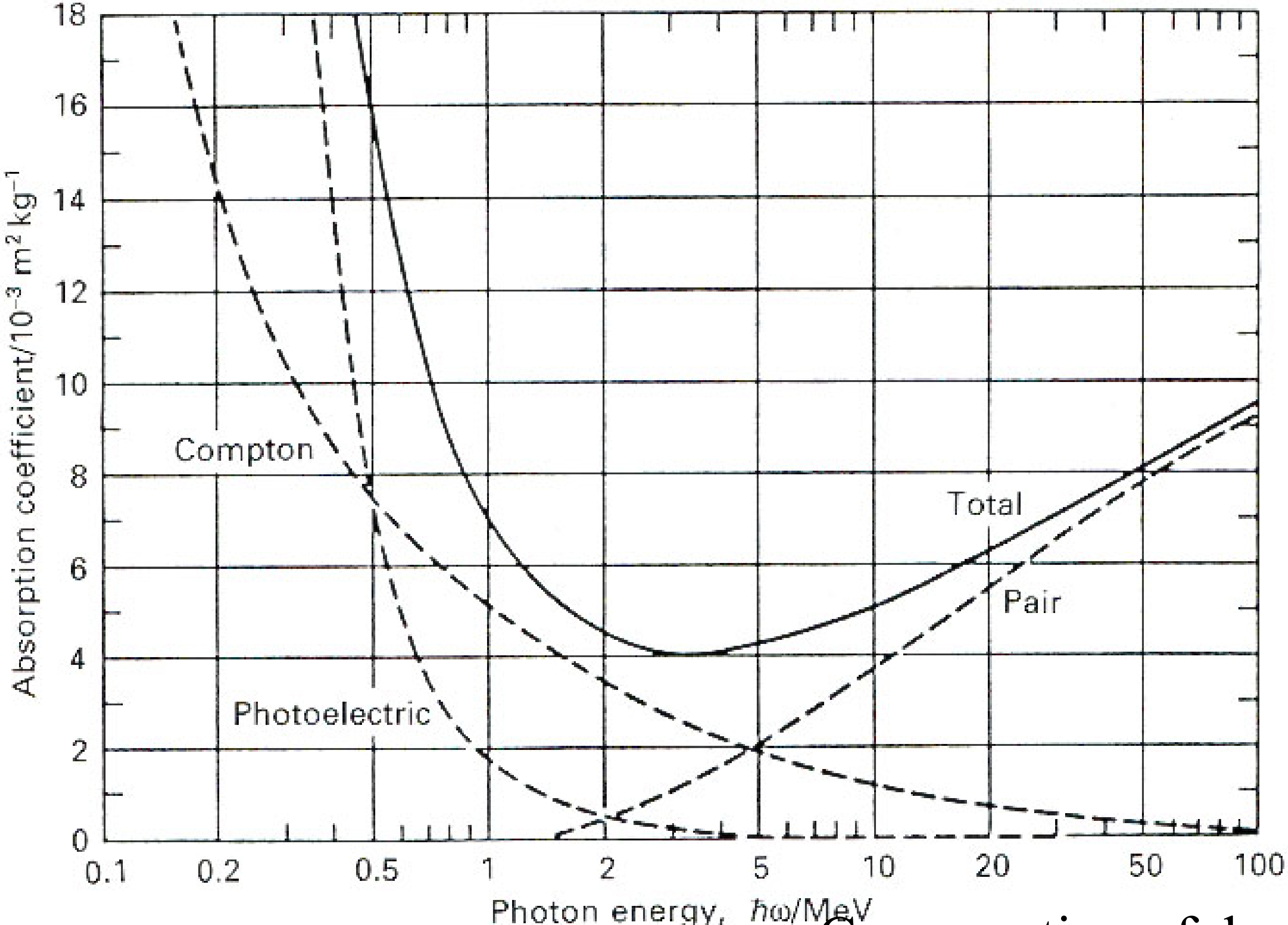

Cross section of lead

Roland Diehl

Interaction of HE photons with matter

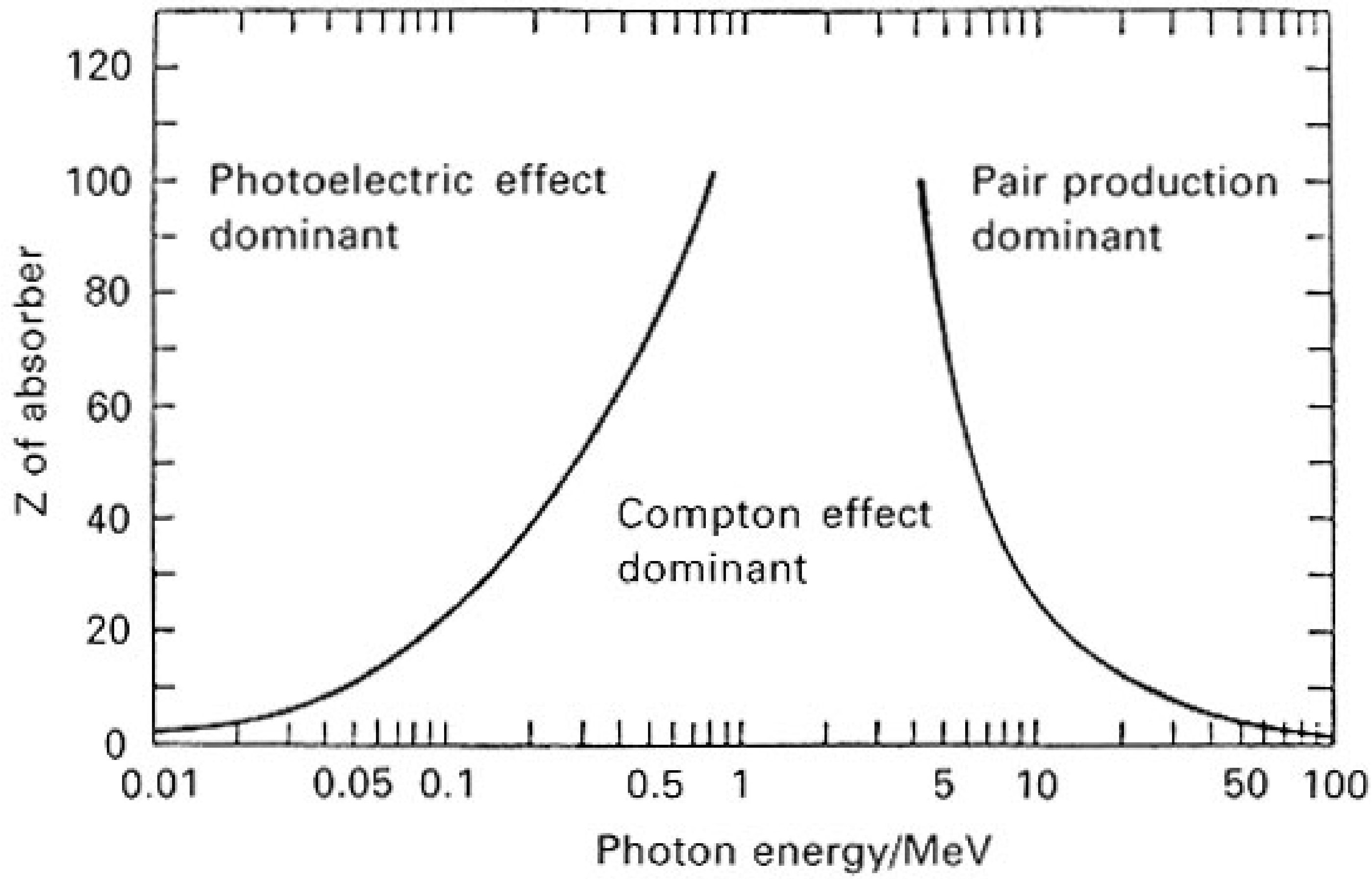

Roland Diehl

Experimental Regimes for the Detection of Gamma Radiation

Interaction Cross Section

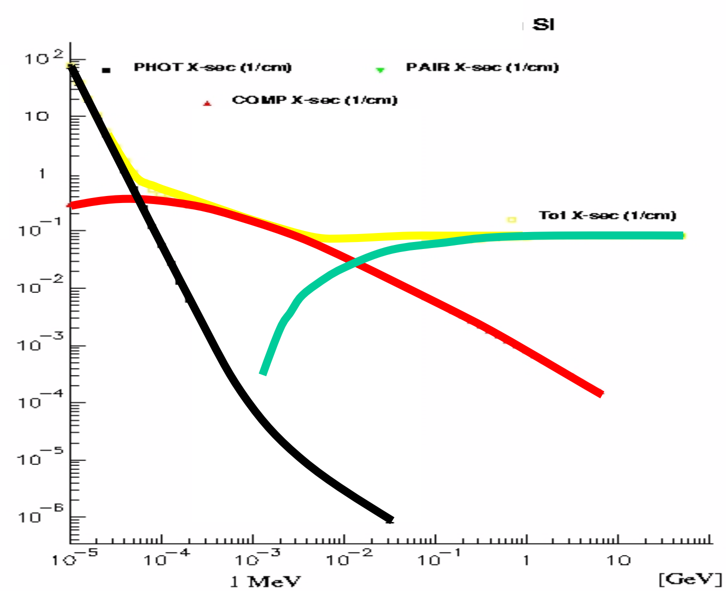

Energy

Photoeffect(< 100 keV)

Photons effectively blocked and stopped

Telescopes:

Collimators
Coded Mask Systems

Compton Scattering (0.2-10 MeV)

Photon Crossection Minimum
Scattered photons with long range

Telescope:

Compton Camera Coincidence System

Pair Creation (> 10 MeV)

Photons completely converted to e^+e^-

Telescope:

Tracking chambers to visualize the pairs

courtesy G. Kanbach

Roland Diehl

Gamma-Ray Telescope Principles

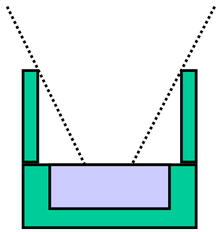

- **Simple Detector (& Collimator)**
  (e.g. HEAO-C, SMM, CGRO-OSSE)
  Spatial Resolution (=Aperture) Defined Through Shield

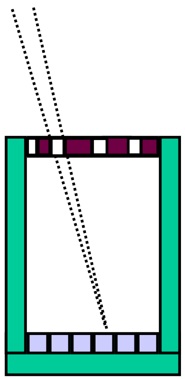

- **Coded Mask & Detector Array**
  (e.g. SIGMA, INTEGRAL)
  Spatial Resolution Defined by Mask & Detector Elements Sizes

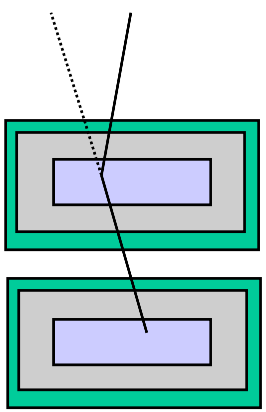

- **Compton Telescopes**
  (Coincidence-Setup of Position-Sensitive Detectors)
  (e.g. CGO-COMPTEL, Athena,...)
  Spatial Resolution Defined by Detectors' Spatial Resolution

Achievable Sensitivity: ~10^{-5} ph cm^{-2} s^{-1}, Angular Resolution ≥ deg

Roland Diehl

Successful Telescopes for Gamma-Rays

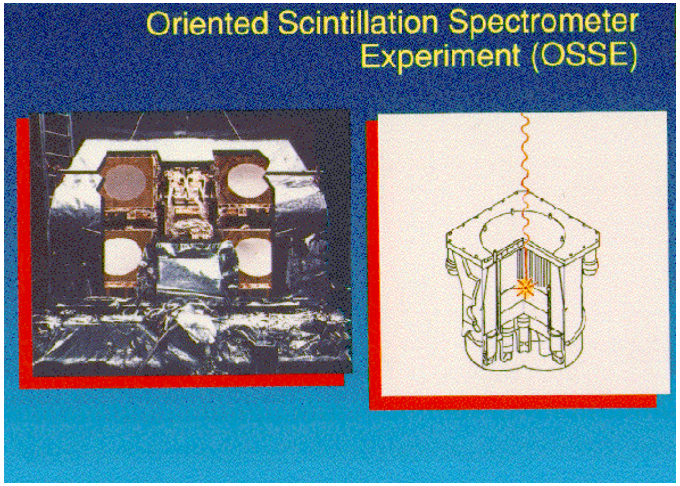

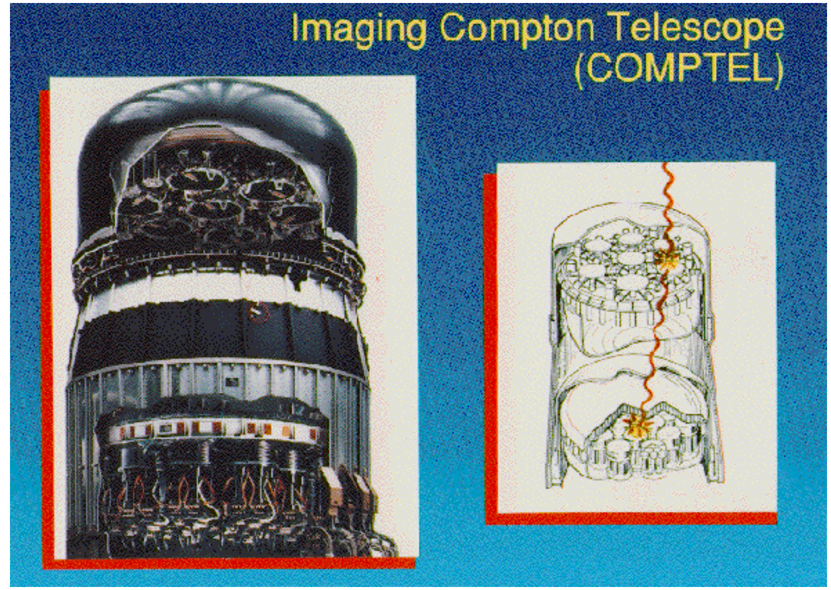

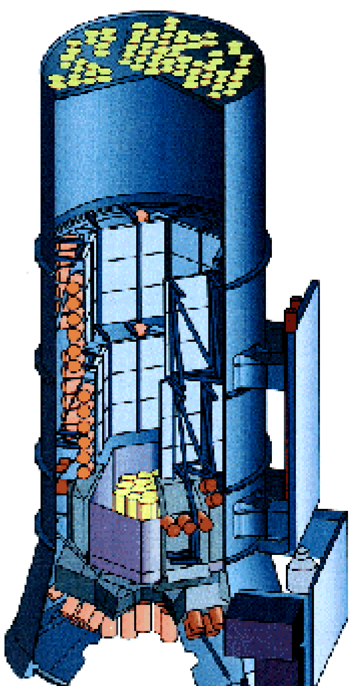

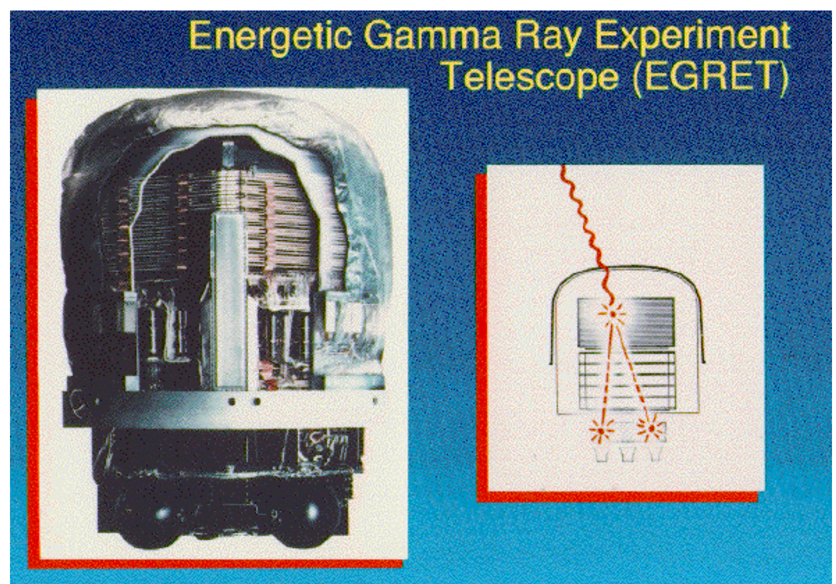

Roland Diehl

Simple HE "Telescope": Collimating Incident Radiation

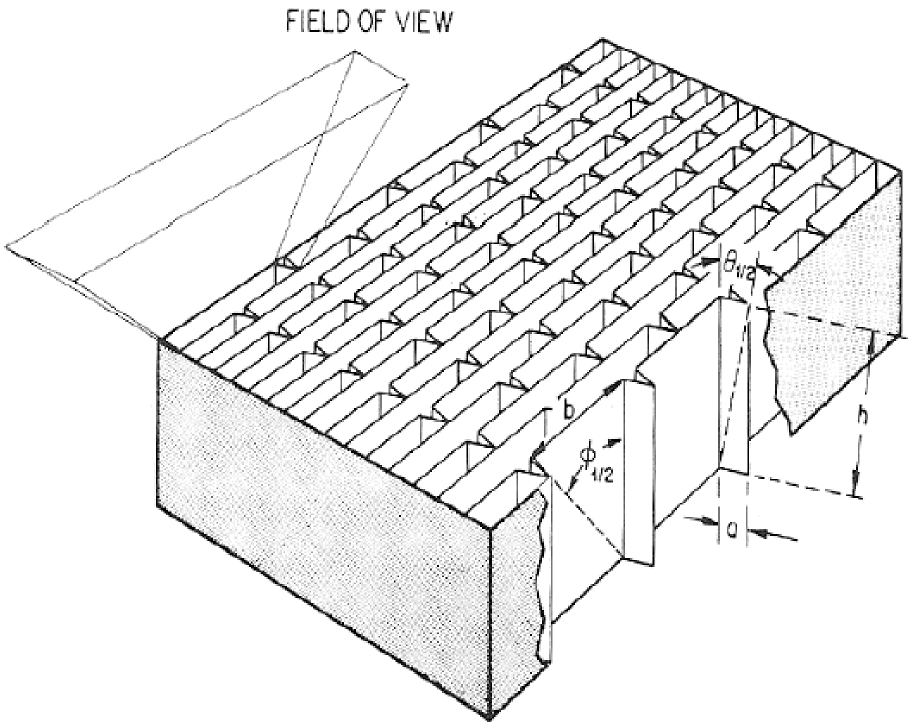

Fig. 2.16. A slat collimator, comprised of rectangular tubes of height h and cross section $a \times b$. X-rays which strike the tubes cannot reach the detector. The response pattern within the field of view has a triangular shape in each of the two orthogonal directions. The half-transmission angles are determined simply by the geometry: $\tan\theta_{1/2} = a/h$; $\tan\phi_{1/2} = b/h$.

- very high-Z material
- walls extremely thin
  ➡ max. aperture
- but thick enough to stop X-rays of the highest energies
- usage for very long time possible
- cheap

Collimated Gamma-Rays: OSSE on CGRO

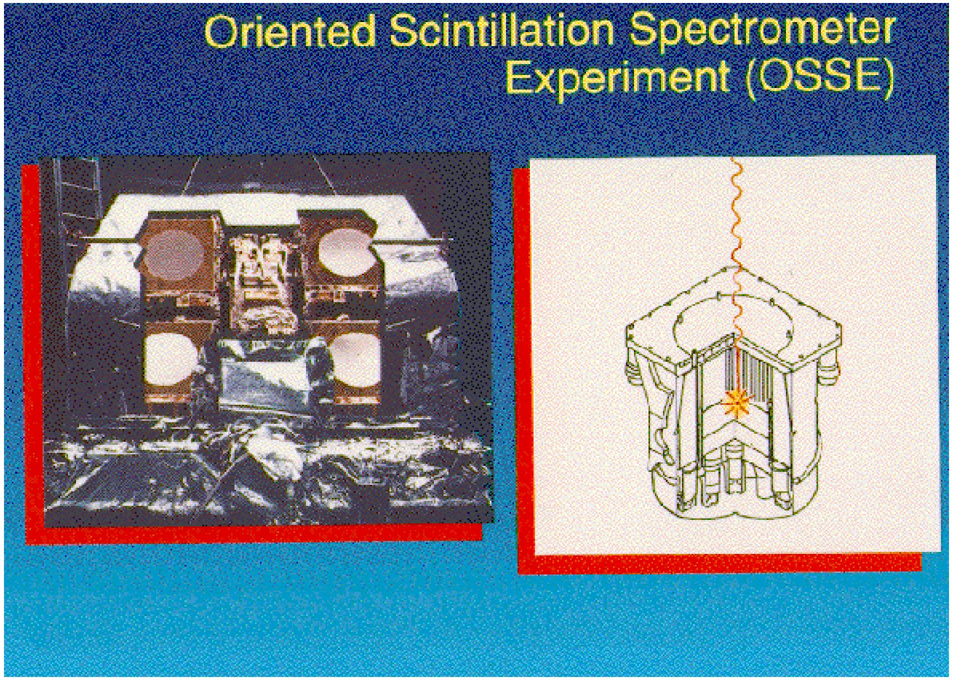

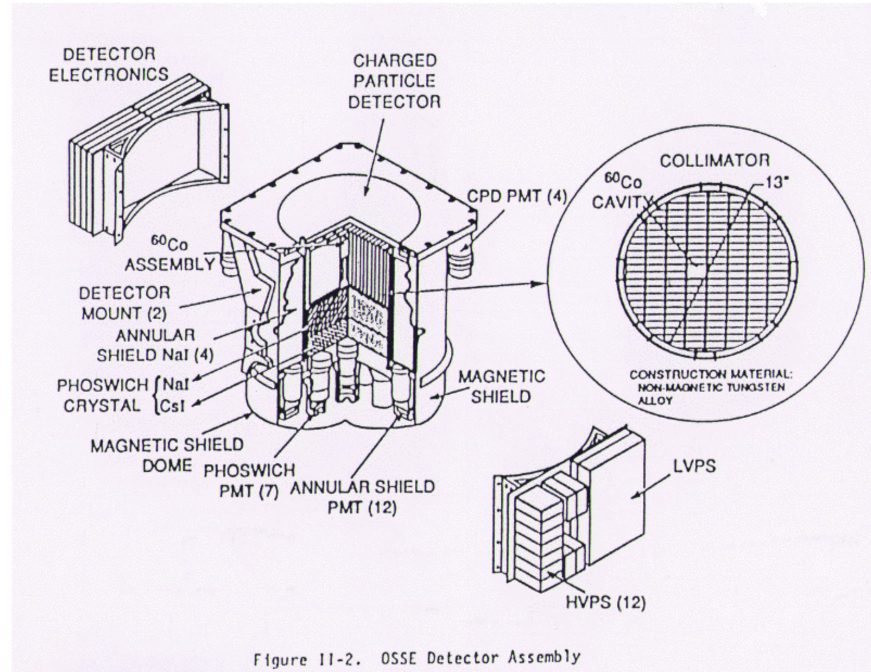

Figure 11-2. OSSE Detector Assembly

☆ **Tungsten Collimators**

- ☞ Field of View 3.8° x 11.4°
- ☞ Scanning Observations, Deconvolution Imaging Analysis

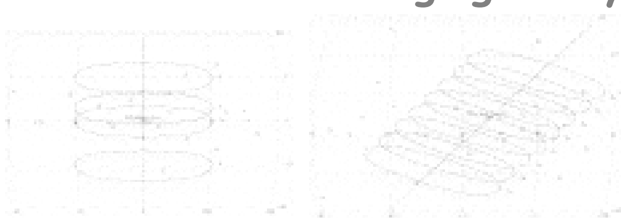

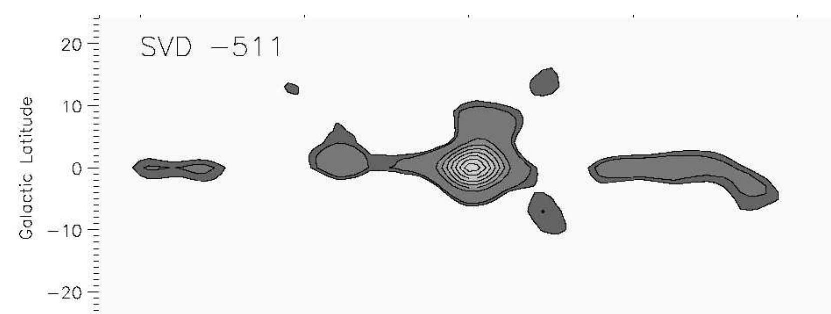

Roland Diehl

Other "simple" Telescopes: GRIS

- High Spectral Resolution through Ge Detectors
- Aperture Defined Through NaI Shield Detectors
- Successful Balloon Flights 1987,... 1995

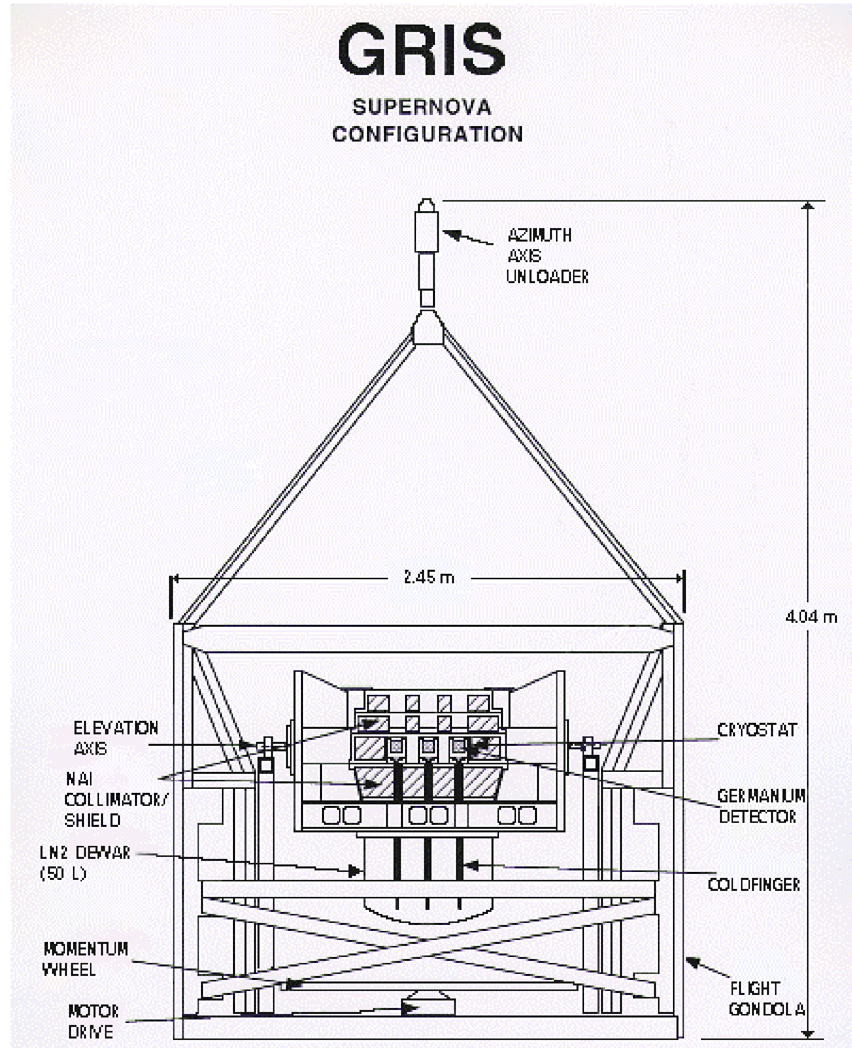

Roland Diehl

Rotation Modulation Collimator

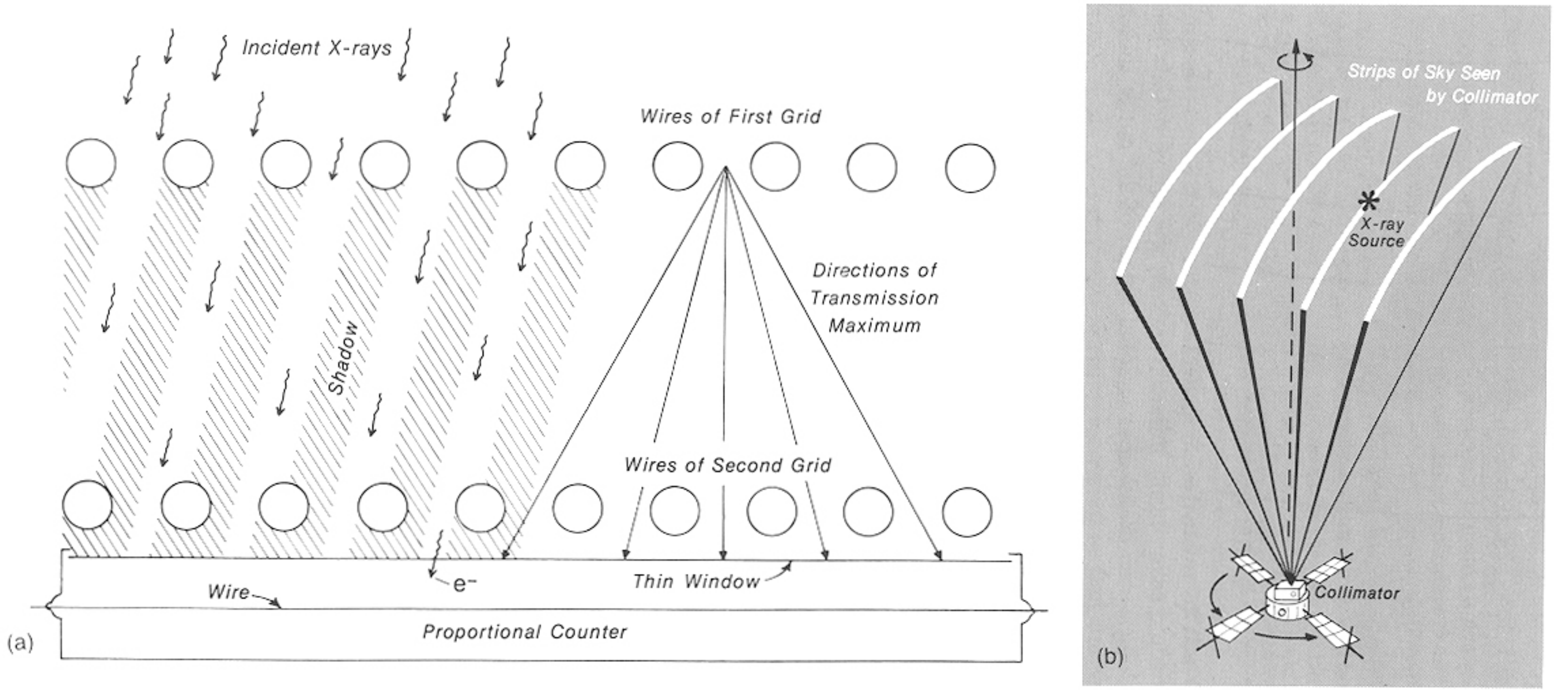

Fig. 2.3 Principle of operation of the modulation collimator, first used in rocket flights in the mid-1960s. Two separated wire grids (a) define a set of bands on the sky through which X-rays can be seen. By rotating the whole spacecraft a point source in this region will cross these bands (b) producing a modulated *count rate as a function of time, as shown in the lower figure (c). This response pattern depends on where the source is within the overall field of view of the collimator, usually 15° or 20° across overall, and hence the location of the source can be determined to typically 1 arcminute. If the source is close to the centre of the rotation then the modulation is very slow compared to if the source were near the edge of the field of view, far from the centre of rotation. It is also possible to model such a detector's response to several X-ray sources in the field of view, thereby simultaneously determining the positions of all the sources. (Based on original diagrams by Hale Bradt and Herb Schnopper.)*

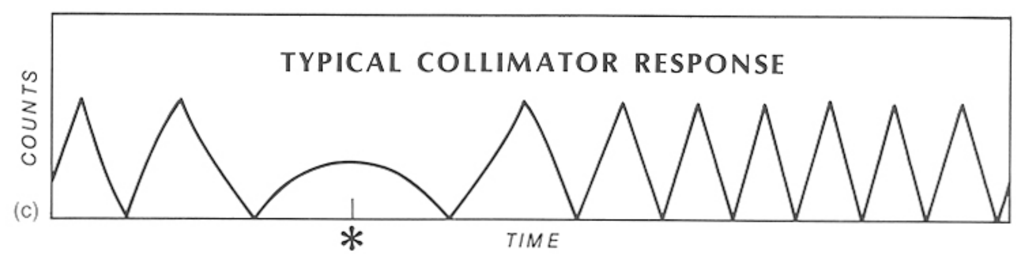

"Imaging" using Earth Occultation

- **Data Selection**
  - ☆ "Source" = Region of Interest Exposed
  - ☆ "Background" = Region of Interest Behind Earth

- **Applications**
  - ☆ BATSE on CGRO
    - ☞ Monitoring of Point Sources; *Harmon et al. 1991; ...*
  - ☆ RHESSI
    - ☞ Imaging Diffuse Galactic Emission; *Smith 2003*

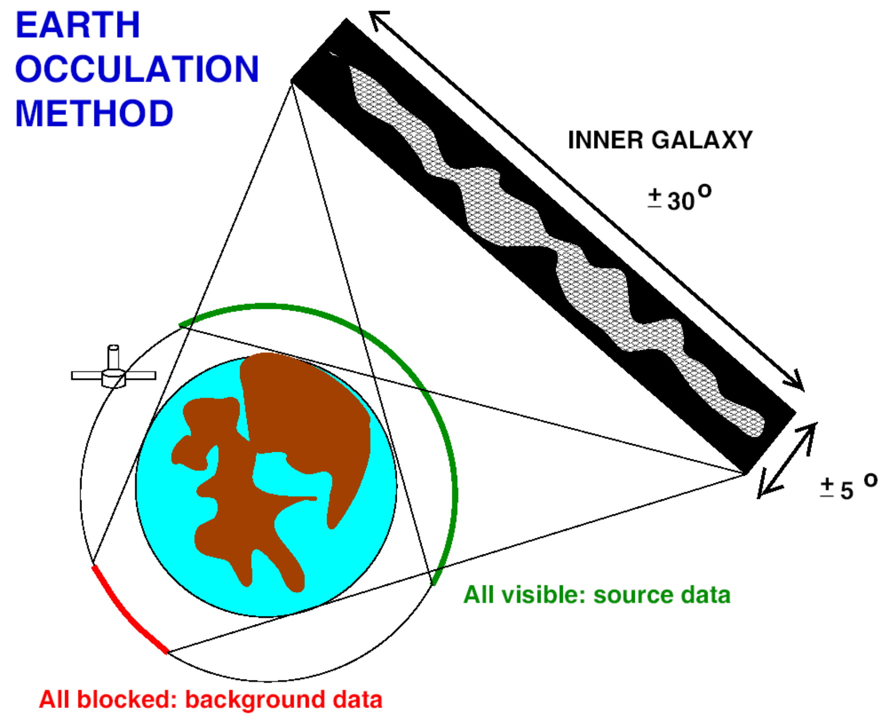

BATSE NGC 4151
(Parsons et al. '98)

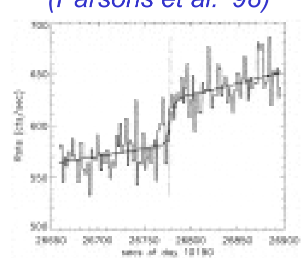

RHESSI SPECTRA: 9 MONTHS OF DATA (3/02-11/02)
(Smith '03)

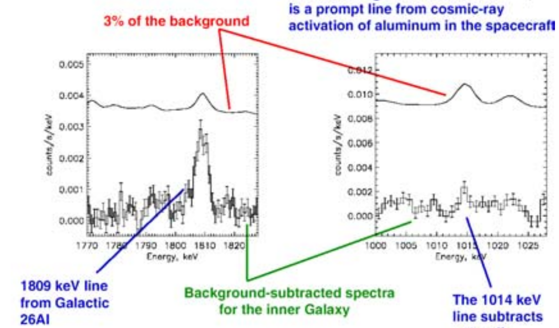

Lunar Occultation

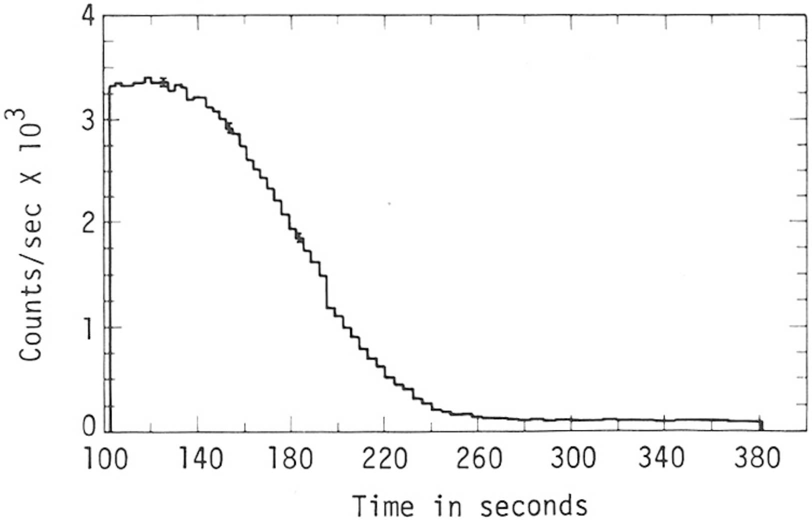

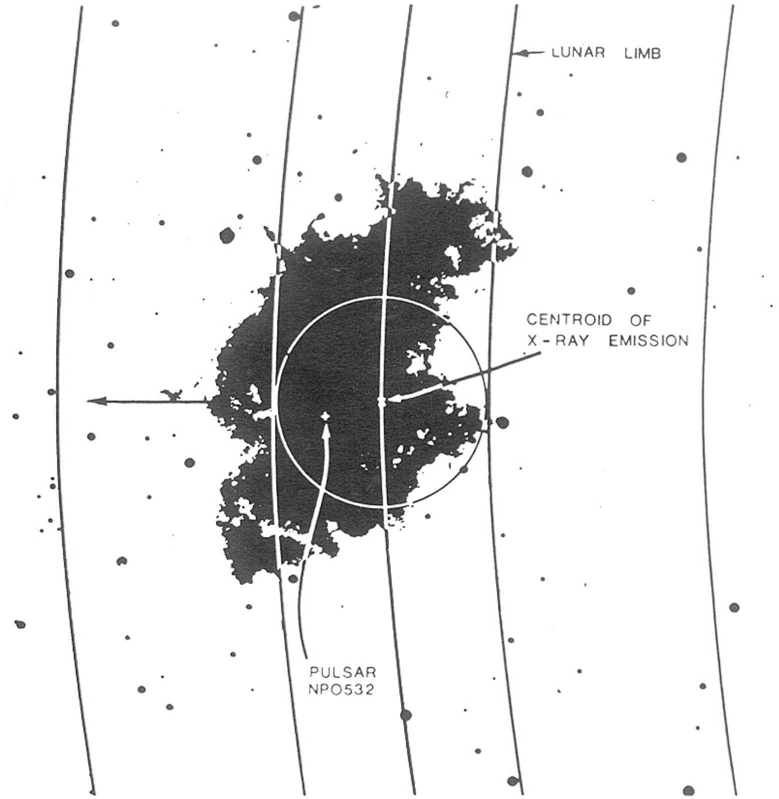

Roland Diehl

Coded Mask Imaging

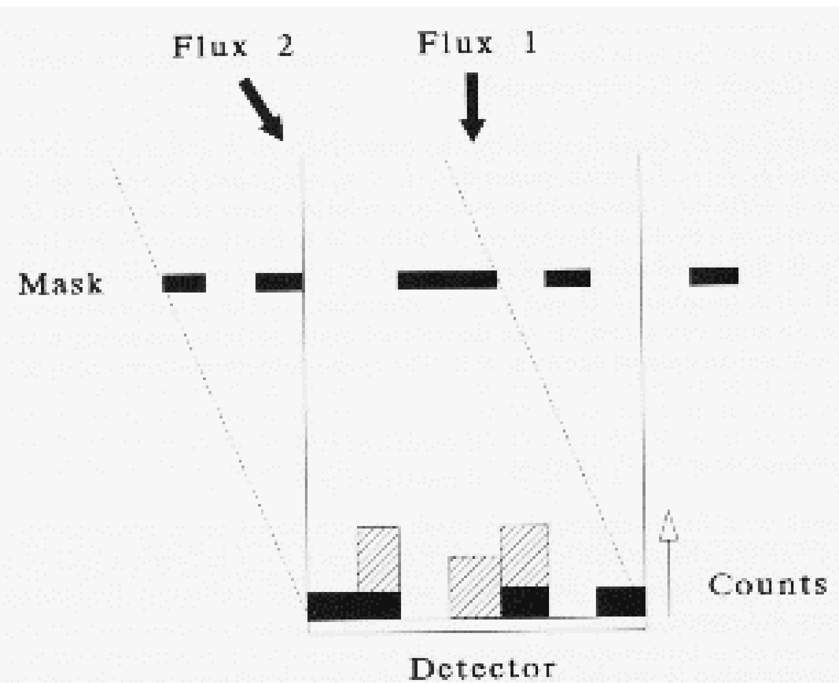

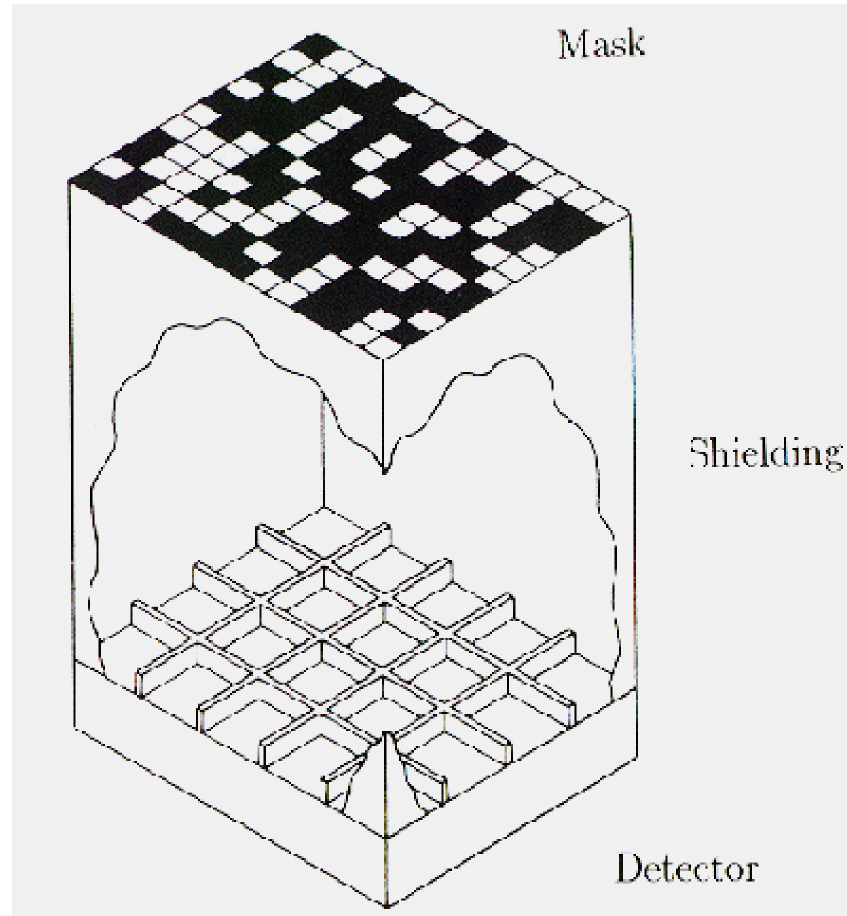

Casting a Source Shadow: Coded Mask Telescopes

ref. e.g.: Skinner

- ☆ A Semi-Transparent Mask Occults Part of the Position-Sensitive Gamma-Ray Detector Plane
- ☆ Recognition of the Mask Shadow in the Detectors' Signal -> "Imaging a Source"
  - Telescope = Mask & Detector Hardware + Imaging Software
- ☆ Masks
  - Uniformly Redundant Arrays
  - Adapted to Detector Spatial Resolution
  - Optimized for Larger Field of View
    - » Partially/Fully Coded FoV
- ☆ Imaging
  - Correlation
  - Fourier-Domain Filtering

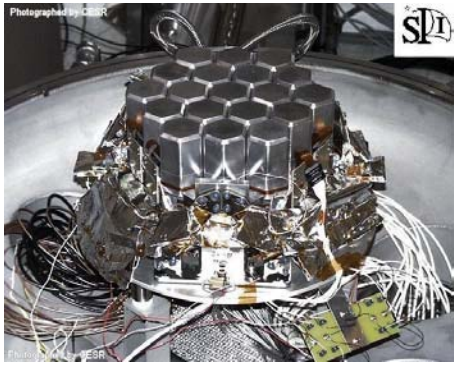

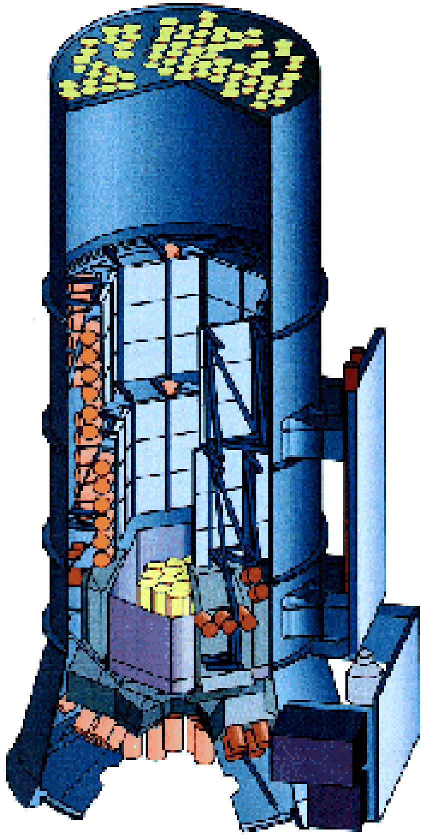

SPI on INTEGRAL

Roland Diehl

Integral

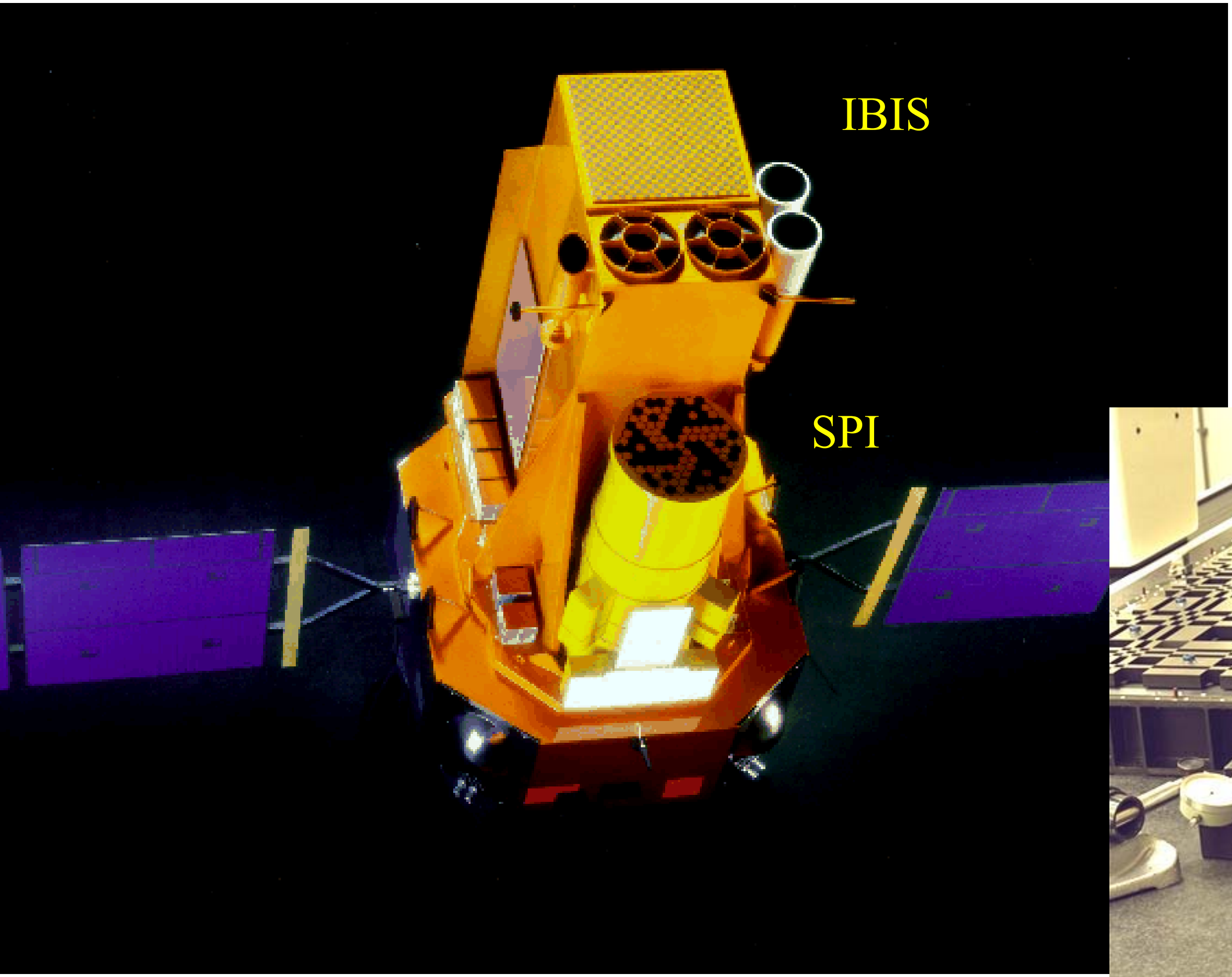

IBIS Coded Mask

BeppoSAX Coded Mask Camera (WFC)

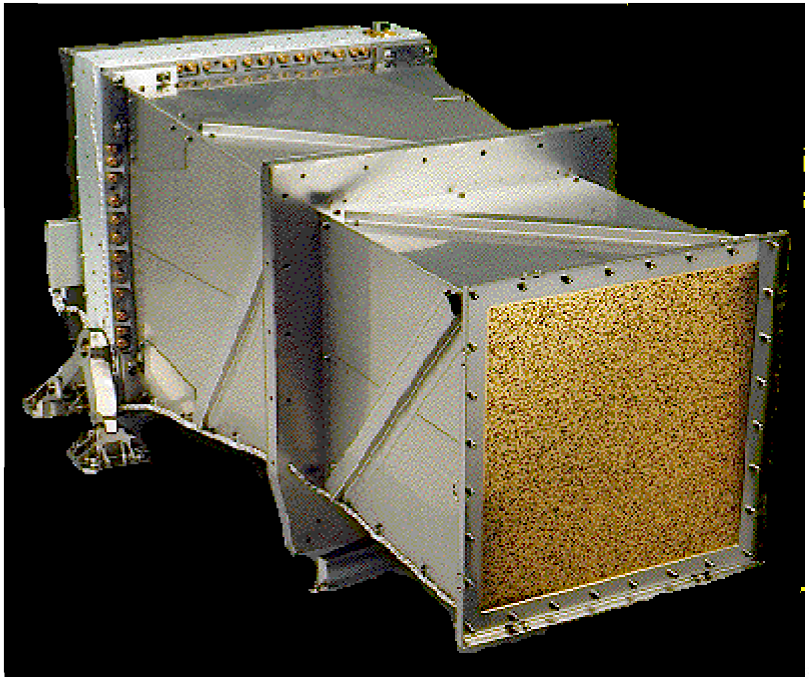

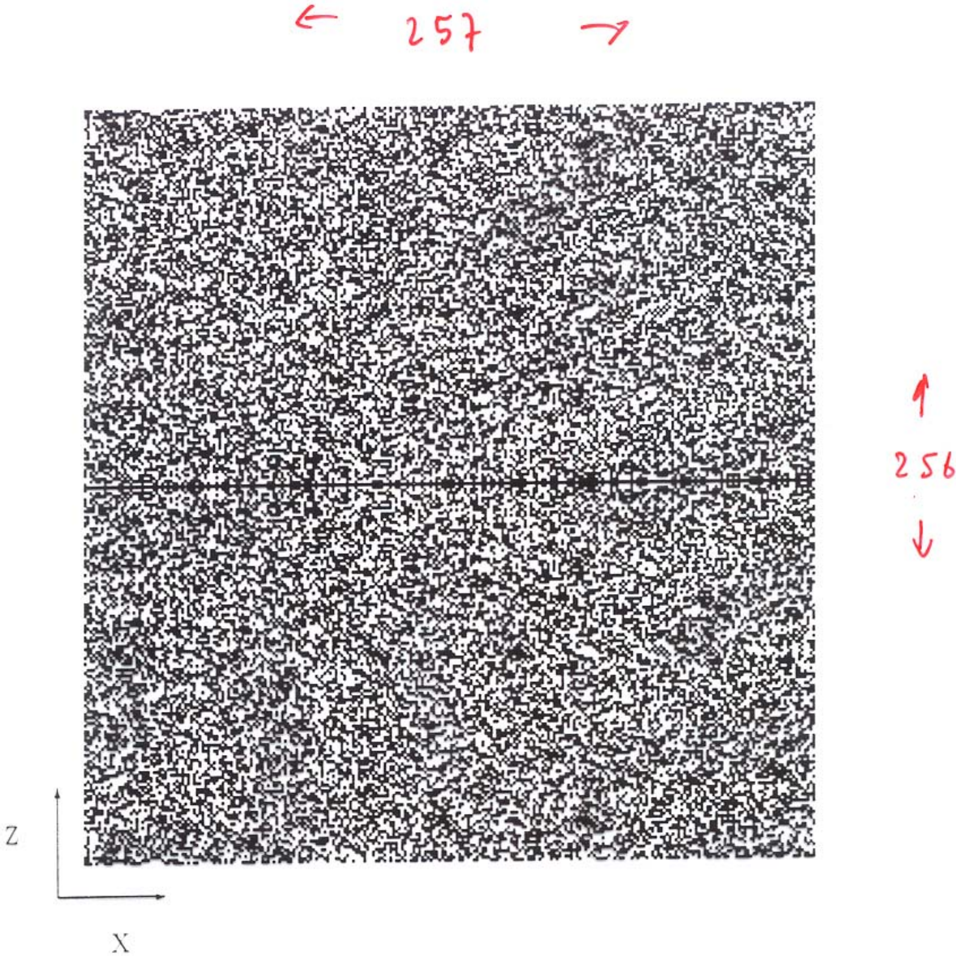

EXIST Mission Concept

Free-Flyer (500 km, i ~ 20°):

- Zenith pointing (Survey mode)
- 3-axis pointing (Observatory *and* survey)
- 3 coded aperture telescopes (60° x 75° each)
  ➞ 180° x 75° fan-beam: all sky per orbit

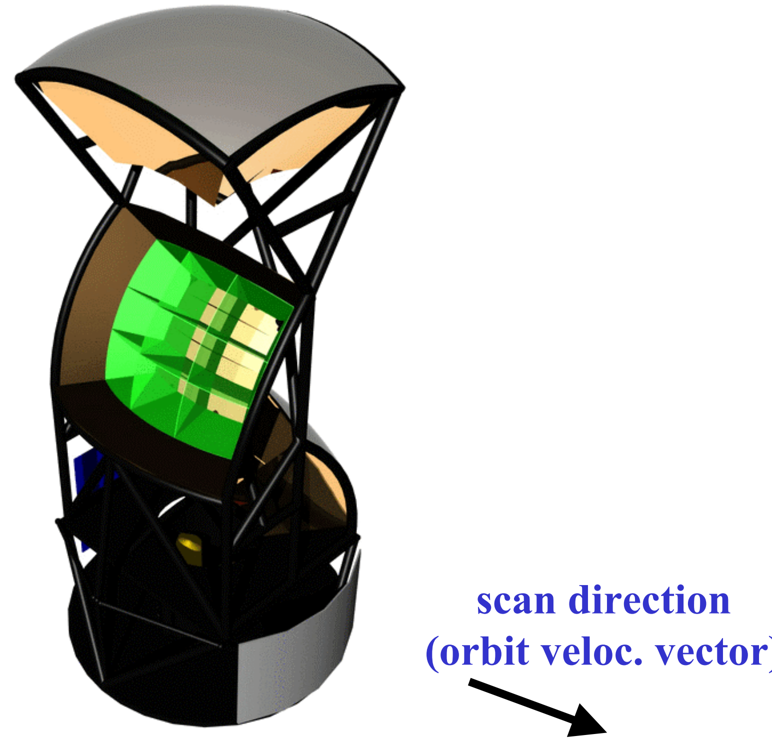

Mission Parameters:

- CZT tiled arrays: 8m² total area
- Passive and active shielding
- Mass, power, telemetry: 8500kg, 1200W, 1.2mbs (X-band)
- Delta-IV launch

Compton Telescope

COMPTEL

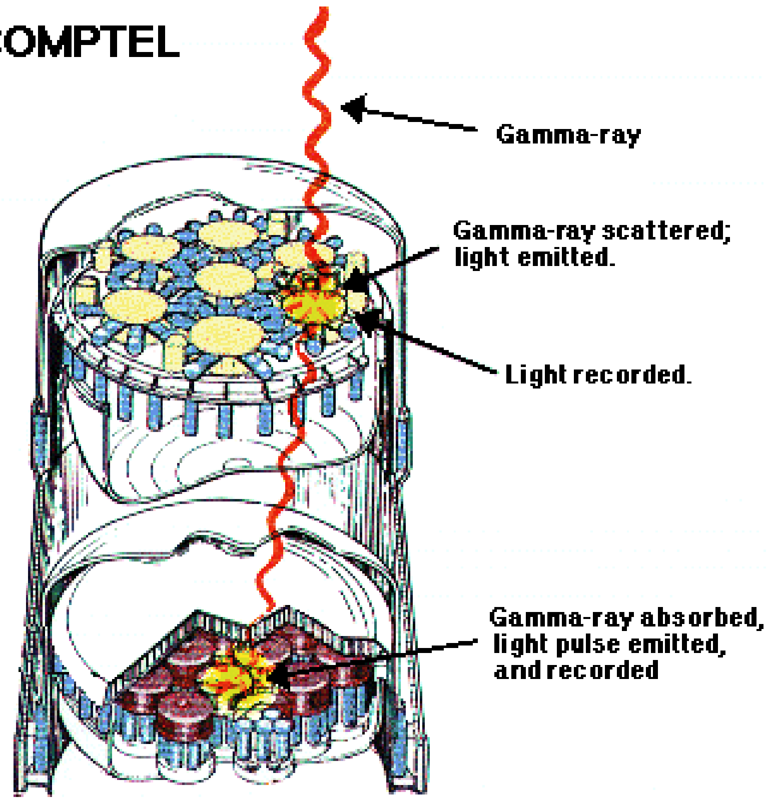

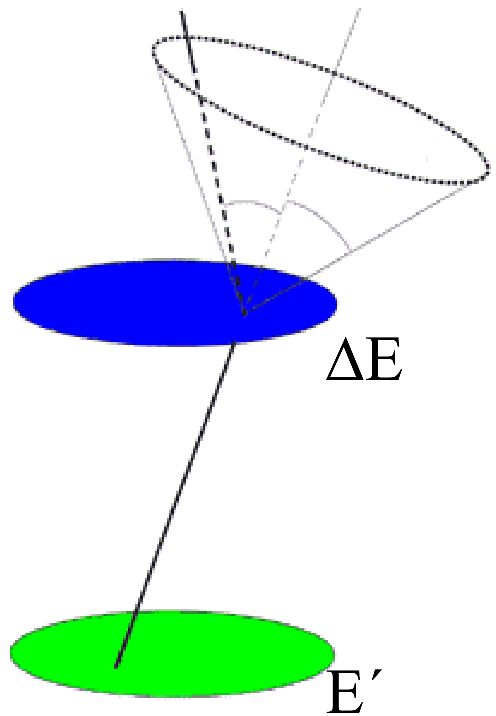

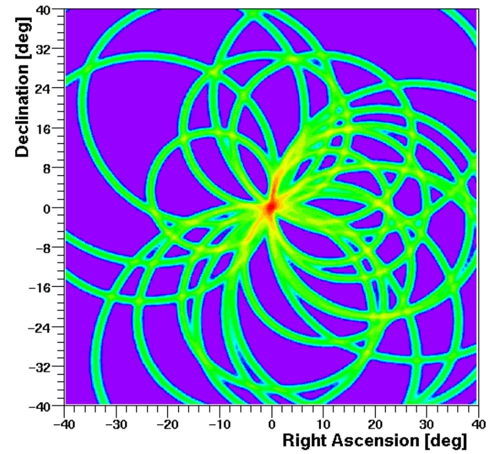

$$E' = \frac{E}{1 + \frac{E}{m_e c^2}(1 - \cos\theta)}$$

$$\varphi_{geometric} = \arccos\left\{1 + m_e c^2 \left(\frac{1}{E_\gamma} - \frac{1}{E_\gamma - \Delta E} \right)\right\}$$

Roland Diehl

Compton Telescope Balloon

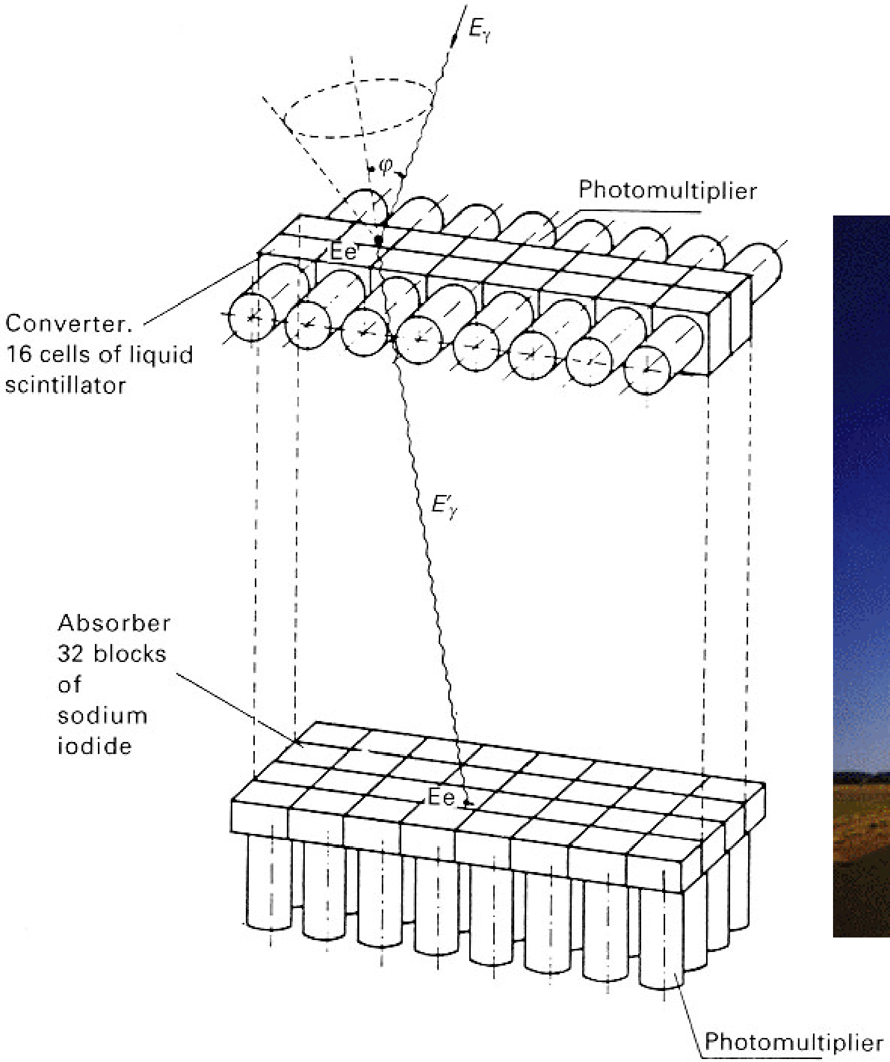

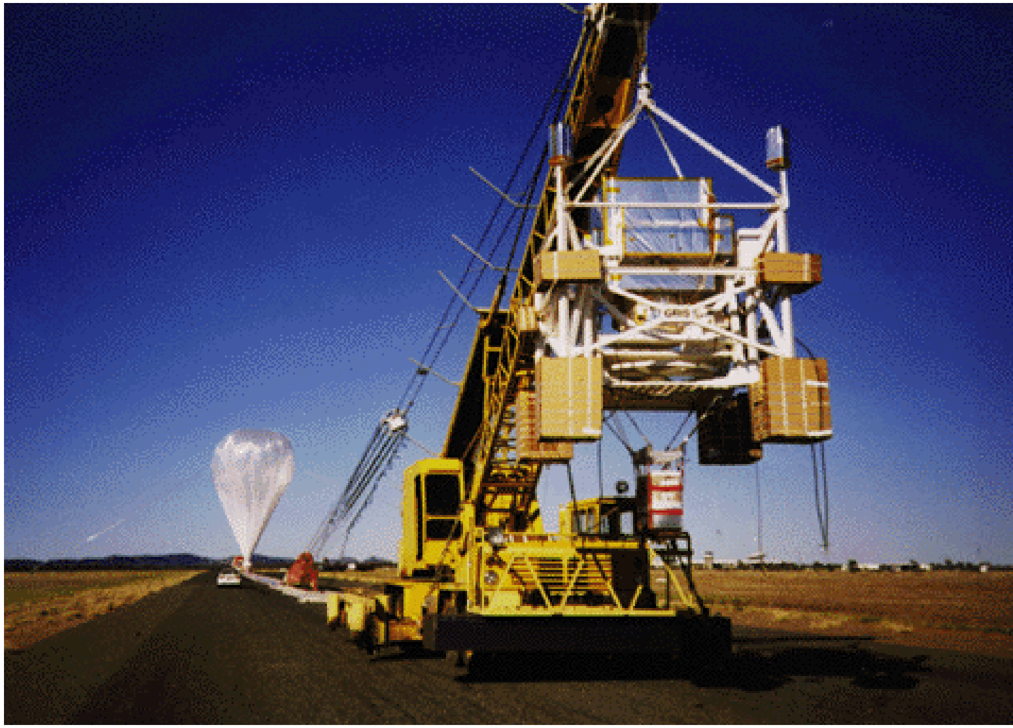

Roland Diehl

Pioneering Space Compton Telescope: COMPTEL on CGRO (1991-2000)

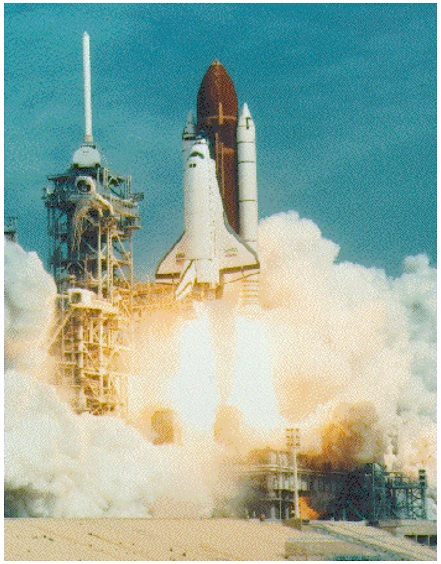
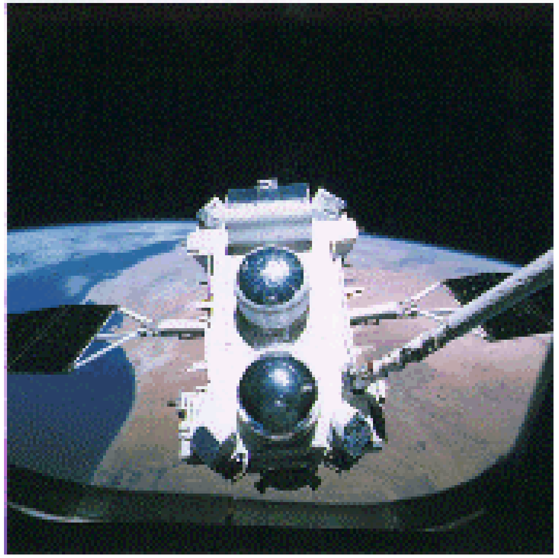
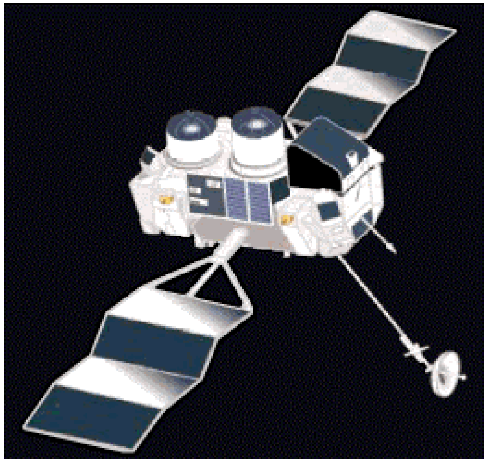
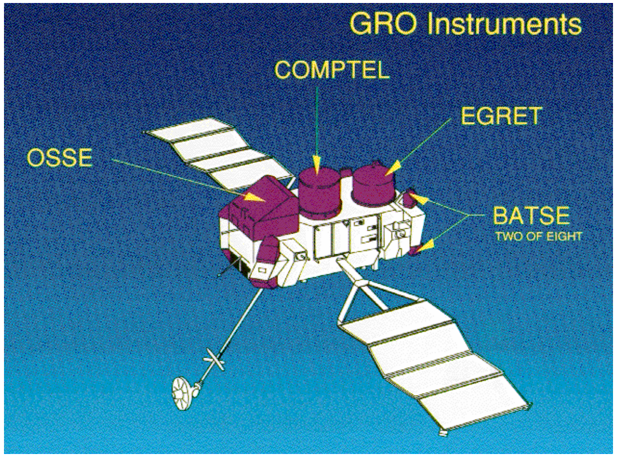

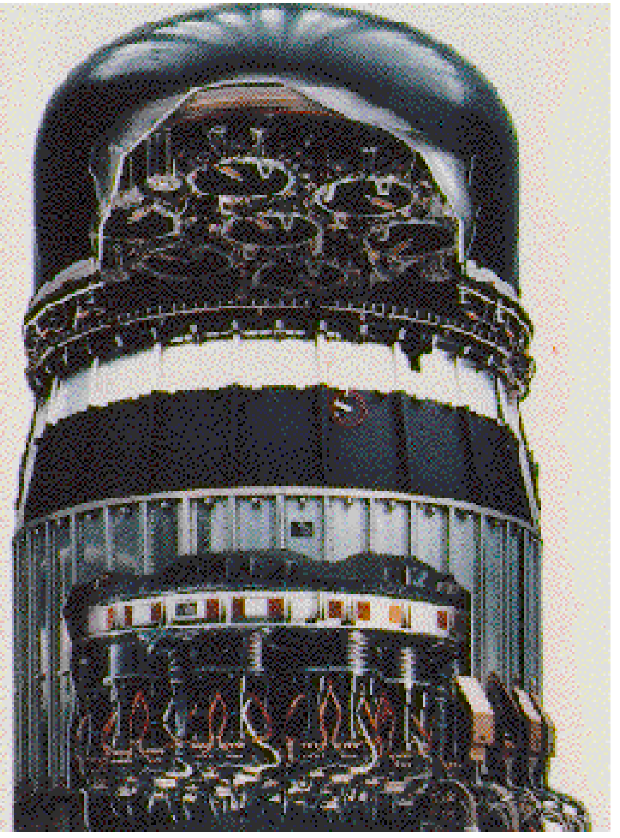

Pioneering Space Compton Telescope: COMPTEL on CGRO

Interaction sequence obtained by time-of-flight (TOF) measurement.

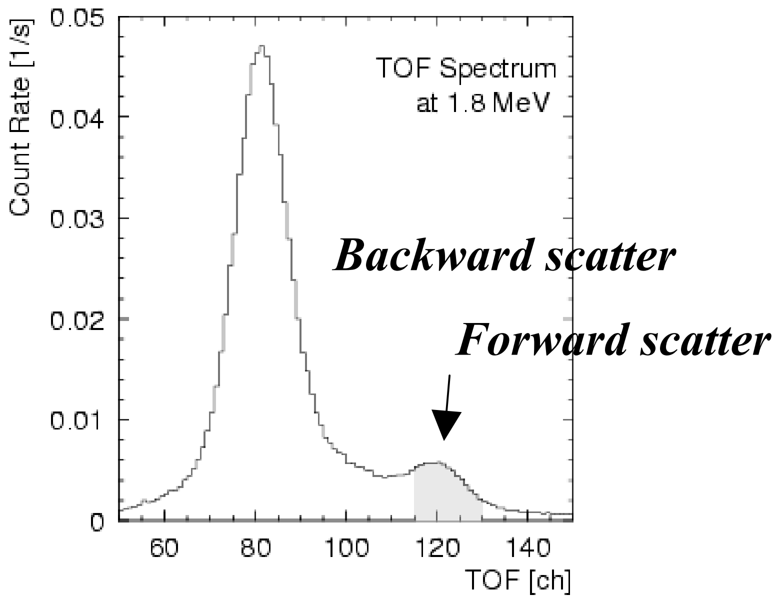

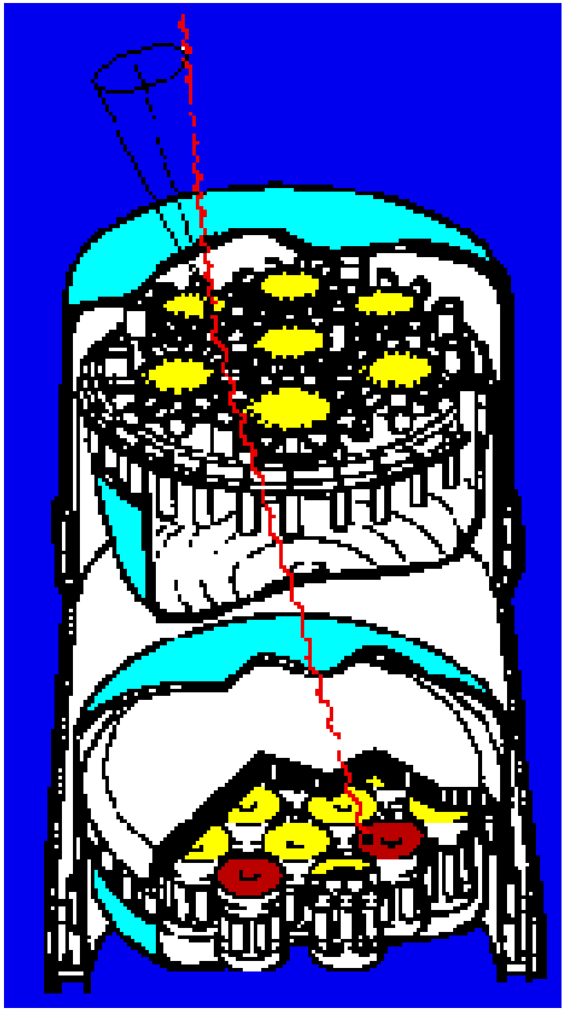

Advantage: clear separation of forward and backward events.
Disadvantage: low efficiency due to solid angle effect.

Roland Diehl

Compton Telescopes

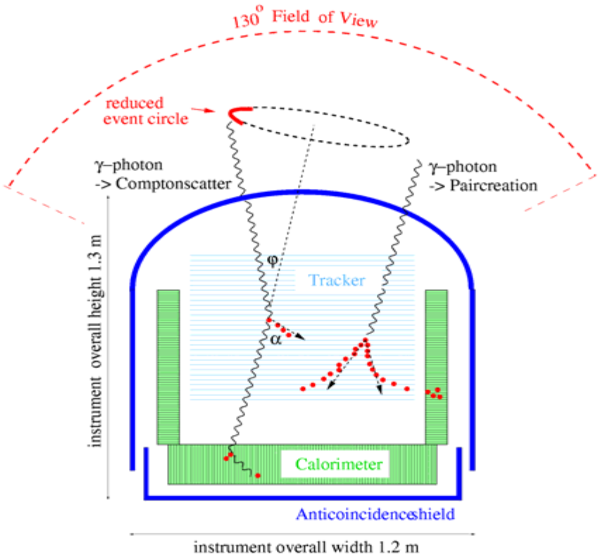

MEGA

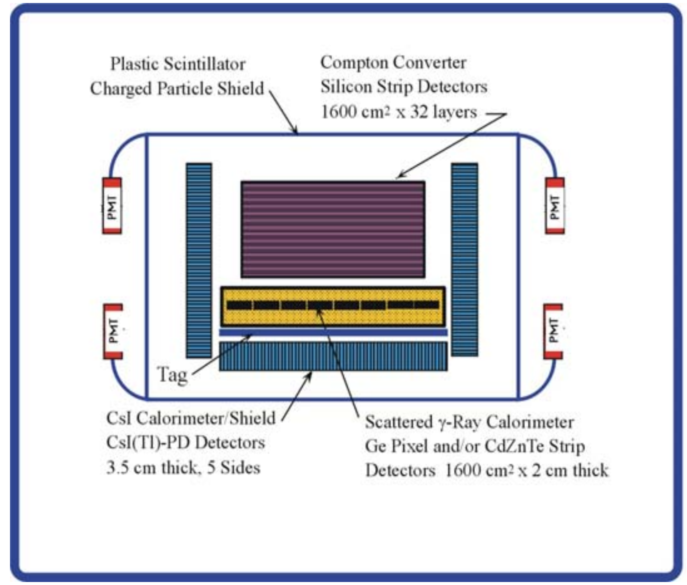

TIGRE

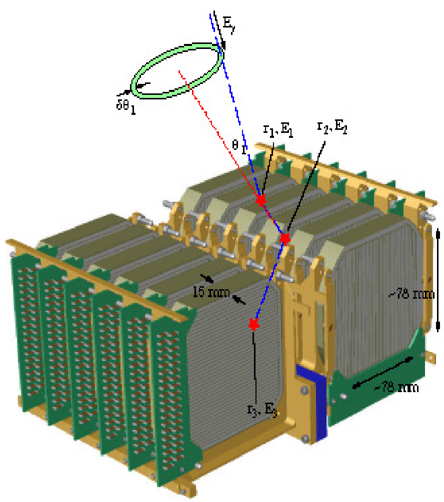

Nuclear Compton Telescope (NCT)

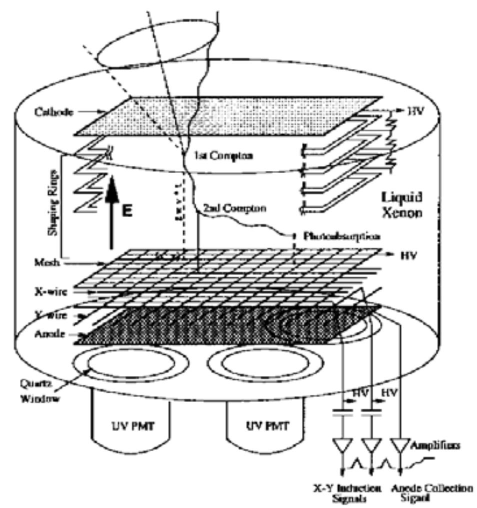

FIGURE 1. Schematic of the liquid xenon time projection chamber

LXeGRIT

Roland Diehl

Compton Imaging: Limits & Improvements

Compton Imaging Measurement of:

- Gamma-ray energy E_g
- Energy transfer to electron E_e
- Direction and orientation of scattered γ-ray

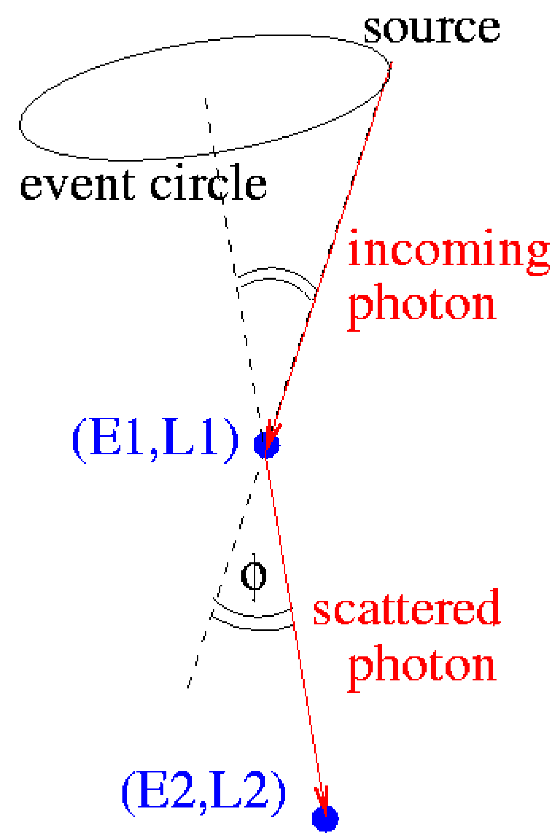

Issues:

- Direction/Momentum of e^-
- Compton-scattered e^- not at Rest
- Multiple Interactions
- Background Events

Angular Resolution Limits due to Doppler Broadening

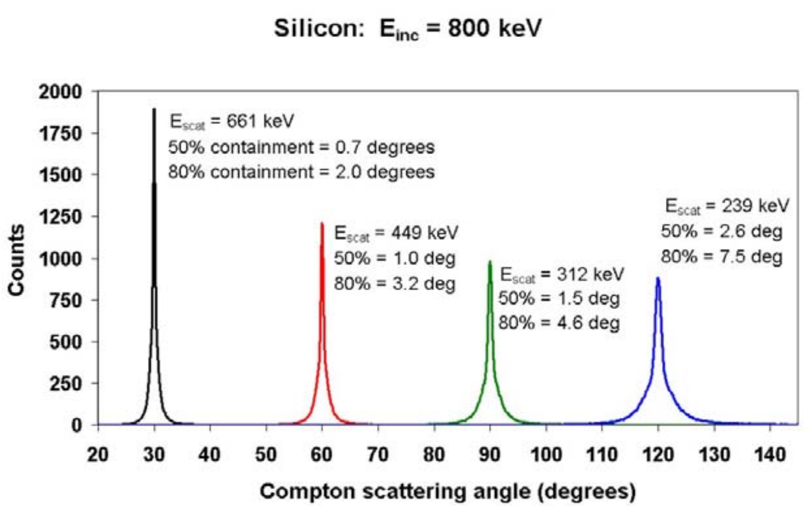

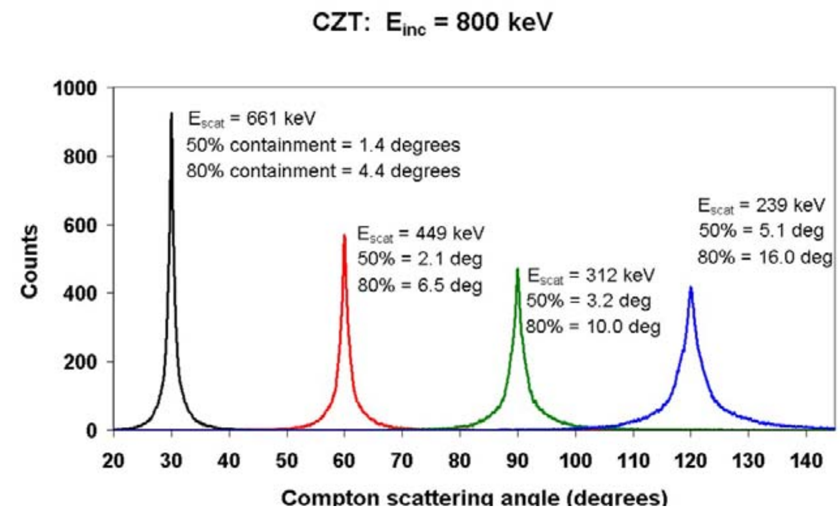

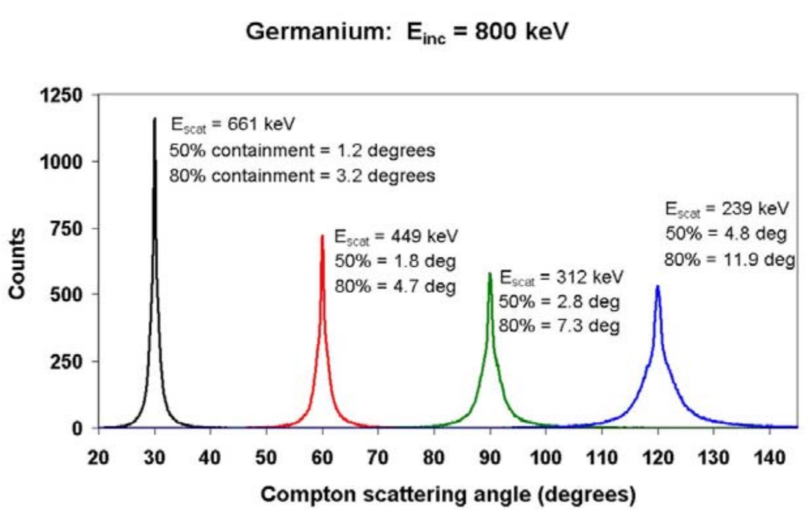

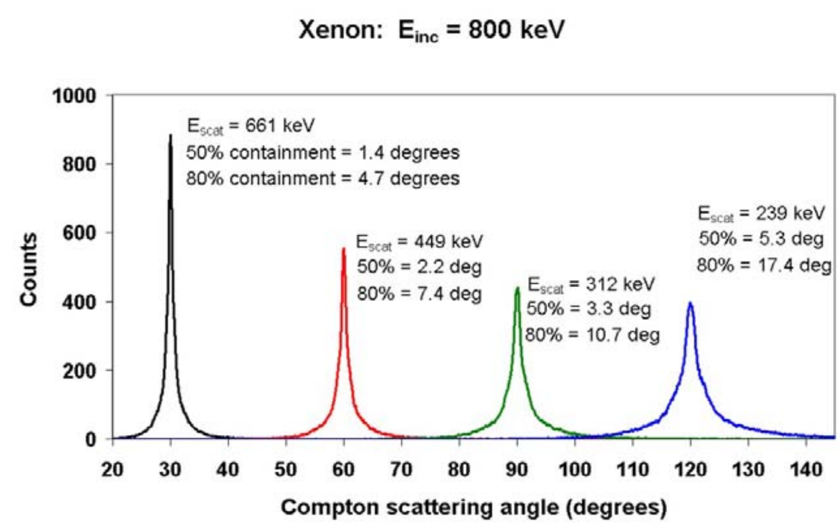

courtesy J. Kurfess

Two-Site Events: The Problem of Time Sequence

Options for Discrimination:

- Time-of-flight
- Electron tracking
- Probabilities of sequences:
  - without assumption of source location: energy sharing.
  - with (some) assumption of source location, e.g., for a gamma-ray originating from the sky (above horizon):
    - locations of interactions
    - orientation

- Allow both sequences in imaging, assign corresponding probabilities in response function.

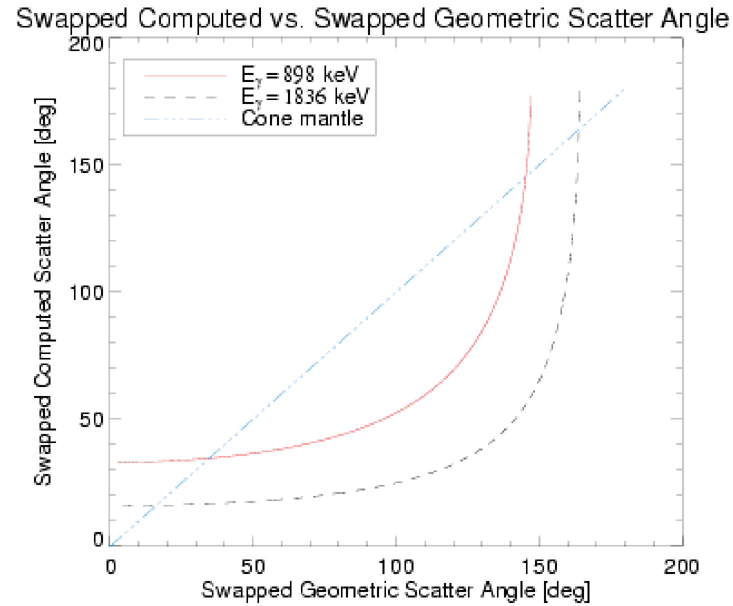

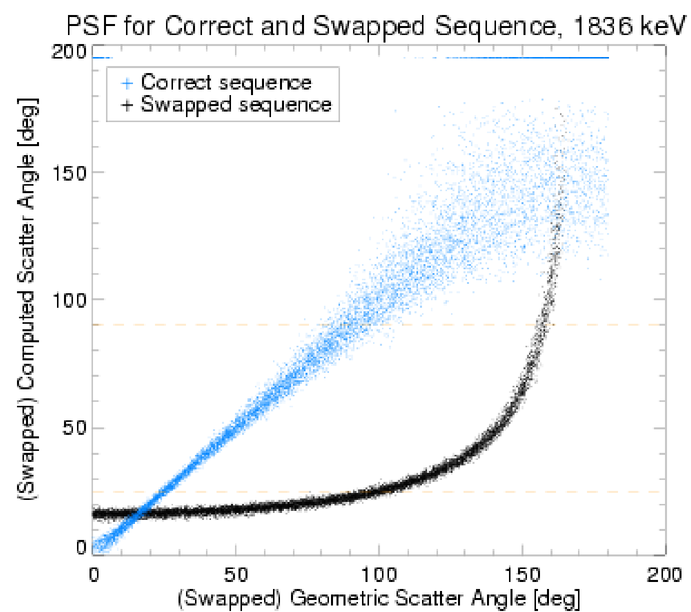

courtesy U. Oberlack

The Problem of the Time Sequence for Multiple-Site (>2) Events

Number of possible scatter directions and orientations grows with n!

Allowing any sequence is therefore *not* an option.

Options (other than TOF or tracking):

- Probabilities of sequences based on Compton kinematics, using redundant information on the interior angles.
- Probabilities of sequences based on additional criteria:
  - separations
  - energy deposit in "last" scatter
  - location of "first" scatter, ...

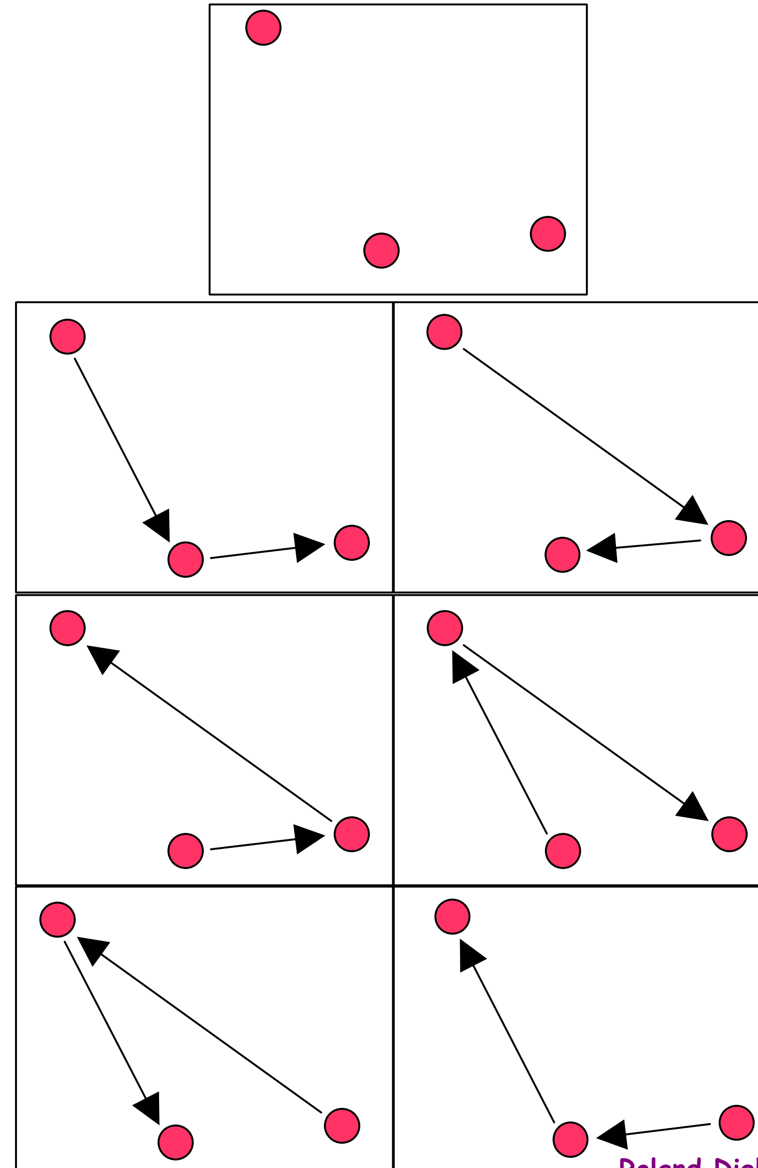

courtesy U. Oberlack

3-Compton Multiple Scatter Technique

$$\cos\varphi_1 = 1 - m_e c^2\left(\frac{1}{E_2} - \frac{1}{E_1}\right) \qquad L_1 = E_1 - E_2$$

$$\cos\varphi_2 = 1 - m_e c^2\left(\frac{1}{E_3} - \frac{1}{E_2}\right) \qquad L_2 = E_2 - E_3$$

$$\cos\varphi_3 = 1 - m_e c^2\left(\frac{1}{E_4} - \frac{1}{E_3}\right) \qquad L_3 = E_3 - E_4$$

$$E_1 = L_1 + \frac{L_2 + \left[L_2^2 + \frac{4 m_e c^2 L_2}{1 - \cos\varphi_2}\right]^{\frac{1}{2}}}{2}$$

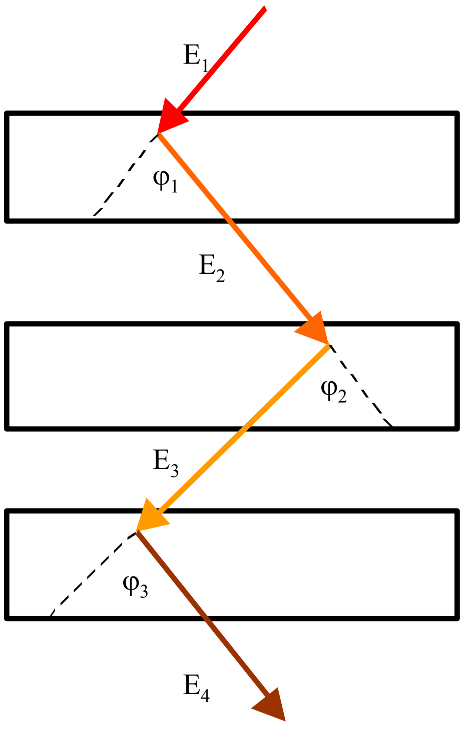

Incident gamma ray energy determined with partial energy loss

- Unknown source: 3 interactions required to determine energy, ***E_1***
- Known source: 2 interactions required to determine energy, ***E_1***
- Dramatic improvement in efficiency
- New alternative: Compton telescope using thick silicon detectors
- Kurfess et al., Proc. 5th Compton Symp. AIP **510**, 789 (2000)

courtesy J. Kurfess

Errors in E_1 *and* ϕ_1

$$dE_1 = \left[dL_1^2 + \left(\frac{1}{2} + \frac{1}{4}\left[L_2^2 + \frac{4mc^2 L_2}{(1-\cos\varphi_2)} \right]^{-\frac{1}{2}} \left[2L_2 + \frac{4mc^2}{(1-\cos\varphi_2)} \right] \right)^2 dL_2^2 + \left(\frac{\sin\varphi_2}{4} \left[L_2^2 + \frac{4mc^2 L_2}{(1-\cos\varphi_2)} \right]^{-\frac{1}{2}} \left[\frac{4mc^2 L_2}{(1-\cos\varphi_2)^2} \right] \right)^2 d\phi_2^2 \right]^{\frac{1}{2}}$$

$$d\varphi_1 = \frac{mc^2}{\sin\varphi_1} \left[\left(\frac{1}{(E_1 - L_1)^2} - \frac{1}{E_1^2} \right)^2 dE_1^2 + \frac{dL_1^2}{(E_1 - L_1)^4} \right]^{\frac{1}{2}}$$

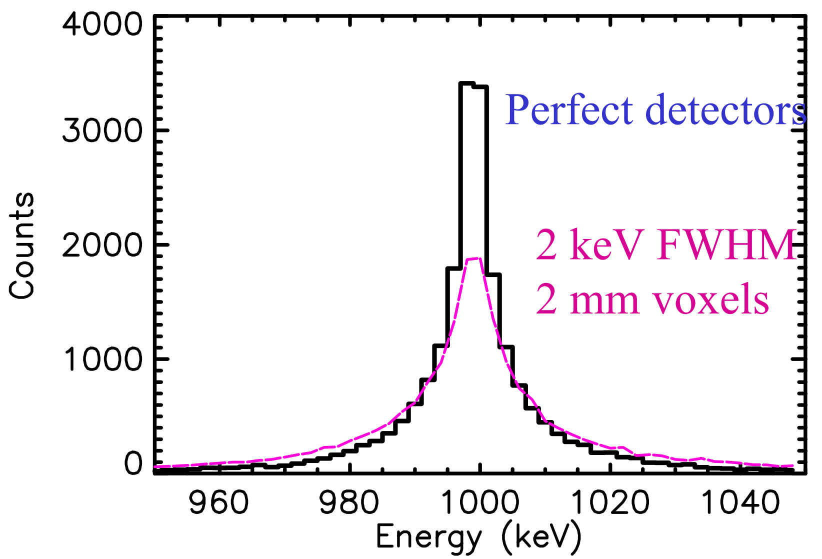

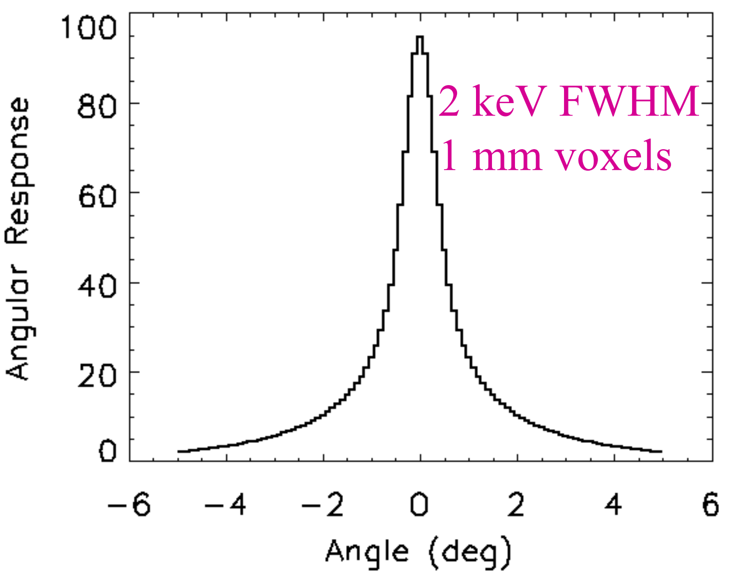

Typical energy and angular response at 1 MeV for 3-gamma instrument

courtesy J. Kurfess

3-Compton Efficiency

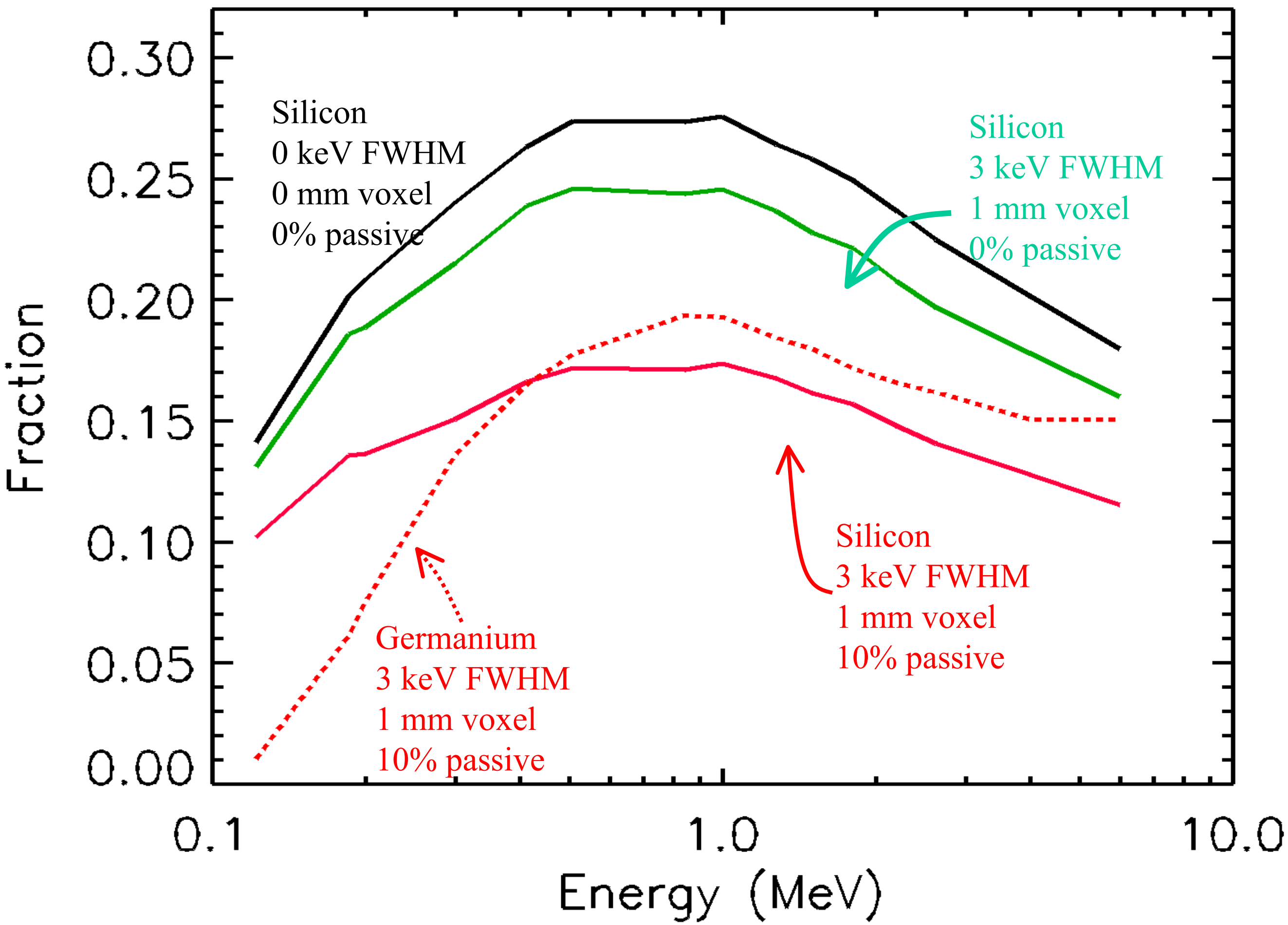

courtesy J. Kurfess

Background Issues for Compton Telescopes

1. Event ambiguity.
   - A. Forward vs. backward
   - B. Neutron vs. γ
2. Accidental coincidences with high count rate from large area.
3. Multiple photon, neutron induced, background.
4. Activation of passive material.
5. Doppler broadening effect.

- COMPTEL suffered from all but 1A and 5.

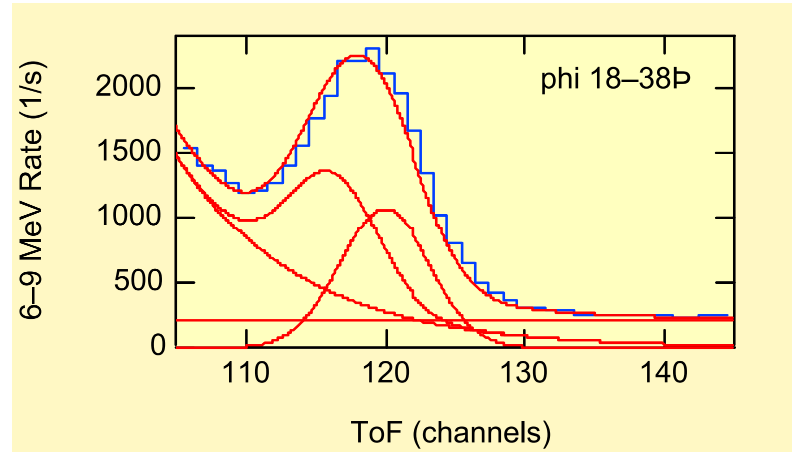

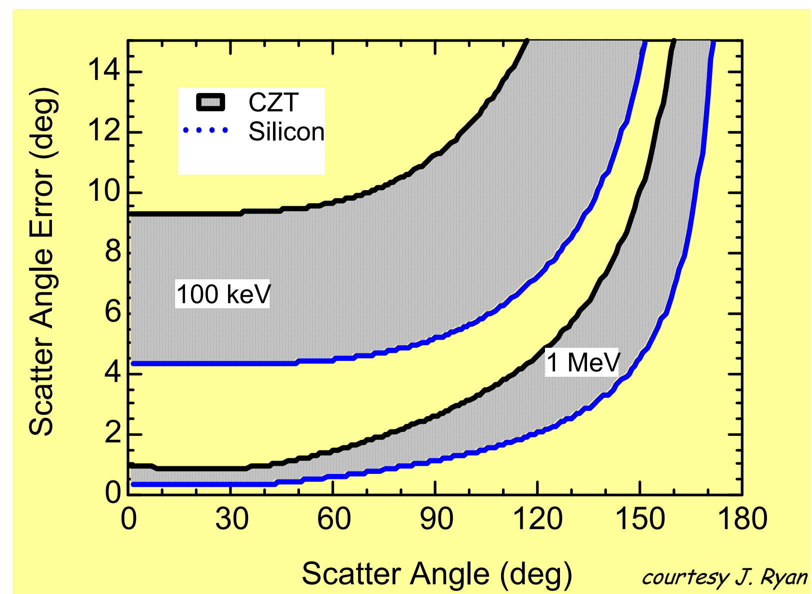

Rejection of Internal Background

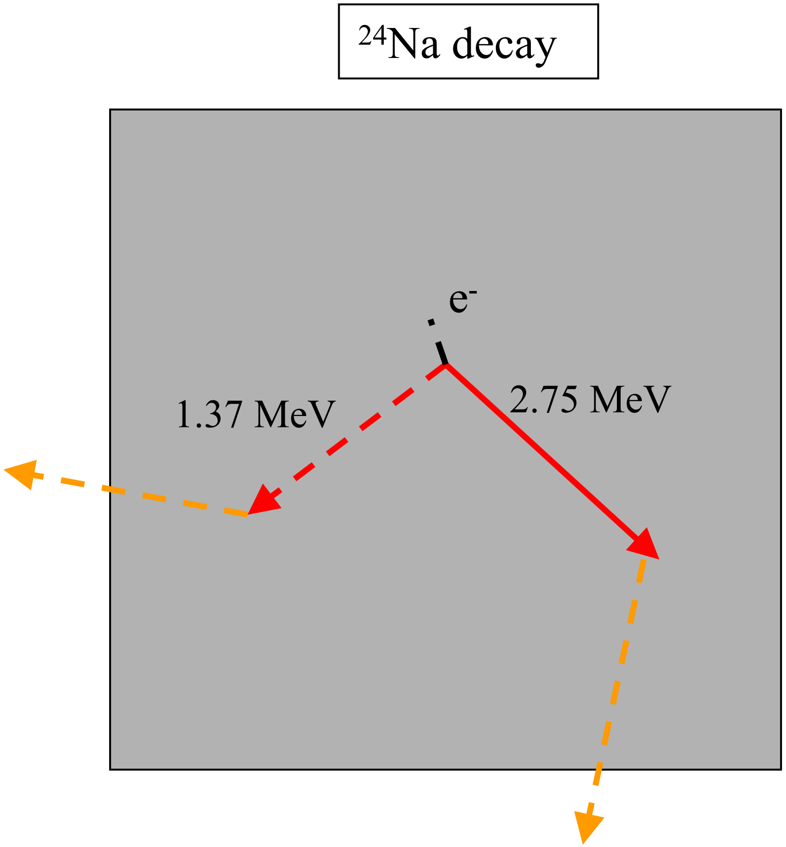

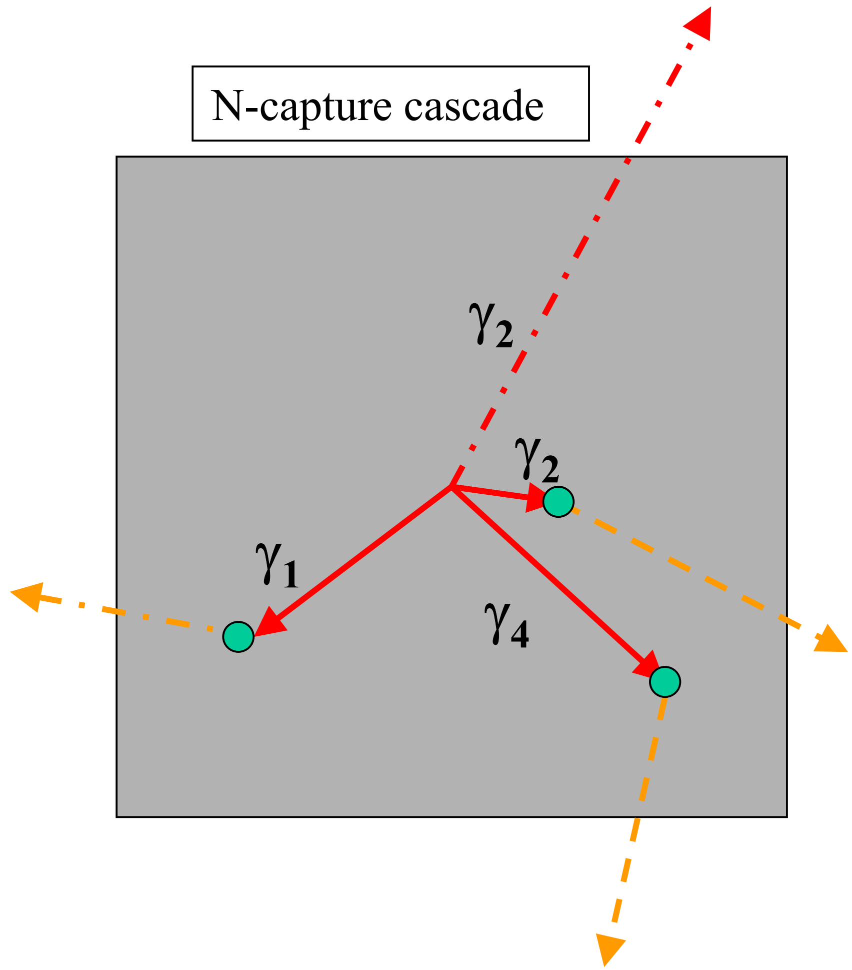

How does rejection efficiency depend on energy and position resolution?

courtesy J. Kurfess

Background Simulations

- ☆ Use Adopted Cosmic-Ray Environment (Flux, Spectrum)
- ☆ Employ Mass Model of Space Experiment
- ☆ Follow CR Interactions
  - ☞ Activated Nuclei
  - ☞ Cascades
  - ☞ Neutrons, Protons, Electrons, Gamma-Rays
  - ☞ Example for SPI/INTEGRAL Ge Dectector Backgorund

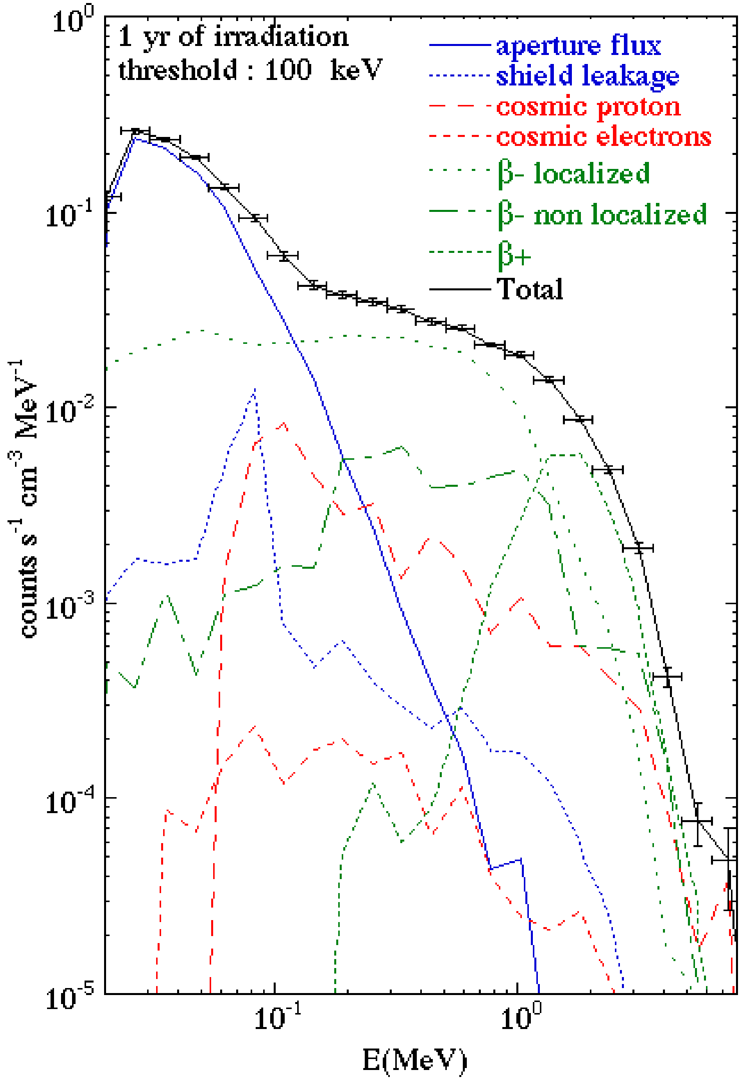

MEGA: Advanced Compton Telescope Imaging

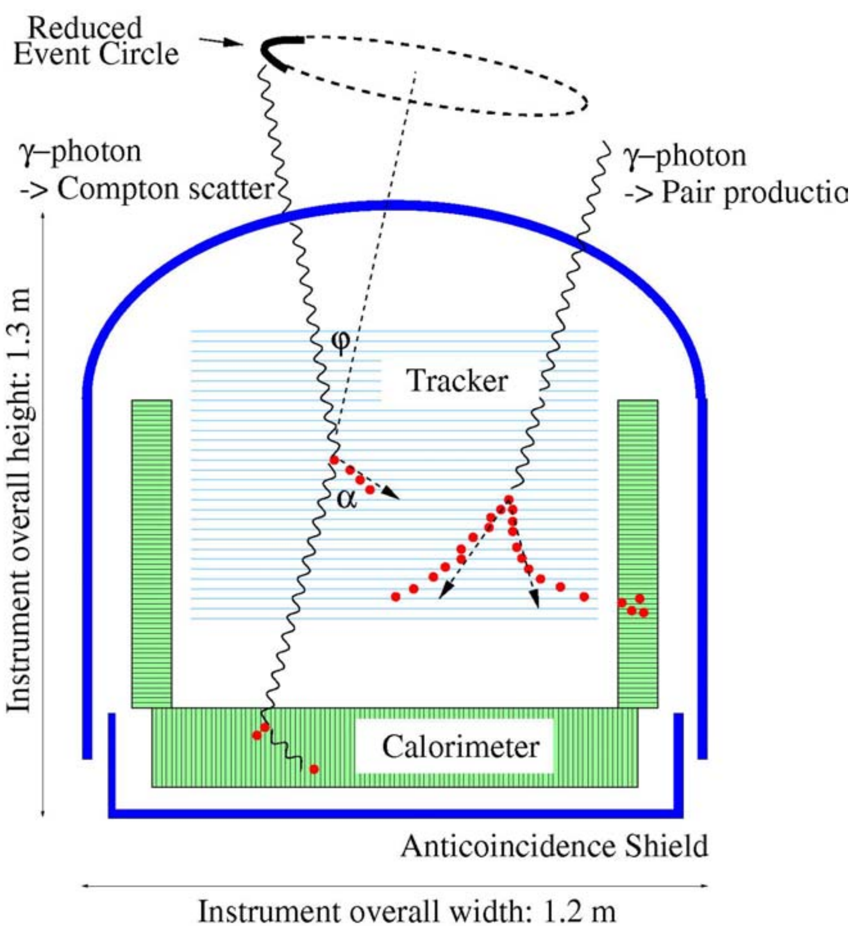

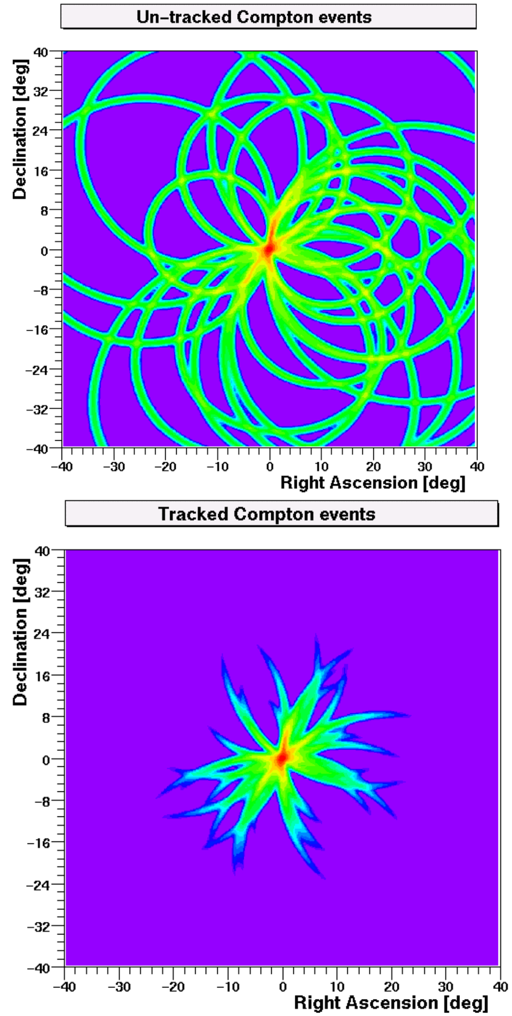

courtesy G. Kanbach

Roland Diehl

MEGA

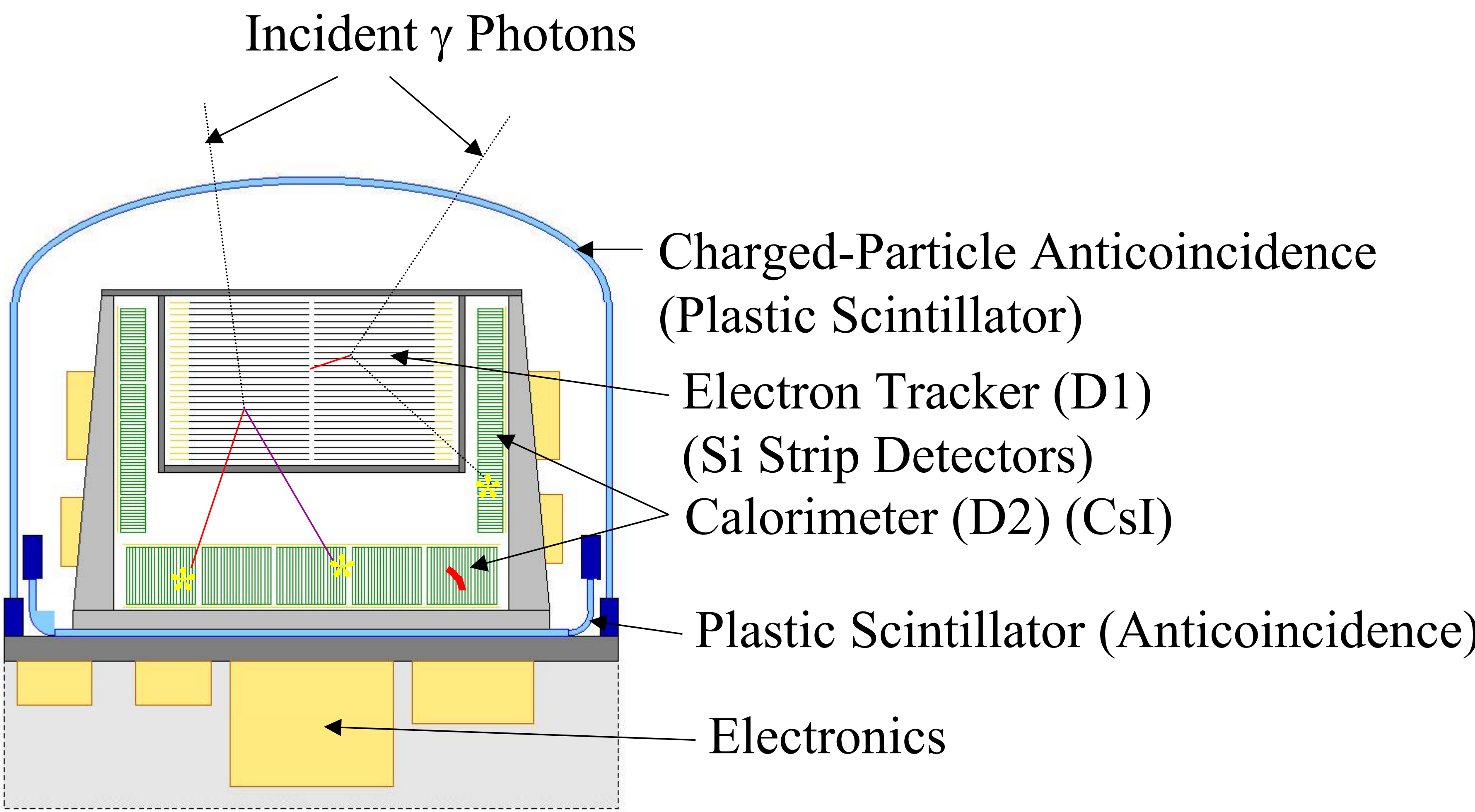

courtesy G. Kanbach

Roland Diehl

Gamma-Ray Detection via Compton and Pair Creation Interactions

- Selective Trigger & good Background Rejection
- Large and Sensitive
- Sensitive to Polarization @ a few MeV
- ‚Matched' Resolution (Angular and Energy)

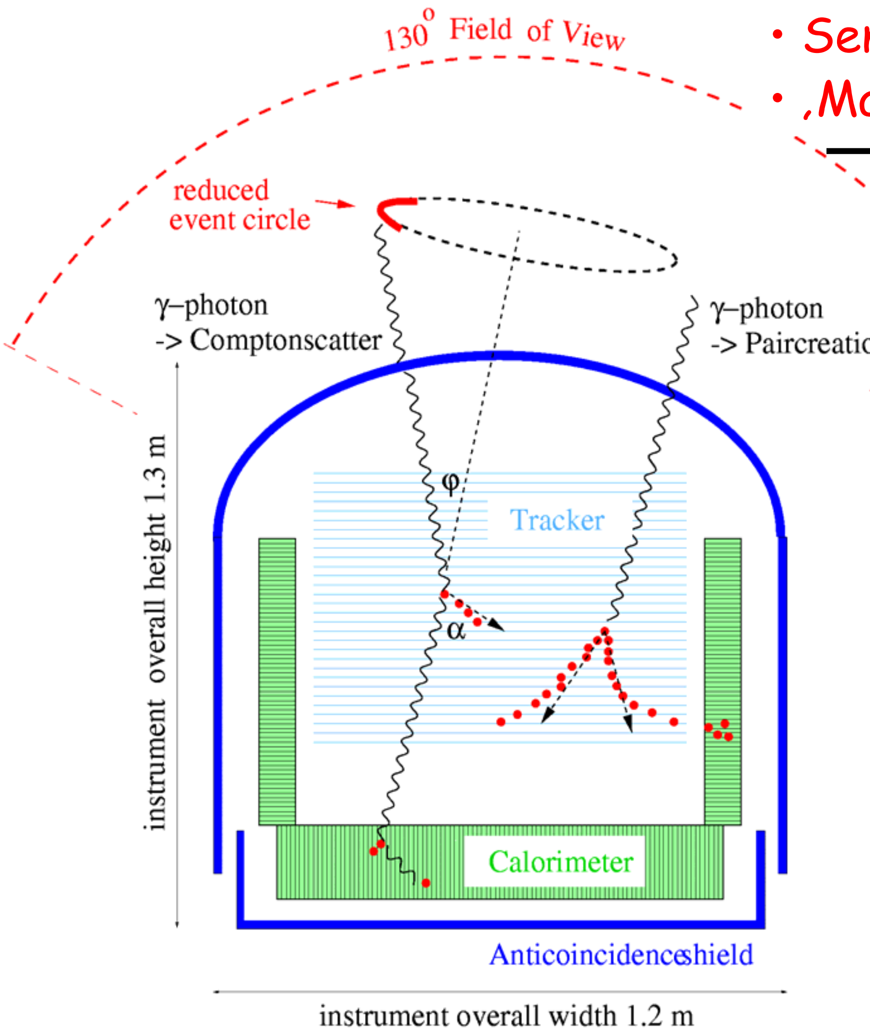

MPE/MEGA choice of technique:

Tracker: double sided Si strip detectors

Calorimeter: CsI/PIN diode pixel arrays

Scale of detector for $A_{eff} \sim 100\ cm^2$?

$A_{eff} = (1-e^{-\mu d})\ A_{geom}\ \eta$

$\mu \sim 0.1\ cm^{-1}$ (>100 keV) in Si
$A_{geom} \sim 1300\ cm^2$ (=36x36 cm^2)
$\eta \sim 0.5$

tracker depth ~ 1.7 cm of Si
i.e. 34 layers of 500μm ; ~ 5 m^2 Si

courtesy G. Kanbach

Prototype and Full-size Instrument

30 layers of Si strip detectors
36 x 36 cm^2 , 0.5 mm thick

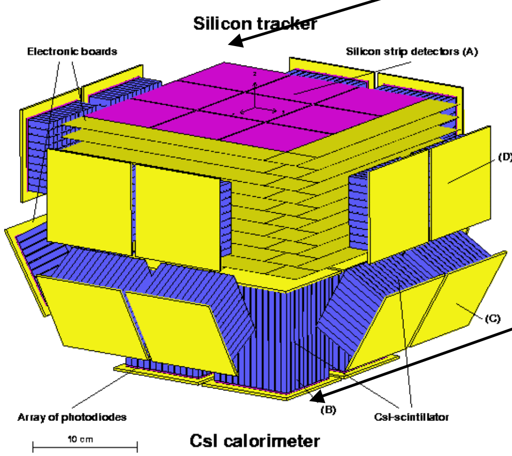

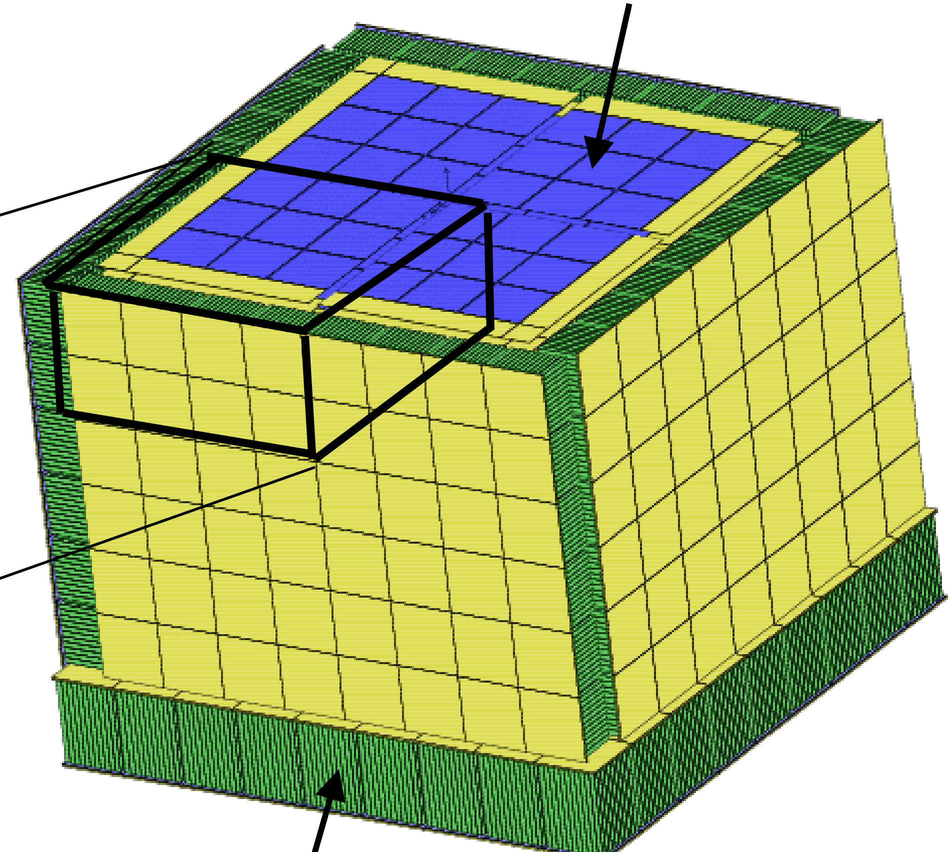

10 layers of Si strip detectors
18 x 18 cm^2 , 0.5 mm thick

10 cm

CsI Calorimeter

courtesy G. Kanbach

Roland Diehl

Prototype

Tracker:
10 (+1) layers of Silicon stripdetectors (wafers 6x6cm²)

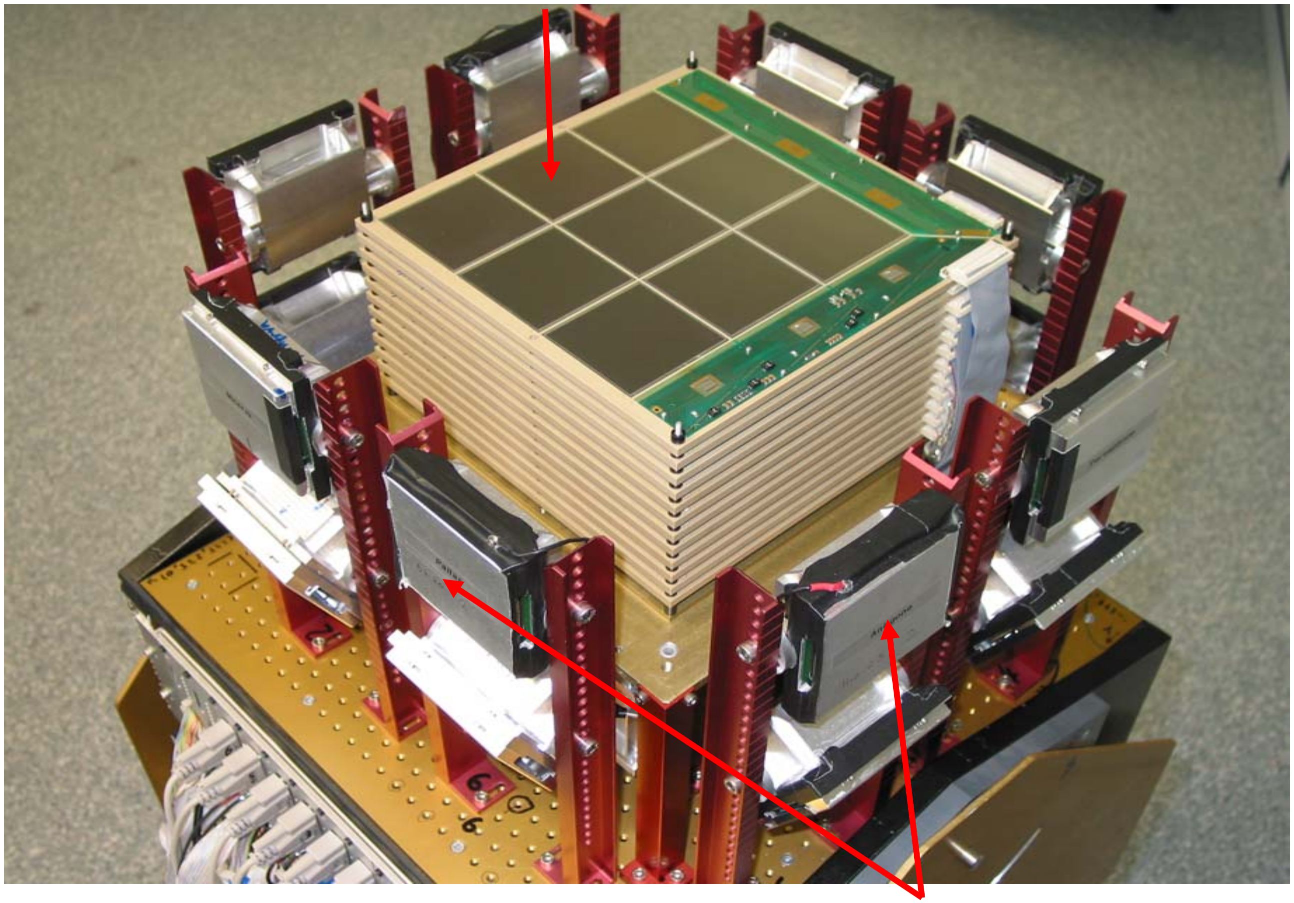

Calorimeter: 20 modules of pixellated CsI(Tl) Scintillators
Fill factor lower hemisphere ~ 40%

A_{eff} estimate :

$$A_{eff} = (1-e^{-\mu d})\, A_{geom}\, \eta = 16\ cm^2\, \eta$$

with $\eta = 0.4 \times 0.3$

$A_{eff} \sim 2\ cm^2$

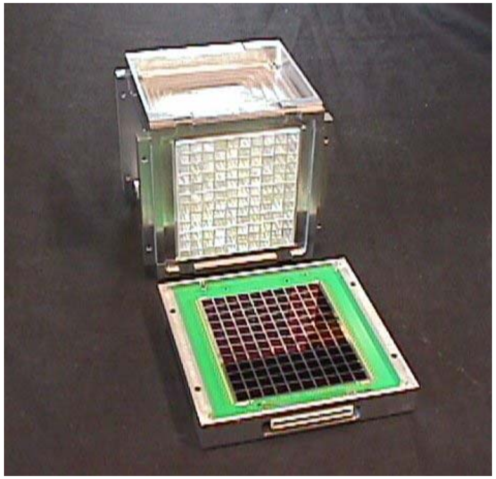

courtesy G. Kanbach

Roland Diehl

LXe for Gamma-Ray Detection

- High detection efficiency

$$\rho = 3.06 g / cm^3, Z = 54$$

- Short radiation length

$$L_{rad} = 2.6 cm$$

- High ionization yield for good ΔE/E

$$W = 15.6 eV / pair, F = 0.04$$

- Sub millimeter spatial resolution

$$D < 80 cm^2 / s, \text{ high } \mu, \text{saturated } \mathrm{v_d}$$

- Excellent scintillator with fast decay time

$$N_{ph} = 4 \times 10^4 / MeV$$

- Three-dimensional localization in homogeneous volume

With TPC mode of operation

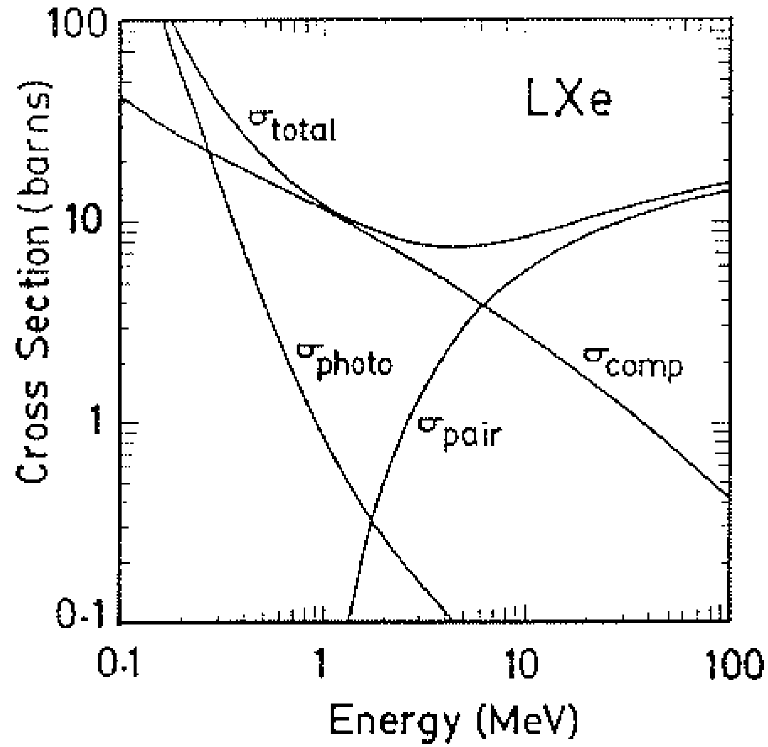

courtesy E. Aprile

A Time Projection Chamber as Compton Telescope

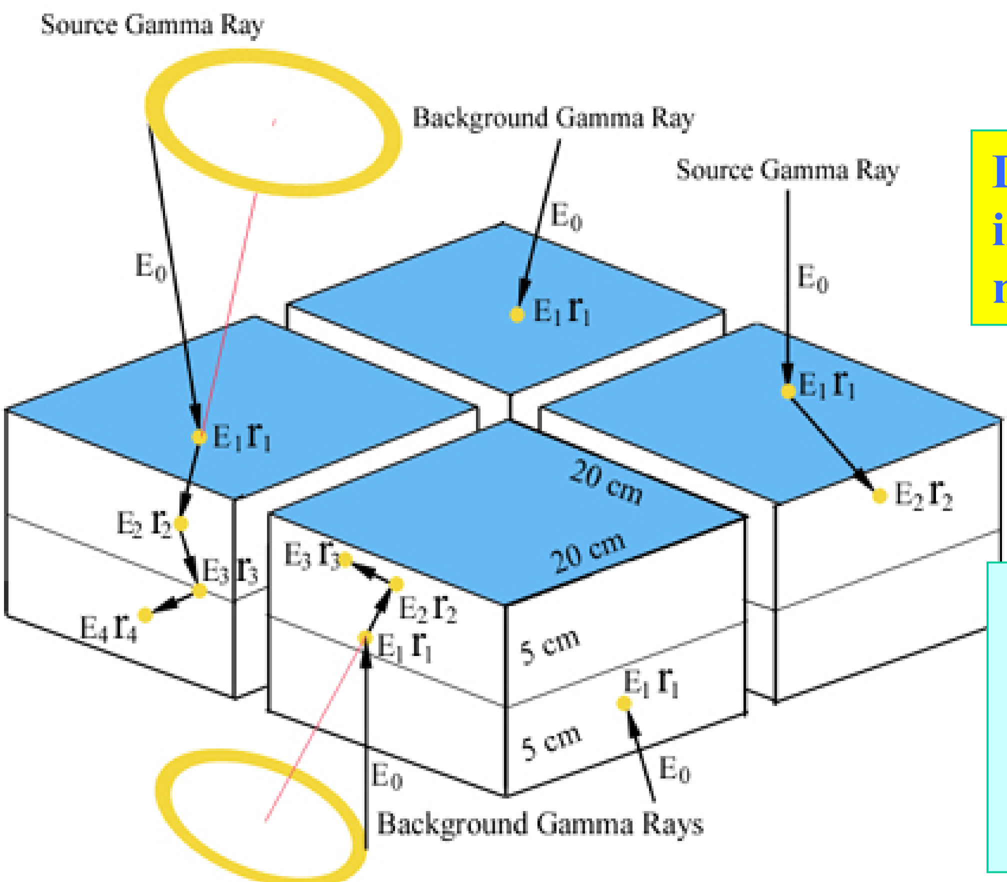

Detection efficiency is dramatically increased by using one homogeneous material as both D1 and D2

With <1 mm position resolution in 3-D and good energy resolution, the complete event interaction history is recorded thus dramatically enhancing background reduction through event reconstruction

High probability to fully contain the scattered photon energy when using a good stopping material such as Liquid Xenon

courtesy E. Aprile

The LXeGRIT Time Projection Chamber

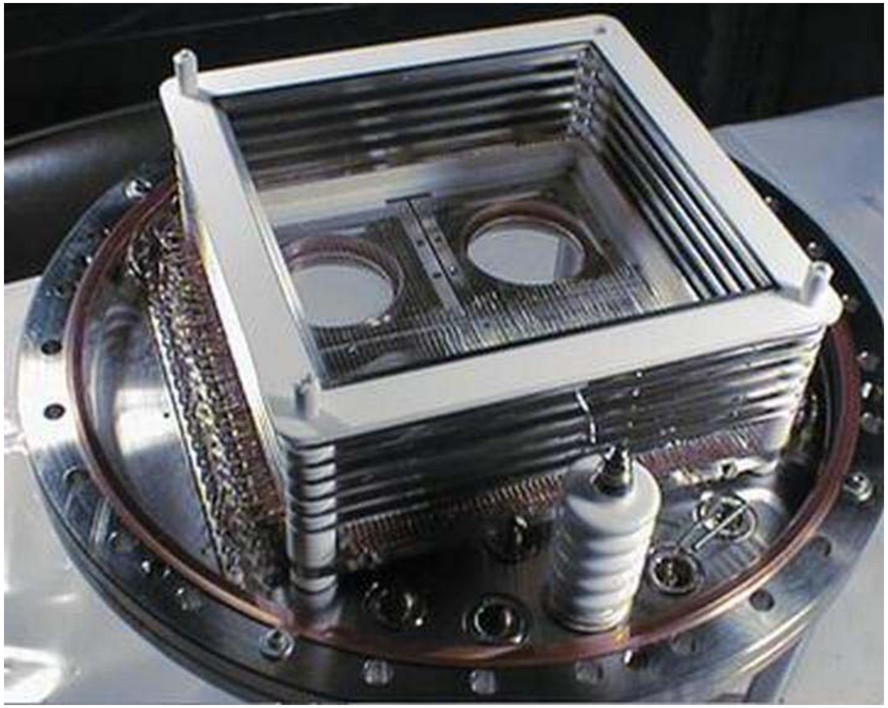

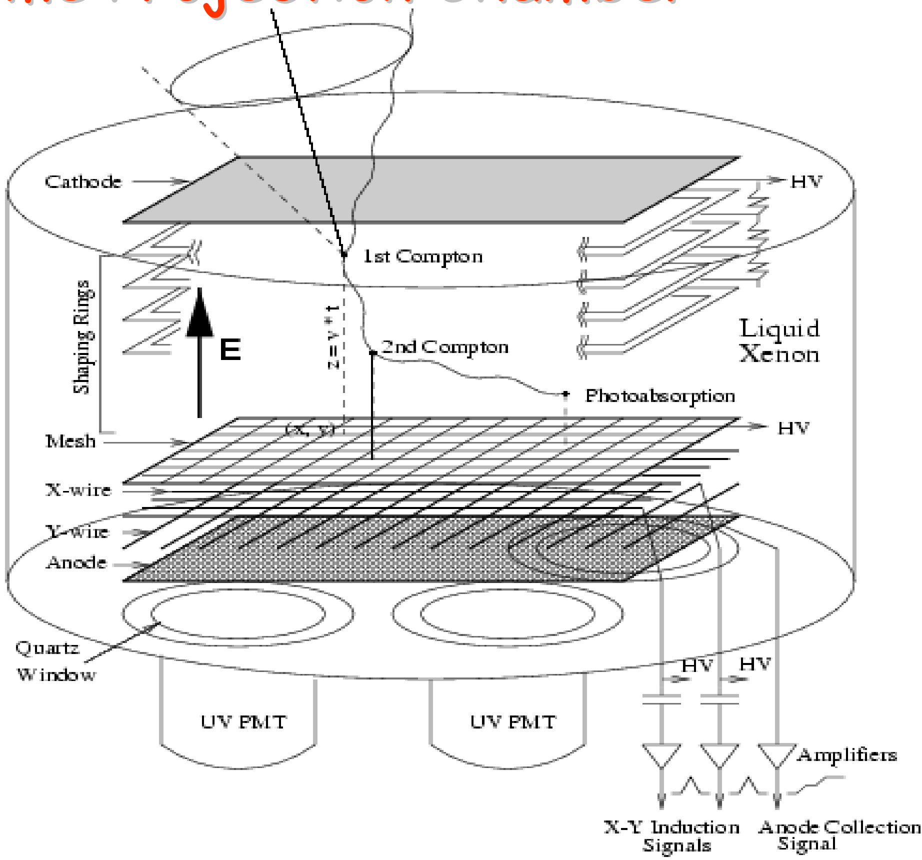

Ionization & Scintillation
20 cm x 20 cm Active Area
Drift Gap = 7cm
Drift velocity ~ 2mm/µs @1 kV/cm
62 X + 62 Y sensing wires (3mm pitch)
4 Independent Anodes for total energy
4 UV PMTs for light detection

(x_1, y_1, x_2, y_2) → scatter direction (χ, ψ)

E_i → total energy and scatter angle φ

$$\cos\varphi = 1 - m_e c^2 \left(\frac{1}{E_2} - \frac{1}{E_1} \right)$$

courtesy E. Aprile

Roland Diehl

The LXeTPC Charge Readout

- non-destructive readout of point-like ionization clouds→ focusing field
- ionization signal on anode ~4000 e/ 100 keV @ 1kV/cm → high purity liquid
- fraction induced on X-Y Wires ~ 40% → Low Noise Amplifier → 350e RMS
- HV on wires for field focusing → Decoupling Network
- preserve max signal information →5 MHz FADC (8/10 bit)

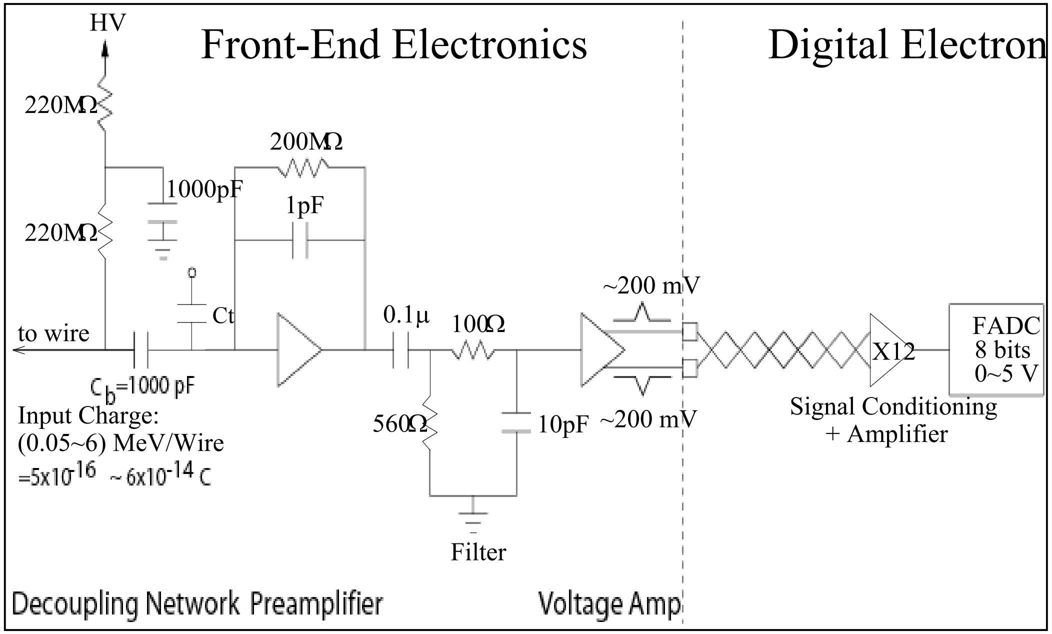

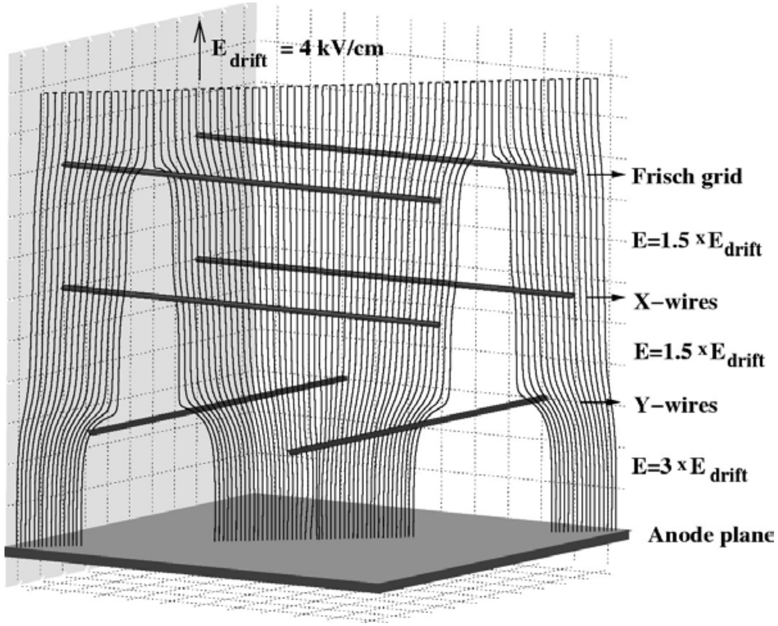

courtesy E. Aprile

Roland Diehl

LXe Compton Telescope Signal Recognition and Event Reconstruction

Analysis Steps

- Find wire signals on each view, collect shared charges.
- Match X- and Y-wire signals.
- Find anode signals, using a digital filter.

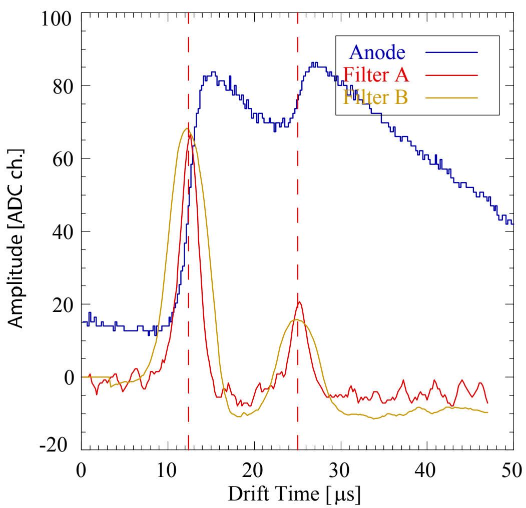

- Fit anode signals. Fit function for an N-interaction event:

$$f_N(t) = \sum_{i=1}^{N} A_i \frac{\exp\left\{\dfrac{t - t_i}{\tau_{decay}}\right\}}{1 + \exp\left\{\dfrac{t_i - t}{\tau_{rise}}\right\}} + B$$

- Match anode and wire signals.

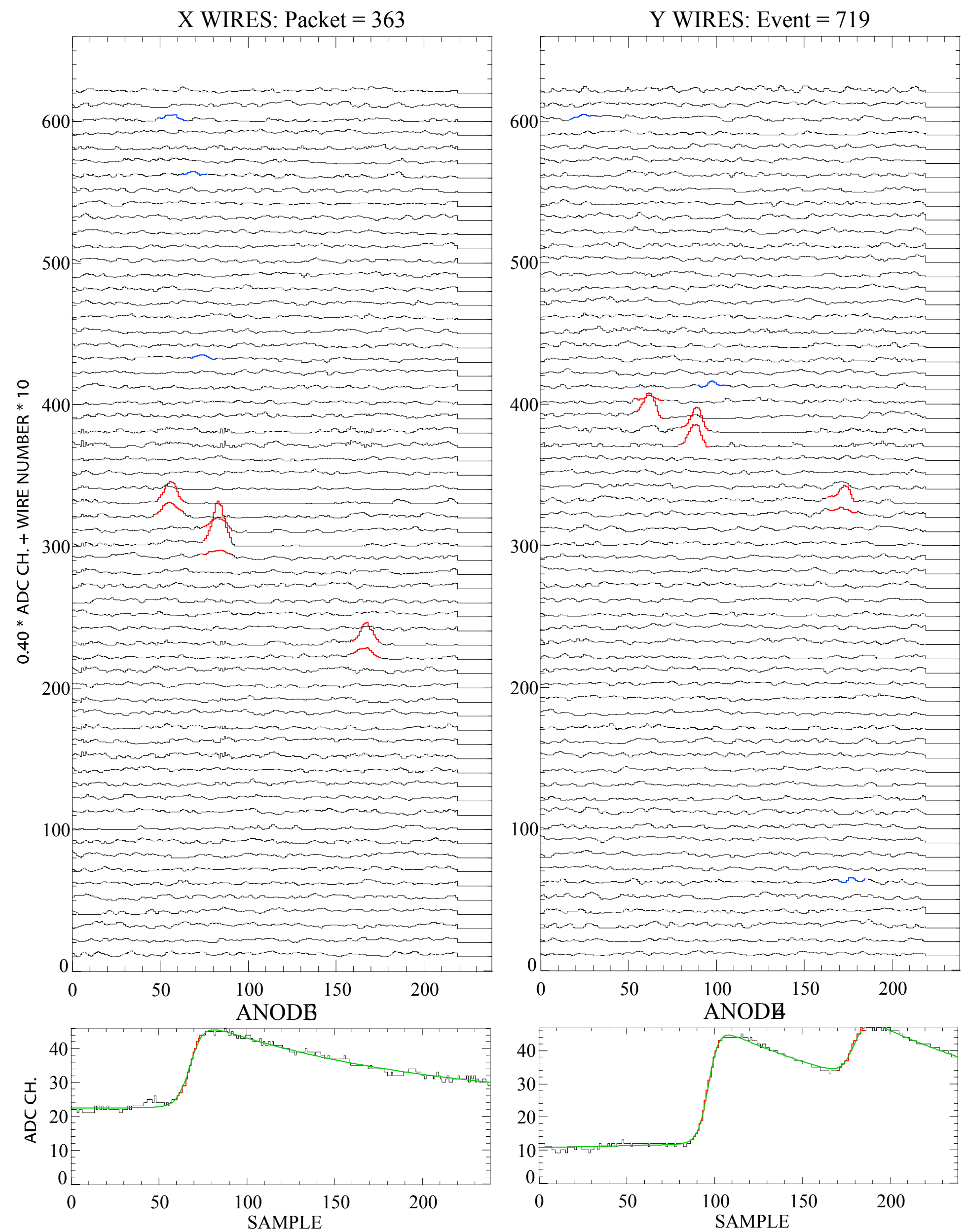

courtesy E. Aprile

LXeGRIT Characteristics: 2000 Balloon Campaign

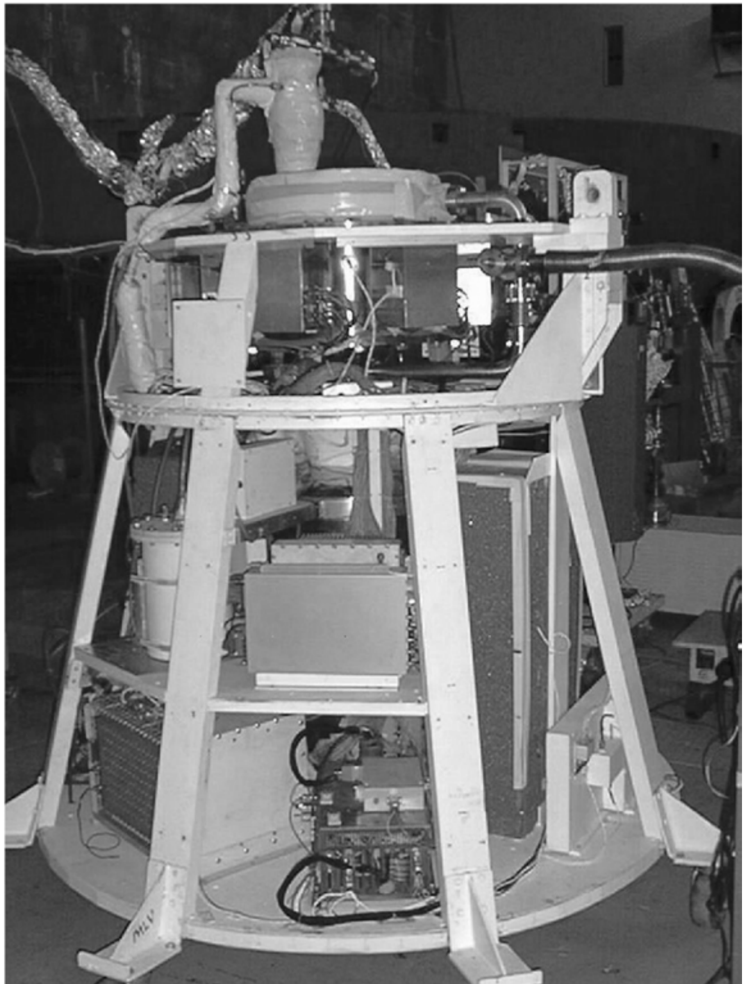

Energy Range	0.15-10 MeV
Energy Resolution ($FWHM$)	$8\% \times (1\,\mathrm{MeV}/E)^{1/2}$
Position Resolution (1σ)	1 mm (3 dimensions)
Angular Resolution (1σ)	3° at 1.8 MeV
Field of View	1 sr
Detector Active Volume	20 cm $\times$ 20 cm $\times$ 7 cm
LN_2 Dewar	100-liter
Instrument Mass, Power	2000 lbs, 450 W
Telemetry	2 $\times$ 500 kbps
Onboard Data Storage	2 $\times$ 36 GB

courtesy E. Aprile

Improvements in Next Generation Compton Telescopes

Increased Efficiency
- More Compact Design
- Monolithic, Position-sensitive detectors

Energy Resolution
- Solid State Detectors
- Gas Detectors

Angular Resolution
- Position-sensitive detectors
- Energy resolution
- Electron tracking

Background Reduction
- Electron tracking
- Event reconstruction
- Choice of orbit

  Note: No time of flight with most systems under consideration

Tracker:
10 layers of Silicon stripdetectors

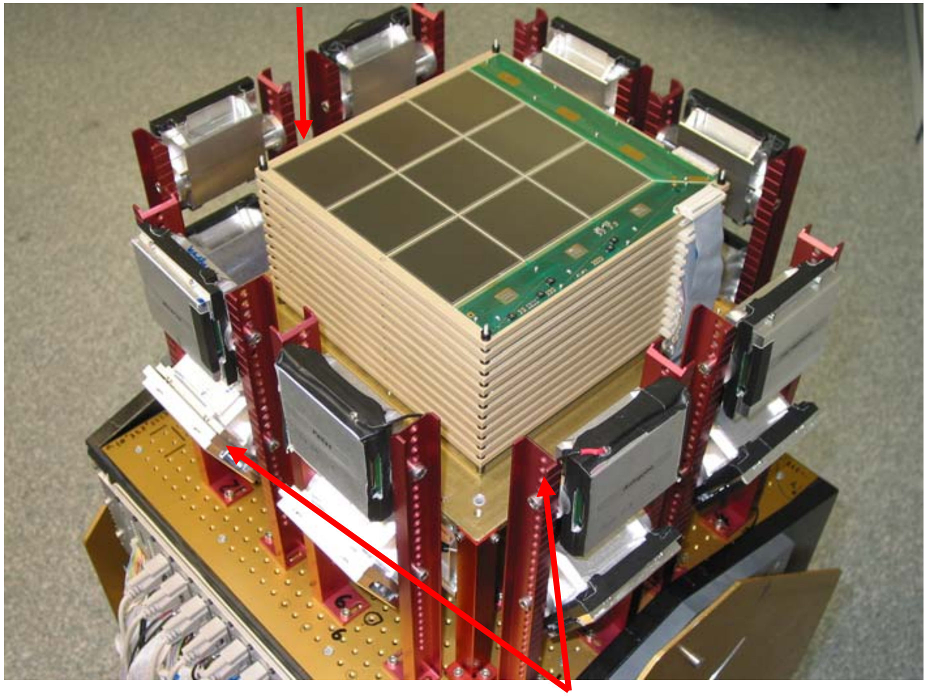

Calorimeter: modules of CsI(Tl) Scintillators

courtesy J. Kurfess

Xe-Advanced Compton Telescope Concept

- Make ACT tracker from large gas volume read out by **pixelized gas micro-well detectors (MWDs)** read out by **thin film transistor (TFT)** arrays
- Advantage of this approach is **excellent electron tracking**: RMS error of 7^{o} for 1 MeV electron for Xe at 3 atm
- Electron tracking dramatically lowers PSF area for higher sensitivity, better imaging, and higher polarization sensitivity
- ACT concept: large Xe gas tracker surrounded by CsI calorimeter

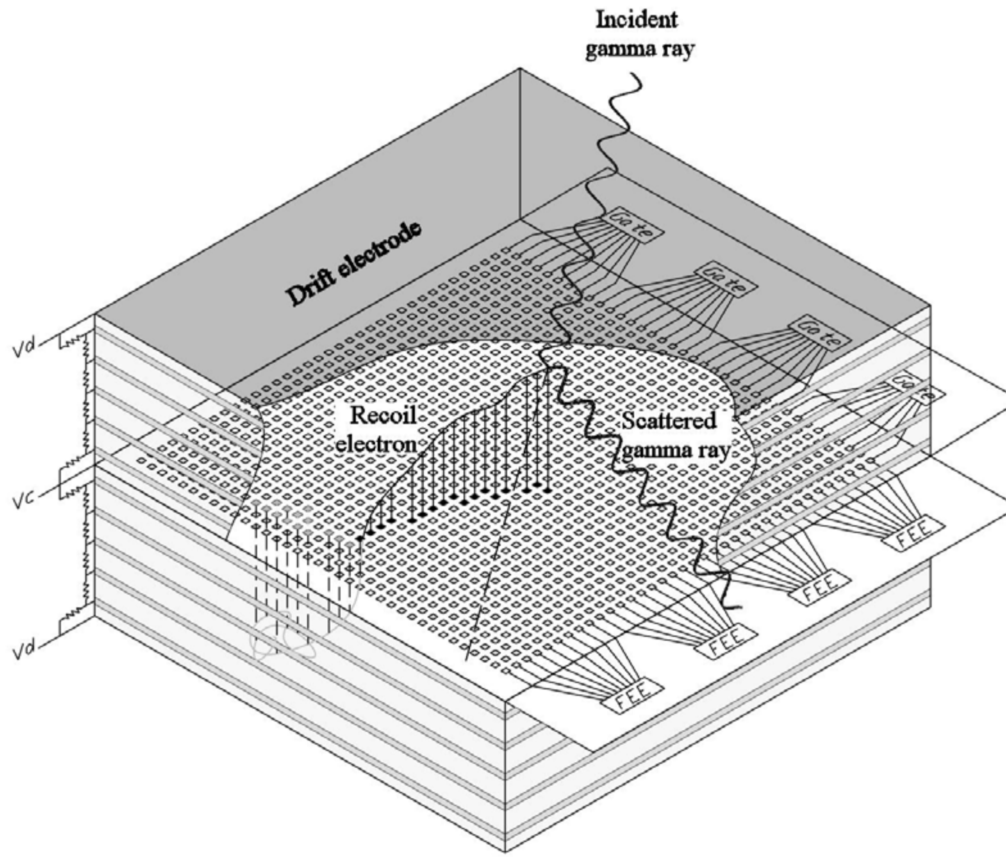

Xe 3-dimensional track imager as module of Compton telescope tracker

courtesy J. Kurfess

Solid-State Detector Advanced Compton Telescope Concept

1 m^2 frontal area

43 g/cm^2 thick

6-mm thick Si(Li) $\langle\rho\rangle = 0.8$
-or-
1 cm thick Ge $\langle\rho\rangle = 2.7$

430 kg active volume

Fluid loop cooling

CMOS electronics

Passive mass <10%

Broad FoV (± 60-75 deg)

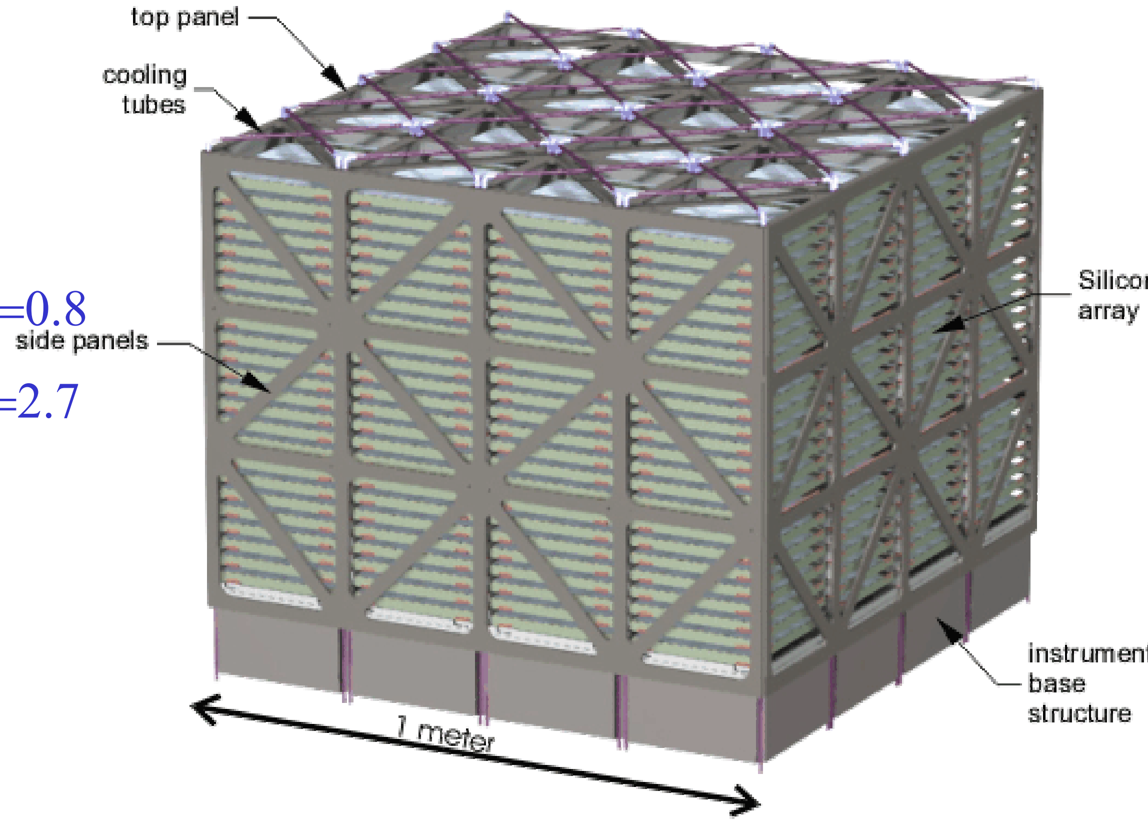

courtesy J. Kurfess

Narrow FOV Compton Telescope for the NeXT mission in Japan

•Incident angle of γ-rays are defined by a well-type active collimator (Extremely Low Background)

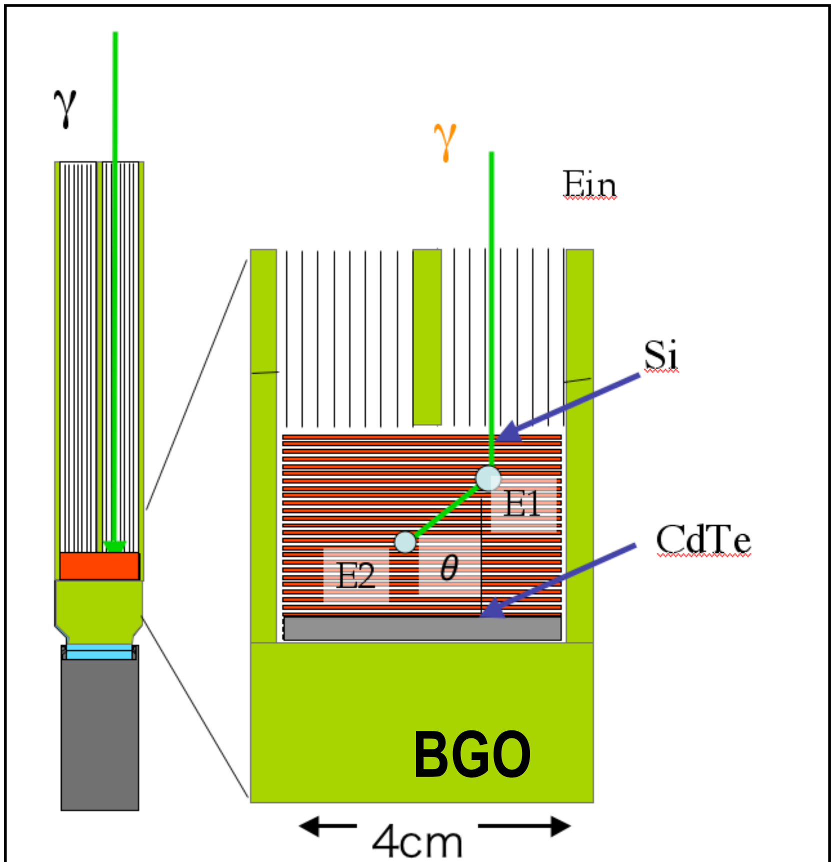

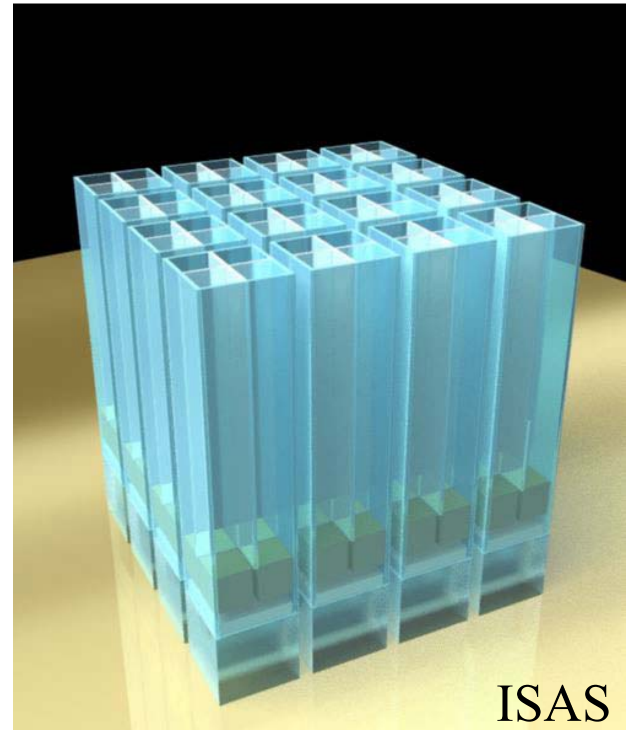

–Stack Configuration

- •Low Energy 24 layers of Strip Strip detectors (res. 400μm) and
  6 mm thick CdTe Pixel (res. 1mm)

–High Energy Resolution of <1 - 3 keV

courtesy J. Kurfess

Mission Options

Large Area Coded Aperture--EXIST

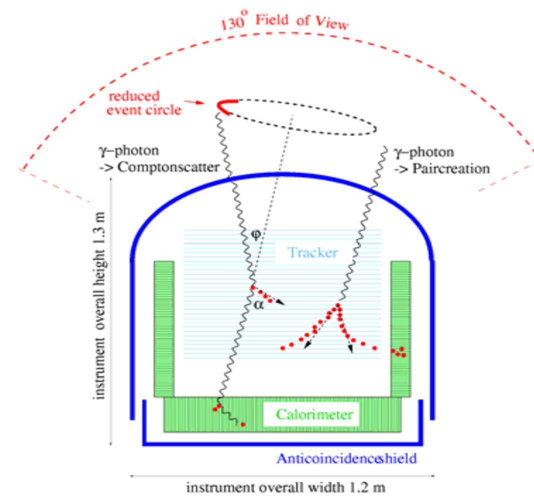

Compton Telescopes

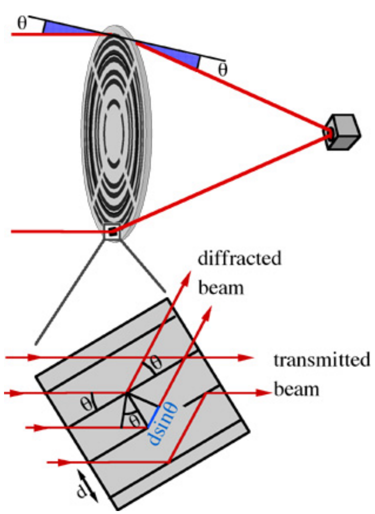

Laue gamma ray collector (Claire)

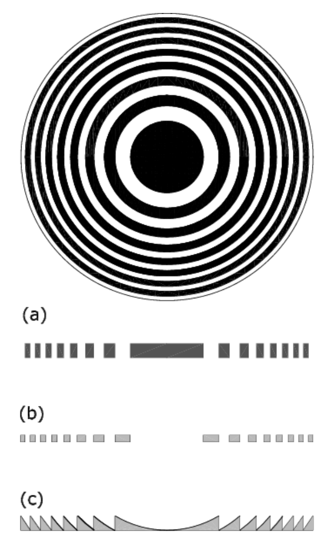

Gamma Ray Lens

Spark Chambers

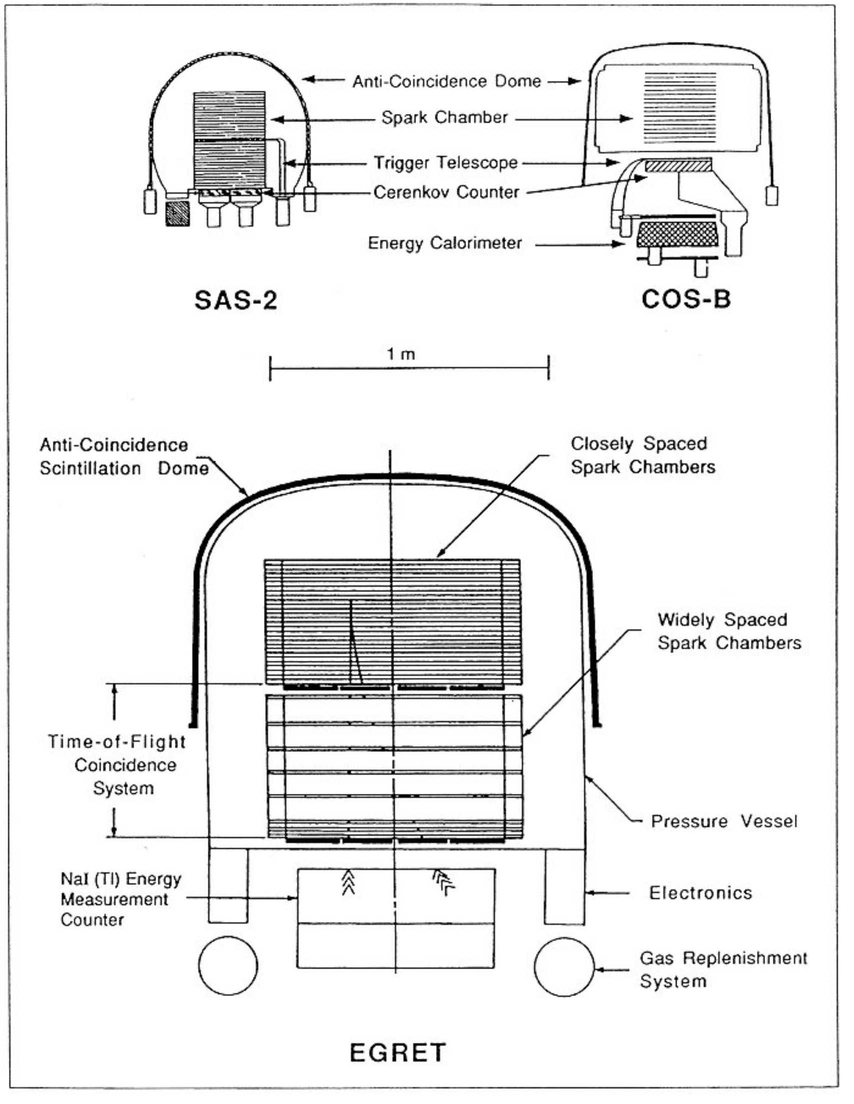

EGRET

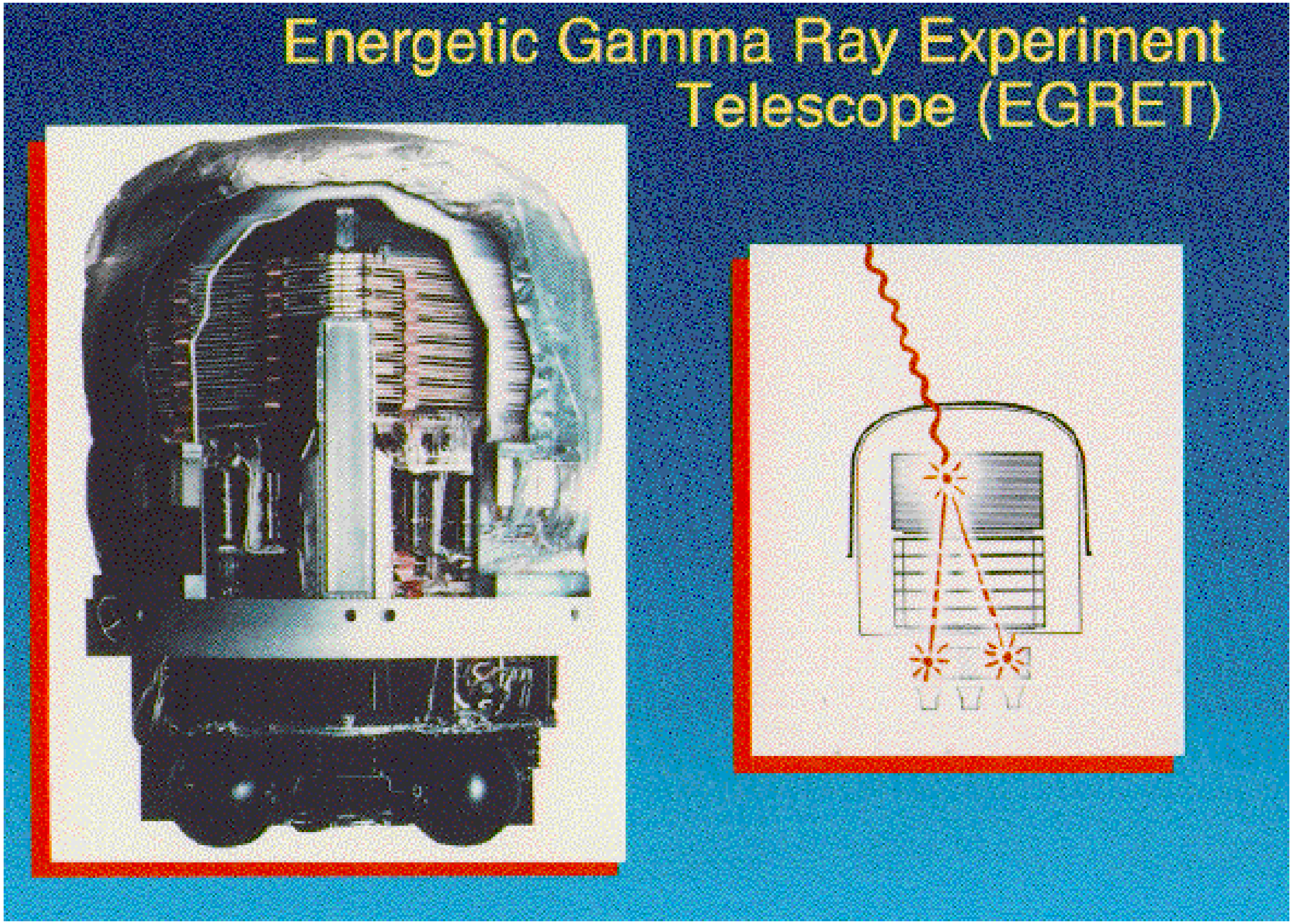

Instrumental Sensitivities

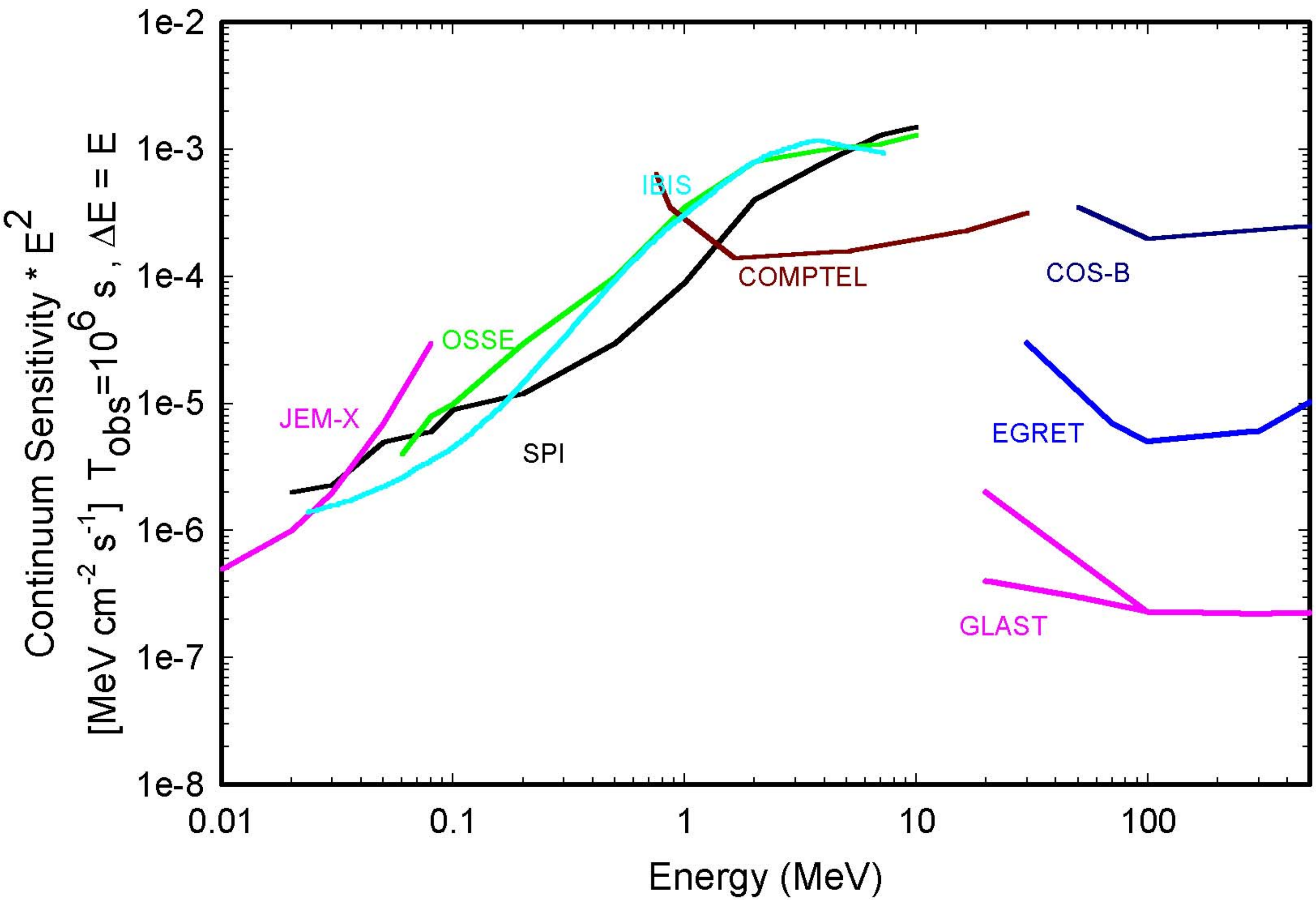

Roland Diehl

We would like something like this at 1 MeV

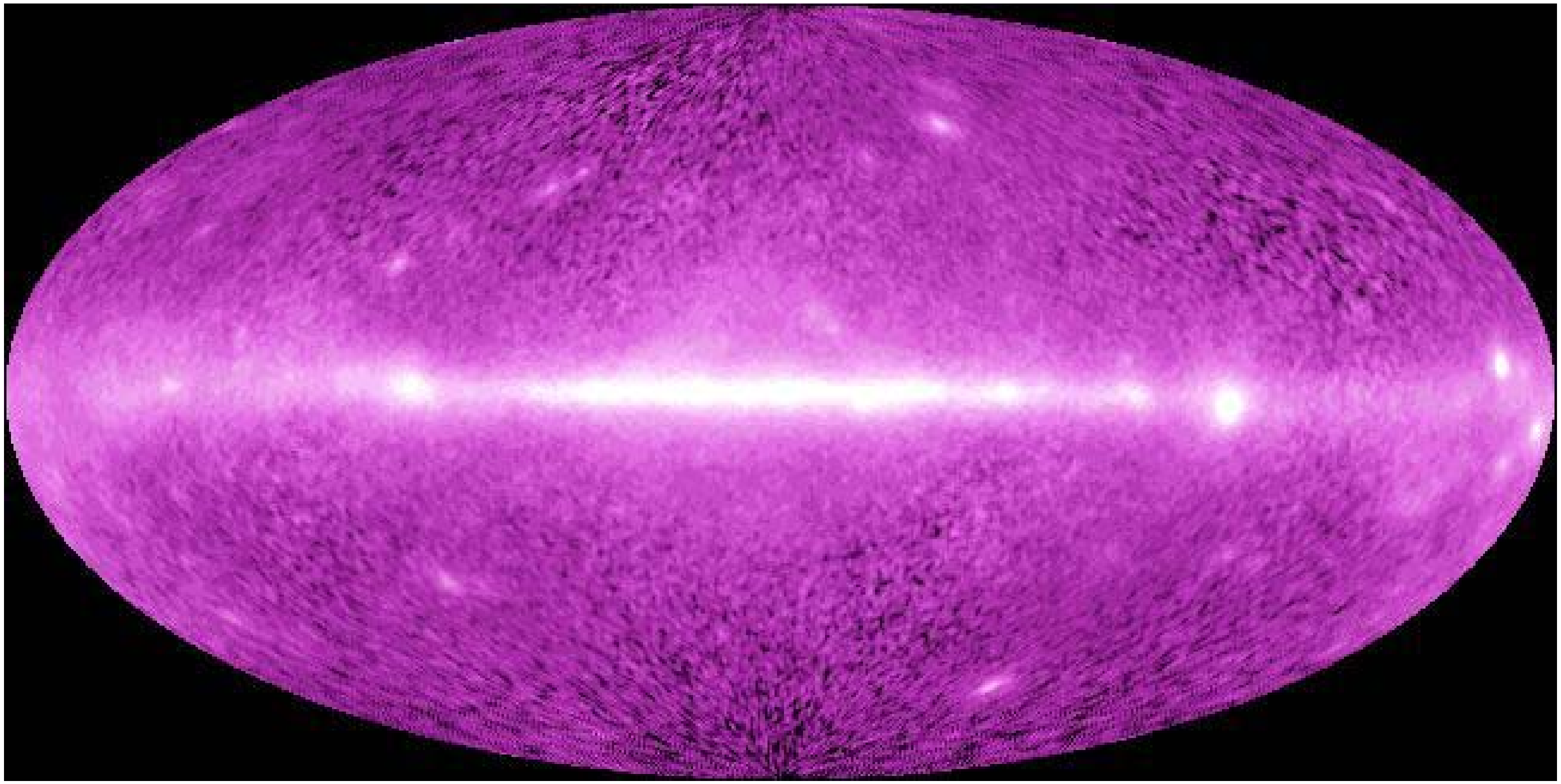

But now, we'd like lots of other things too, now that we know what is out there.

COMPTEL Sky maps

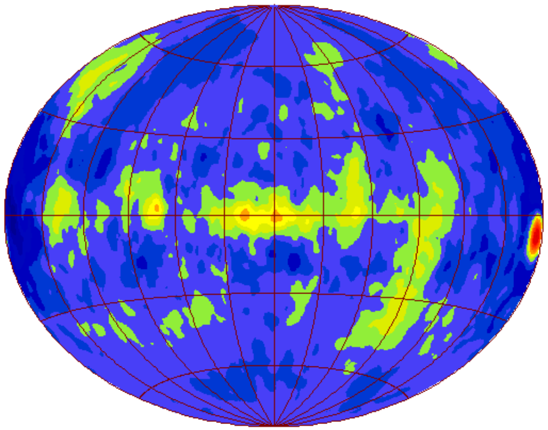

1–3 MeV

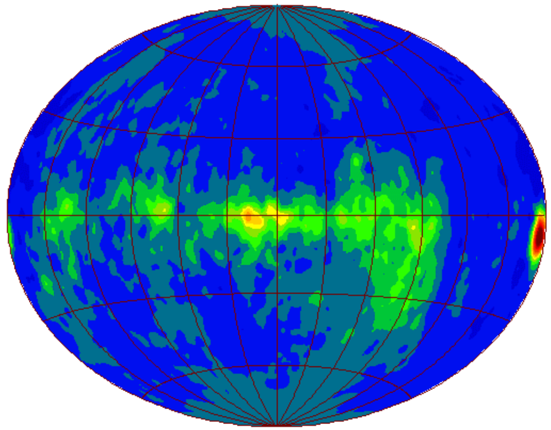

3–10 MeV

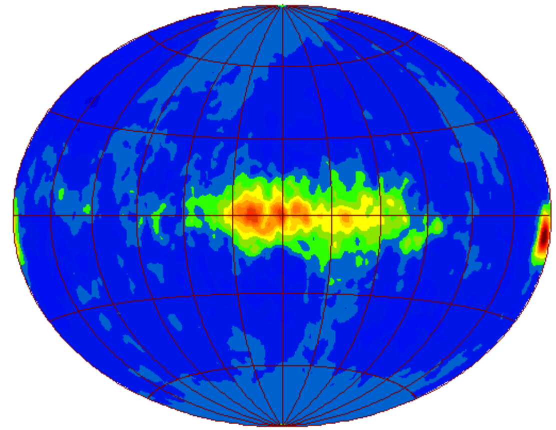

10–30 MeV

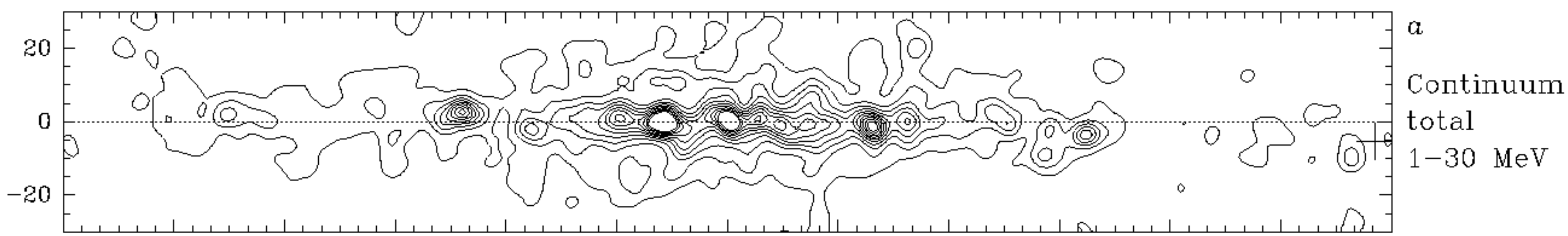

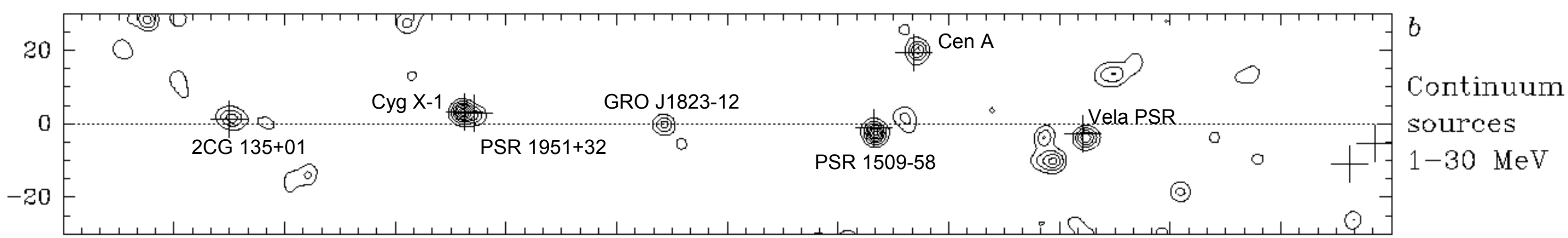

Roland Diehl

SN1987A: First Supernova Gamma-Rays

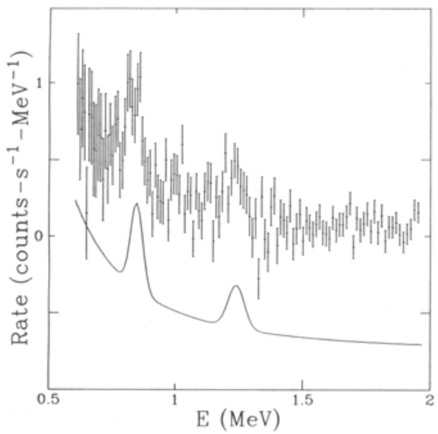

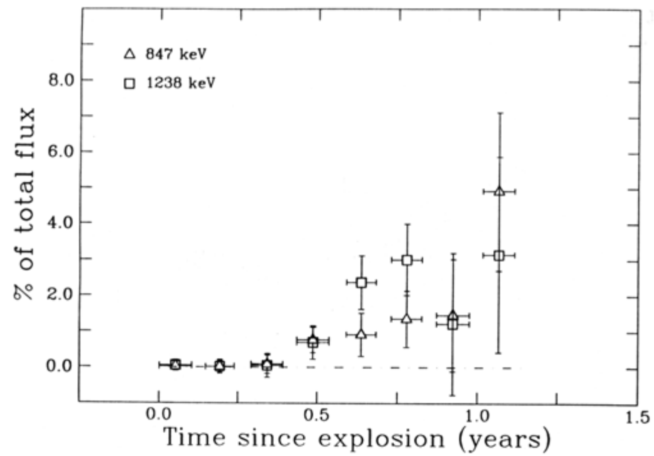

- SN1987A ^{56}Co Decay Gamma-Rays Detected Earlier Than Expected; First Proof of Supernova ^{56}Ni Synthesis
  (SMM; Matz et al. 1988)

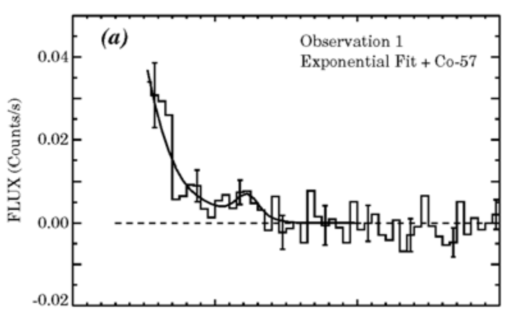

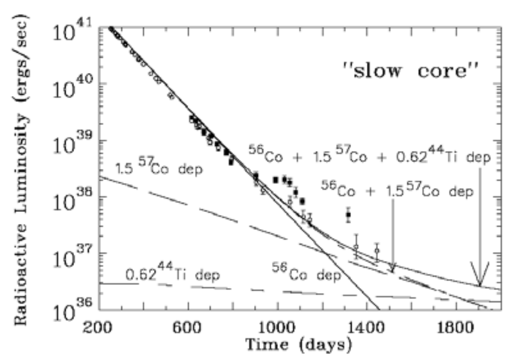

Figure 1.

- SN1987A ^{57}Co Decay Gamma-Ray Detection Used to Infer Co Isotopic Ratio (~1.5 x solar)
  (OSSE; Kurfess et al. 1992; Clayton et al. 1992)

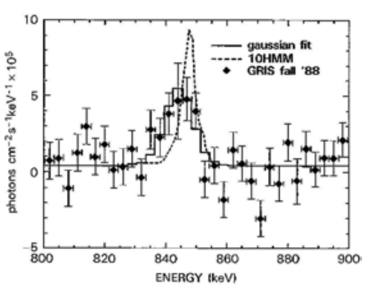

- SN1987A ^{56}Co Line at 847 keV Used for Line Shape Analysis
  (GRIS; Teegarden et al. 1988)

Roland Diehl

Core-Collapse Supernovae: ^{44}Ti from Cas A

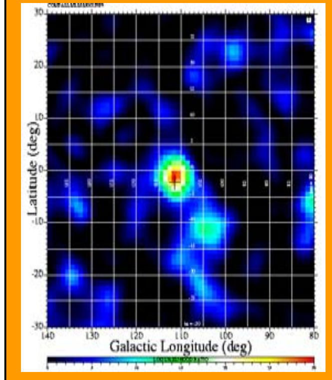

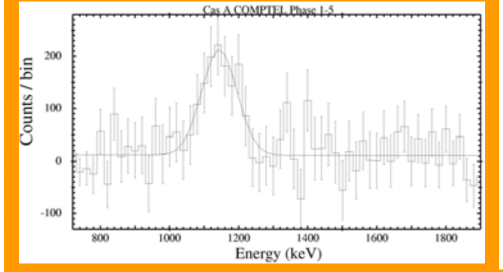

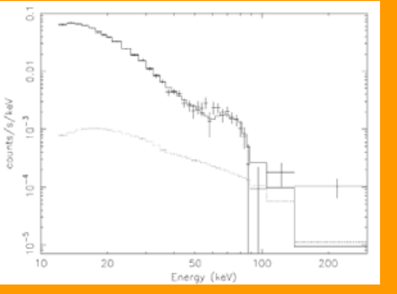

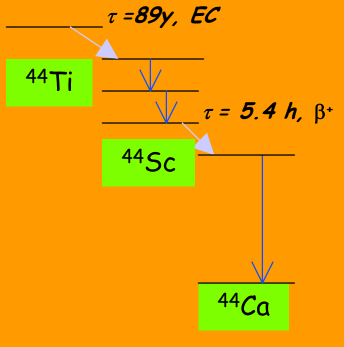

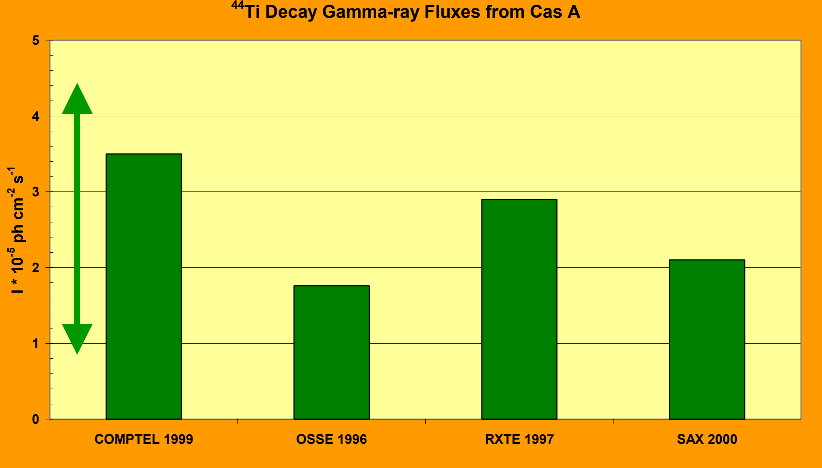

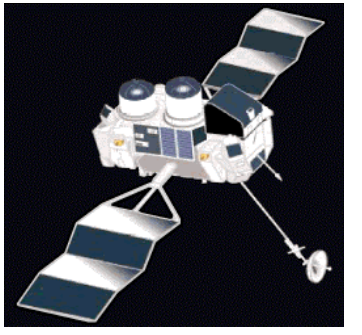

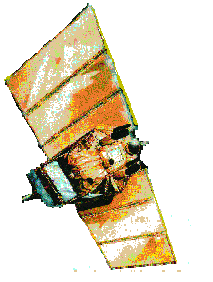

- ^{44}Ti Decay: τ~89y -> Young SNR
- Difficult γ-Ray Region (78, 68, 1157 keV) -> Uncertain Iγ

-> ^{44}Ti Ejected Mass ~0.8-2.5 10^{-4} M_o

The Sky at 1809 keV: ^{26}Al

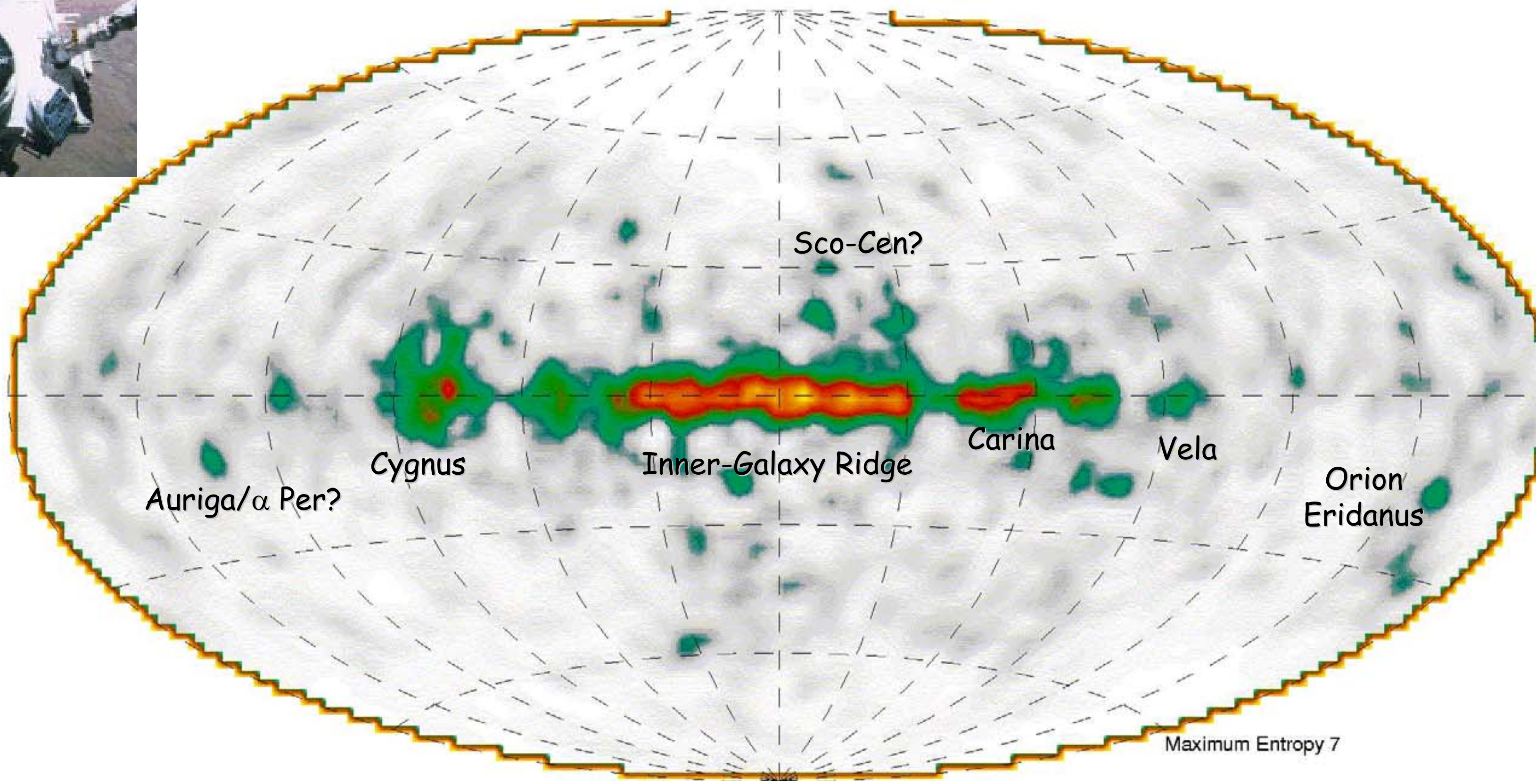

Complete CGRO Mission
(Plüschke et al. 2001)

Roland Diehl